NASA Contractor Report 177586

Soft Hub for Bearingless Rotors

Peter G. Dixon

Contract Number NAS2-13157
June 1991

National Aeronautics and
Space Administration

NASA Contractor Report 177586

Soft Hub for Bearingless Rotors

Peter G. Dixon

Advanced Technologies, Inc.
812 Middle Ground Blvd.
Newport News, VA 23606

Prepared for
Ames Research Center
Contract Number NAS2-13157
June 1991

National Aeronautics and
Space Administration

Ames Research Center
Moffett Field, California 94035-1000

TABLE OF CONTENTS

TABLE OF CONTENTS (cont'd)

1.0 SUMMARY AND CONCLUSIONS

This study of soft hub concepts has shown that to share the rotor tilt motions between the composite blade root flexures and a gymballed hub with composite drive torque and hub stiffening devices is structurally feasible. A comparison of estimated weight and drag of the two soft hub concepts analyzed with the equivalent BO-105 rotor hub is made together with a count of non-standard parts and ROM cost.

	SOFT HUB		BO-105
	w/Flexures	w/Bellows	
Weight (lb)	200.6	194	197
Drag (ft^2)	2.43	1.31	
Cost ($)	129,750	58,050	92,460
# Non-std Parts	53	7	162

Reliability of either concept is estimated to require scheduled inspection of the hub components no more freqently than every 500 hours and the maintenance needed should be neglibible.

This study has established feasibility and it is recommended that a selection of one hub concept should be made for Phase II effort which would include detail design, fabrication and evaluation through structural testing of a prototype system.

2.0 INTRODUCTION

This document describes the results of a NASA-monitored small business contract to evaluate a Soft Hub/Elastic Gymbal concept that would enhance bearingless/hingeless rotor structural performance by sharing the tilt of the rotor disc between the blades and the flexible hub. A Design Criteria and Specifications Document has been derived, based upon the specification and loads data for the 5050 lb. DGW BO-105 hingeless rotor helicopter with a reduced hub moment stiffness equivalent to a three percent (3%) radius equivalent flap hinge offset, instead of the eleven percent (11%) that was characteristic of the bearingless version. By meeting these criterion, bearingless rotor systems, with their characteristic low life cycle cost, low weight, low drag, and low maintenance features can be retro-fitted to current helicopter systems. The concepts studied are each centered around a single, universally articulated, elastomeric bearing co-axial with the rotor shaft which transmits the rotor thrust from the hub to the rotor shaft while free to articulate and follow the rotor disc tilt. This bearing type is now widely used for rotor blade retention, however, it is even more suited to hub use since the articulation requirements are the same as a blade but the axial load requirement is less than one-quarter of the centrifugal force at the root of the blade. This hub application is shown in Figure 1. The biggest design challenge, however, is the transmittal of the high shaft torque from the high power-absorbing rotor running at a low RPM, and then there is the necessity to provide additional hub teetering stiffness (to enhance the controllability of the helicopter, see Appendix 1) by some device that can withstand the fatigue environment of the teetering hub.

The first approach, detailed in our proposal and shown in Figure 2, was to transmit torque through bellows which were expected to permit an articulation restrained only by that stiffness intentionally added therein to provide the required controlling hub moment.

The second approach, shown in Figure 3, was to transmit torque through composite flexure/hairpin elements which also provide hub stiffness. These elements were of fiber composite/elastomer laminates which were intended to have reduced bending strains due to hub tilt without impairing the flexures' capability to transmit torque.

The third approach was to transmit torque through upper and lower fixed ended hairpin flexures and provide additional hub moment stiffness as required through changeable hairpin flexures mounted in elastomeric end supports as shown in Figure 4.

A fourth approach, shown in Figure 5, used a single bellows to transmit torque and utilizes only the universal elastomeric bearing to augment hub moment stiffness.

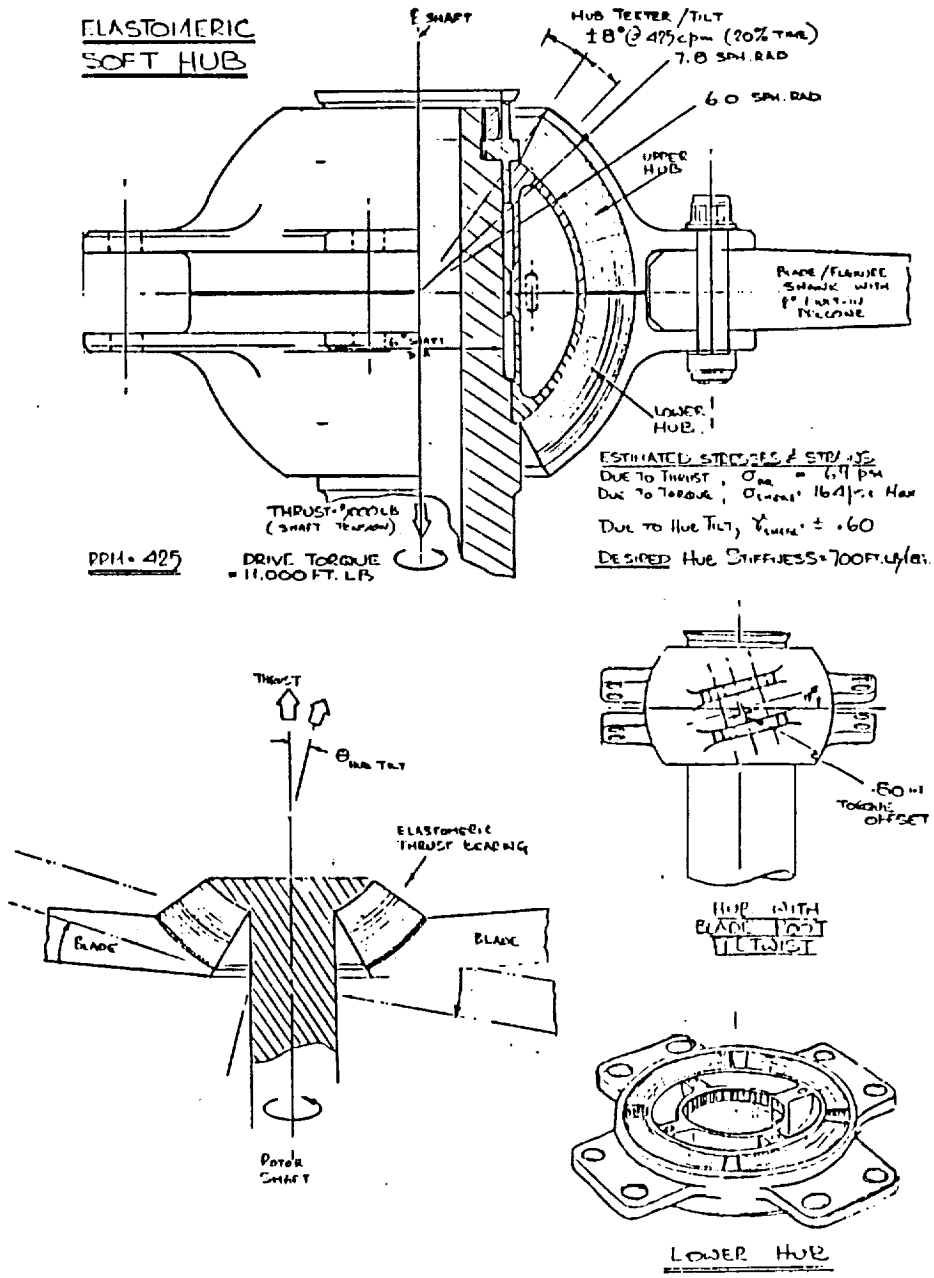

Figure 1. Hub Application for Elastomeric Bearings

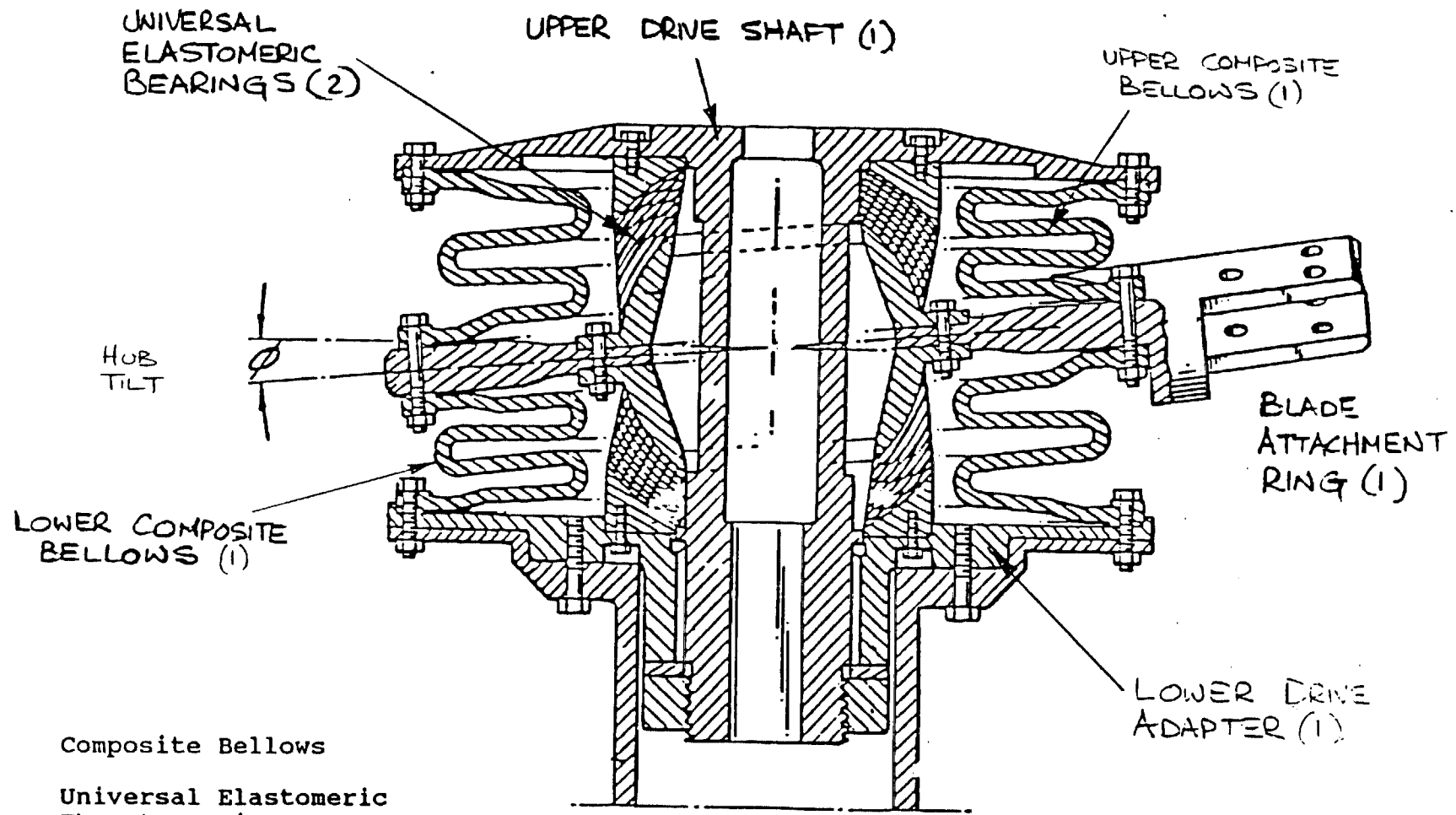

- Composite Bellows
- Universal Elastomeric Thrust Bearings
- 7) Non-Standard Parts

Figure 2. Soft Hub with Two Composite Bellows Torque Drive/Hub Stiffening Flexures

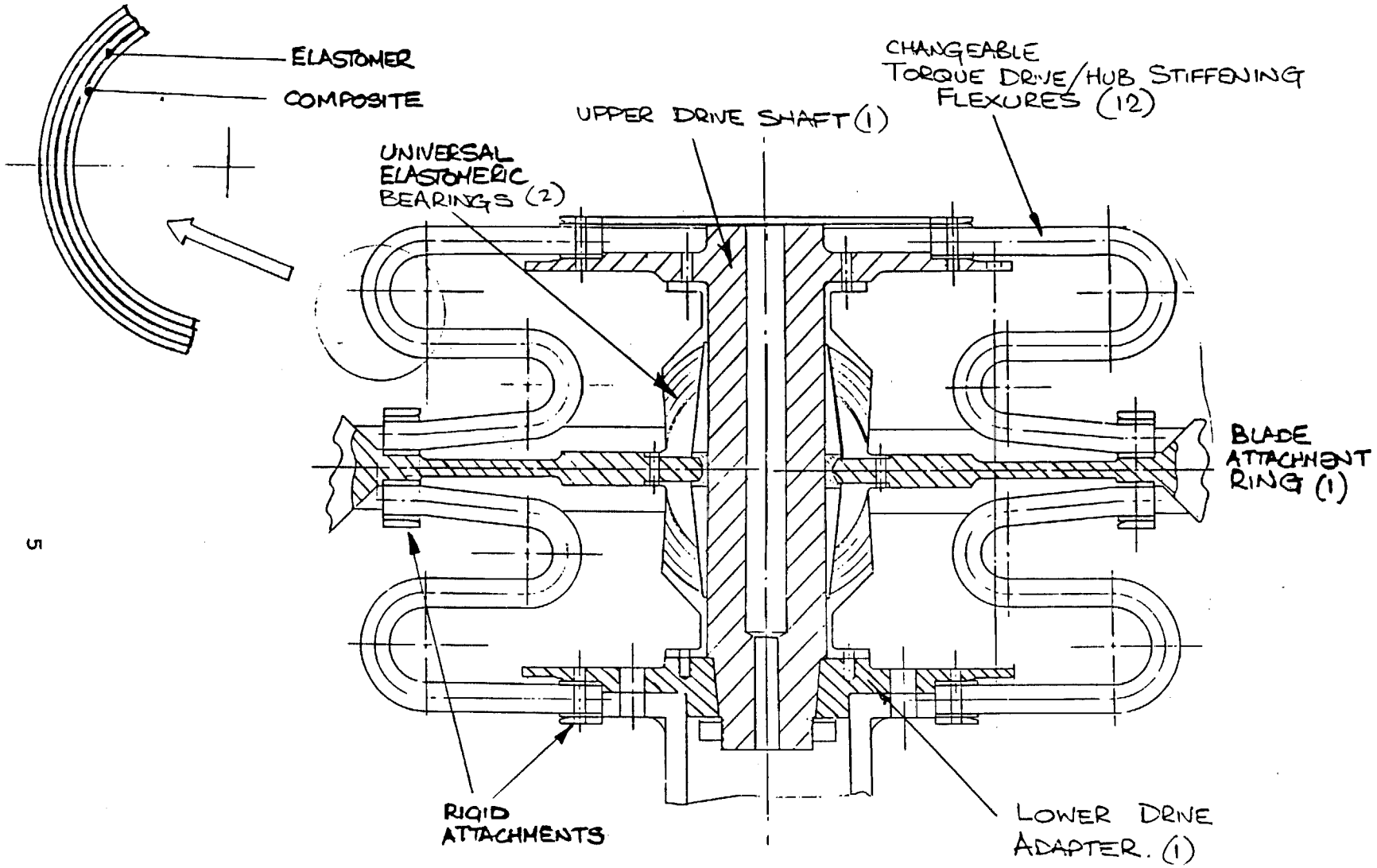

- F/E - Elastomer Composite Torque Drive/ Hub Stiffening Flexures
- Universal Elastomeric Thrust Bearings
- 17 Non-Standard Parts

Figure 3. Soft Hub with Fiber Epoxy/Elastomer Composite Hairpin Flexures

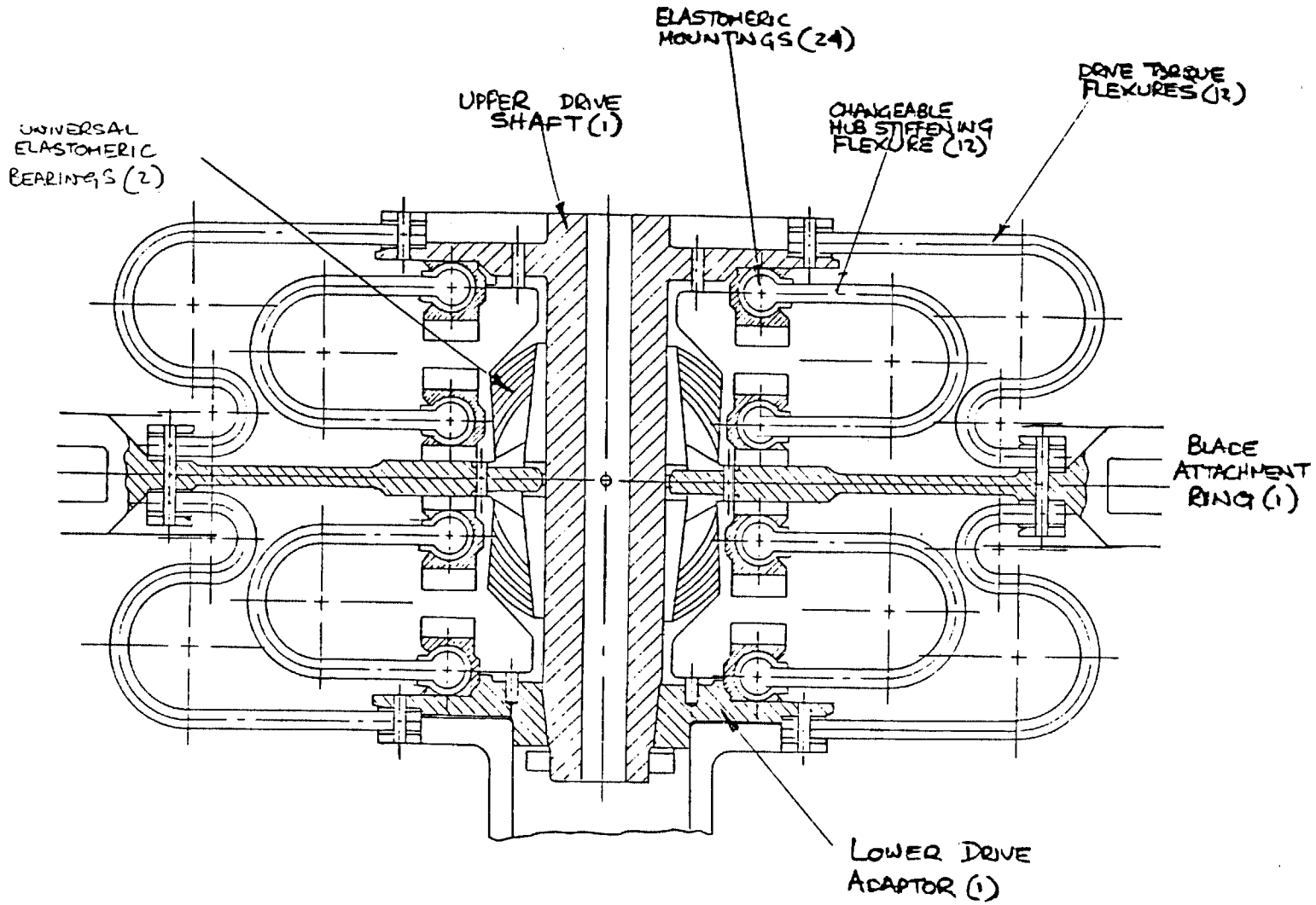

- Universal Hub - Changeable Composite Stiffening Flexures
- Universal Elastomeric Thrust Bearings
- Composite Torque Drive Flexures
- 53 Non-Standard Parts

Figure 4. Soft Hub with Torque Drive Flexures and Hub Stiffening Flexures

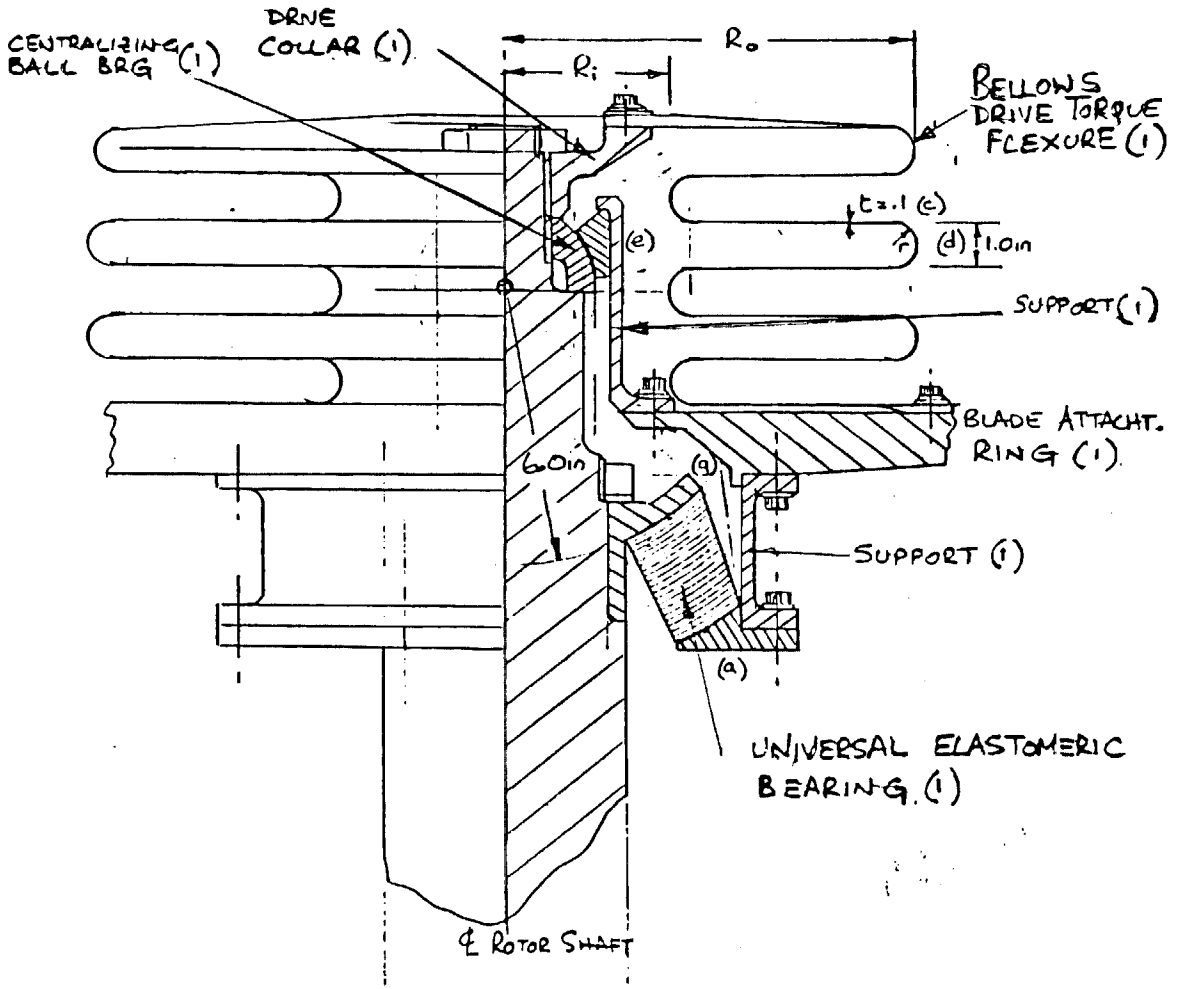

- F/G Composite Bellows Torque Drive Flexure
- Universal Elastomeric Thrust Bearings
- 7 Non-Standard Parts

Figure 5. Soft Hub with One Bellows Drive Torque Flexure

Through analysis, each of the four systems were shown to exhibit their own advantages and disadvantages and these are discussed herein.

Mathematical tools for analyzing a bellows, convolute, and hairpin section flexure therefrom were generated under this program. All degrees of flexural freedom were considered which enable the investigators to identify and improve upon the disadvantaged features of a concept and capitalize the promising ones.

3.0 A SOFT HUB WITH HUB STIFFENING AND TORQUE DRIVE FLEXURES

3.1 GENERAL DESCRIPTION

This hub concept (see Figure 4) is intended to suit a range of helicopter sizes and types. The gymbal is a dual spherical elastomeric bearing between which is sandwiched a horizontal disc which supports the rotor blades and root articulation systems at its perimeter. These elastomeric bearings, besides providing the tilt freedom, also transmit the rotor thrust from the disc to the rotor shaft. They are not critical in the design and are not analyzed herein since they are under-utilized and state-of-the-art.

The key features of this system are (a) the hub stiffening flexures which are changeable to a size required according to the helicopter application and (b) additional torque drive flexures which are stackable laminates separated by elastomeric to allow each laminate to act as a single beam when required to flex as the hub tilts. The number of these laminates within the torque drive flexure is changeable according to the helicopter application.

To allow the hub stiffening flexure to bend according to hub tilt requirements without experiencing excessive fiber strains, each end of this flexure is mounted in an elastomeric frictionless bearing which permits normal end rotations which are approximately twice the magnitude of the hub tilt. Detail design of these attachments is to be included in any Phase II effort of this program.

Appendix 3 discusses the options for stiffening flexure installation and concludes that if the pinned open end of the hairpin is towards the shaft (i.e., normal) then more hub stiffness can be achieved without an increase in flexure strain. This is the configuration chosen for this concept.

3.2 ASSESSMENT OF THE HUB STIFFENING FLEXURE

Figure 6 shows a U-shaped hairpin flexure element for varying the hub stiffness in the soft hub concept shown in Figure 4. To best use the available space and produce the required stiffening effect, the flexure is tapered in width similar to a sector of a bellows convolute.

To avoid the high flexural strains at the ends of the hairpin due to end fixity, they are attached to the hub hardware through cylindrical elastomeric bearings which allow the ends to rotate as the hub is tilted.

With reference to Figure 6, typical dimensions of the flexure are:

length of straight portion	(ℓ)	= 2.65 in.
mean radius of the outer end	(r)	= 1.50 in
width at the outer end	(b)	= 4.20 in.
width at the inner end	(b_1)	= 1.60 in.
radial position of the inner attachment	(d)	= 3.50 in.

3.2.1 Flexure Deflection (Δ) Due to Hub Tilt (ϕ)

Total deflection (Δ) consists of two parts, (Δ_1) for a constant width flexure ($b_1 = b$) and (Δ_2), the additional deflection due to the width taper thus;

$\Delta = \Delta_1 + \Delta_2$, but $\Delta = d \sin \phi$, where (ϕ) is the hub tilt angle.

Figure 7 presents views of the flexure for which the equations relating deflection (Δ) to applied shear load (P) material modulus (E) and flexure geometry have been derived in Appendices 3 and 4.

FOR CONSTANT WIDTH FLEXURE DEFLECTION $\Delta_1 = \frac{2*P}{EI_o}\left[\frac{\ell^3}{3} + r\left(\frac{3}{2}\ell^2 + \frac{\pi}{4}r^2 + 2\ell r\right)\right]$ FROM APPENDIX 4,

$= 74.65 * \frac{P}{EI_o}$ WHERE $EI_o = E * \frac{b * t^3}{12}$

ADDITIONAL DEFLECTION FROM TAPER, IF $b_1 = 1.6$, FROM APPENDIX 5, (APPROXIMATION)

$\Delta_2 = \frac{2}{3} * \frac{P}{EI_o}\left(\ell + \frac{\pi r}{2}\right)^3 * \frac{1}{3}\left(1 - \frac{b_1}{b}\right)$

$= 11.51 * \frac{P}{EI_o}$

TOTAL DEFLECTION IS: $\Delta = \Delta_1 + \Delta_2 = 86 * P/EI_o$

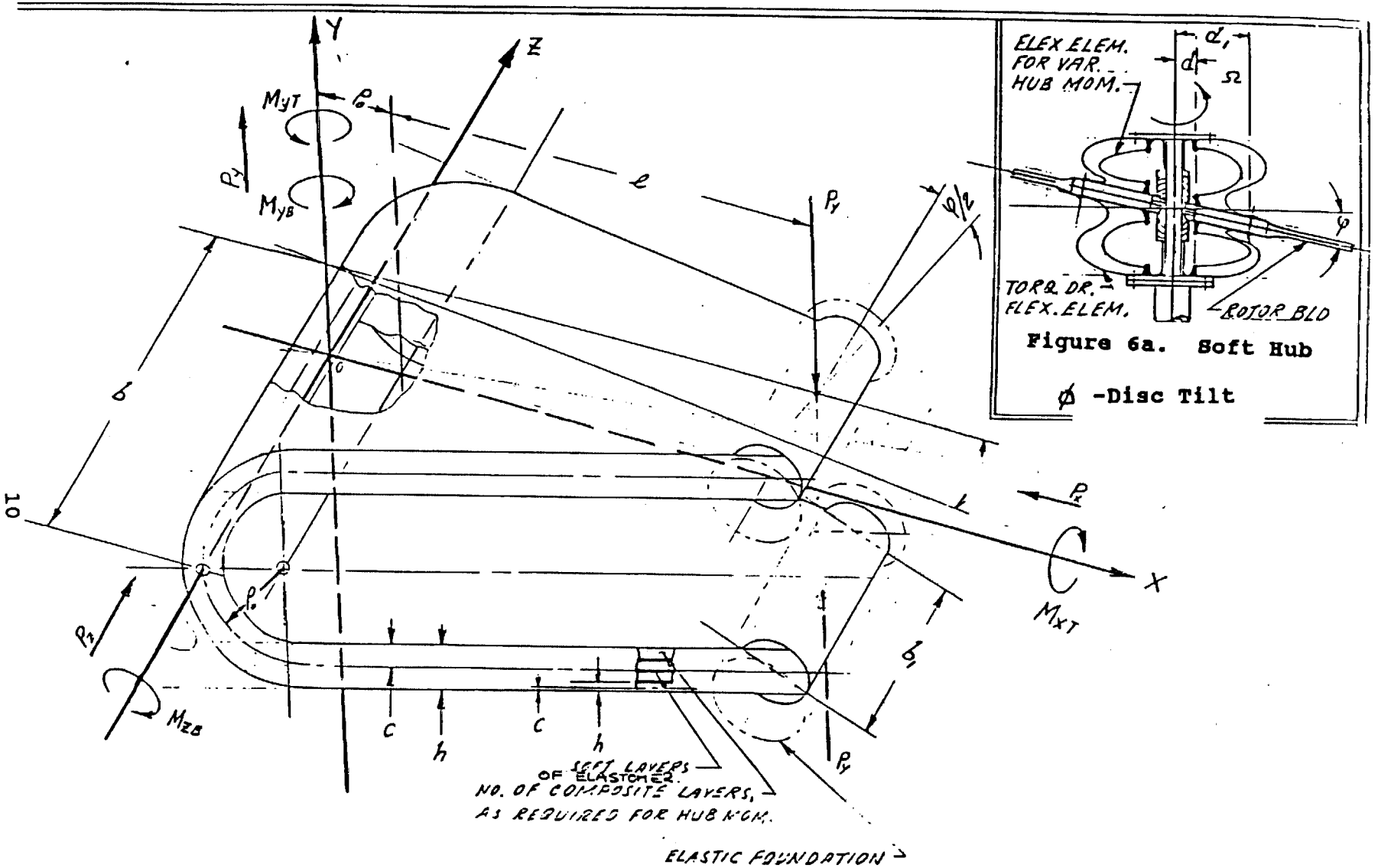

Figure 6. Soft Hub Flex Element for Variable Rotor Hub Moment Stiffness

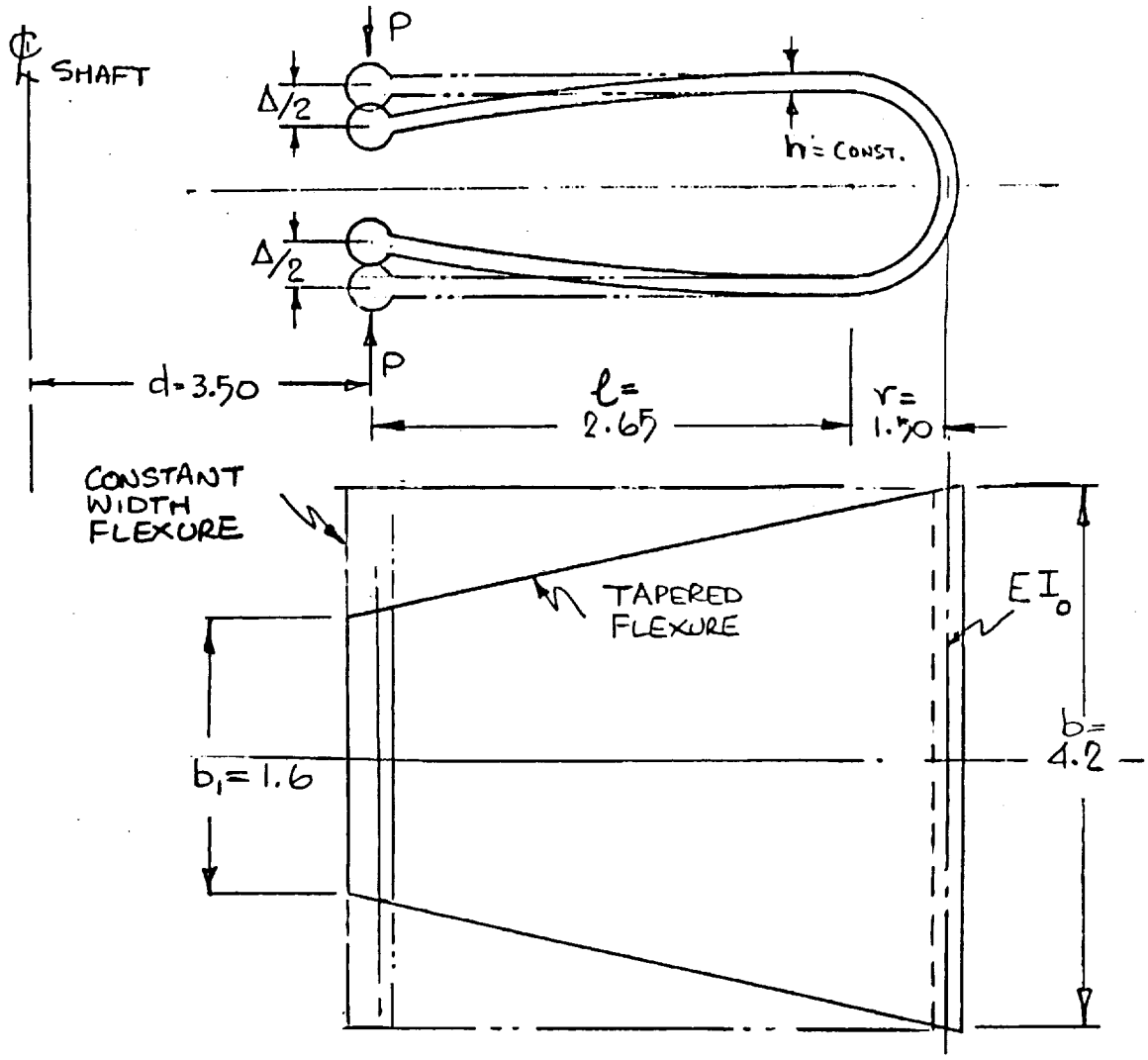

Figure 7. Geometry of the Hub Stiffening Flexure

This total deflection can be related to hub tilt (ø) through the equation:

$$\Delta = 3.5 \sin \phi = \frac{86P}{EI_o}$$

then

$$EI_o = \frac{24.57P}{\sin \phi}; \text{ or } \quad P = .0407\ EI_o * \sin \phi$$

3.2.2 Maximum Alternating Bending Stress (@ x = 0)

The maximum alternating bending moment (M_{ZB}) will occur at point 0 (x = 0) in the Figure 6. The maximum bending stress,

$$\sigma_b = \frac{M_{ZB} * E_c * c}{EI_o} \text{ p.s.i.}$$

where (E) is the elastic modulus of the critical fiber and (c) is the location of the critical fiber from the neutral axis of bending.

$M_{ZB} = P\ (\ell + r) = 4.15P$ in. lb.
$E_c = 6.5 * 10^6$ psi (for fiberglass 1002-S2)
$E_{eg} = E = 5.5 * 10^6$ psi (0° F/G + ±45° GR. Fabric)

The allowable alternating stress $\sigma_b = \pm 12{,}000$ p.s.i., then

$$\text{(a)} \quad c_{max} = \frac{12000 * 24.57 * P}{4.15 * P * 6.5 * 10^6} * \frac{1}{\sin \phi} = \frac{.01093}{\sin \phi} \text{ in}$$

Flexure thickness $h_{max} = 2 * c_{max} = \frac{.0219}{\sin \phi}$ in

then,

$$\text{(b)} \quad I_o = \frac{bh^3}{12} = \frac{4.2 * 10.45 * 10^{-6}}{12 * \sin^3 \phi} = \frac{3.66 * 10^{-6}}{\sin^3 \phi} \text{ in}^4$$

$$\text{(c)} \quad EI_o = \frac{20.11}{\sin^3 \phi} \text{ lb in}^2$$

$$\text{(d)} \quad P = \frac{M_{ZB}}{415} = \frac{.818}{\sin^2 \phi} \text{ lb}$$

The stiffness of one flexure (k) is:

$$(e)\quad k = \frac{P}{\Delta} = \frac{.2337}{\sin^3 \phi} \text{ lb/in}$$

3.2.3 Contribution to Hub Stiffness

If the number of flexures (= N) in each of both the upper and lower hub are evenly distributed azimuthially around the hub then the spacing of each is (2 π /N) RADS

Then about the axis y, each flexure attachment is at a moment arm $d_n = d * \cos(2\pi * n/N)$ $n = 0 \rightarrow (N - 1)$.

The displacement Δ, however, is also reduced proportionately since $\Delta_n = \Delta * \cos(2\pi * n/N)$ as is the flexure load P where $P_n = P * \cos(2 \quad n/N)$.

The contribution to total hub stiffness (K_H) is M_H/ϕ where

$$\frac{M_H}{\phi} = \frac{P * d}{\phi} * \quad \cos^2(2\pi . n/N) \qquad \text{in. lb./RAD}$$

Note:

- all flexures contribute to stiffness, independent of which side of the axis they are located
- an equal number of stiffeners are located above and below the hub plate.

If d = 3.5 in and N = 1/2 total number of hub stiffening flexures, hub moment stiffness

$$(f)\ K_H = (3.5 * N * P)/\phi \text{ in. lb./RAD} \quad (N \geq 3).$$

3.2.4 Selection of Flexure Quantity and Thickness

For a desired hub stiffness $K_H = ((N * P * d)/\phi)$ to suit a particular helicopter application and endurance limit of hub tilt (ϕ) the equations (d) and (f) become:

$$(f)\quad K_H = \frac{3.5 * N * P}{\phi} \text{ in. lb./RAD where } (d)\quad P = \frac{.818}{\sin^2 \phi} \text{ lb.}$$

For small angles of tilt when $\sin \phi \approx \phi$,

$$K_H = 2.86 * N/\phi^3$$

or

$$(g) \quad N = .35 * K_H * \phi^3$$

For example: for a 5000 lb. G.W. helicopter, the desired hub moment stiffness = 700 ft. lb./deg. Allowing 25% of this to be available from the elastomeric bearing, etc., and for a desired endurance hub tilt of $\pm 8°$ (= ø) then the number of flexures required in the hub, based upon a hub stiffness contribution of .75 * 700 * 12 = 6300 in. lb./deg. is obtained:

$$2N = 2 * 6300 * .35 * (8°/57.3)^3$$

$$2N = 12 \text{ Flexures (6 upper and 6 lower)}$$

Flexure thickness (h) is given by equation (a)

$$h = 2 * c = \frac{.0219}{\sin \phi}$$

$$h = .156 \text{ in.}$$

3.2.5 Conclusion

For a BO-105 size of soft hub shown in Figure 4 with a stiffness of 700 ft. lb./degree of hub tilt, 12 flexures are required. To achieve unlimited life at an endurance limit hub tilt of $\pm 8°$, the flexures must be no thicker than .156 inches if made in fiberglass epoxy and they must be support in attachments which will permit end rotation.

3.3 ASSESSMENT OF THE TORQUE DRIVE FLEXURE

Figure 8 shows a double-U hairpin flexure for transmitting the shaft drive torque to the hub. It is fixed at A to the drive shaft and at B to the Blade Attachment ring which is free to tilt about the hub center on the shaft axis. Contrary to the requirements for the hub stiffening flexure, bending stiffness is not a requirement for the torque drive flexure, however, it must still be able to withstand the cyclic tilting motions of the hub. This torque flexure is constructed of thin fiberglass epoxy laminates separated by layers of elastomeric rubber material to allow the laminates to flex as independent elements. This feature will allow the ends of the hairpin to be rigidly attached without the complexity of elastomeric mountings to permit flexure end rotation as is necessary for the hub stiffening flexures shown in Figure 4.

Typical dimensions of this flexure are given in Figure 9.

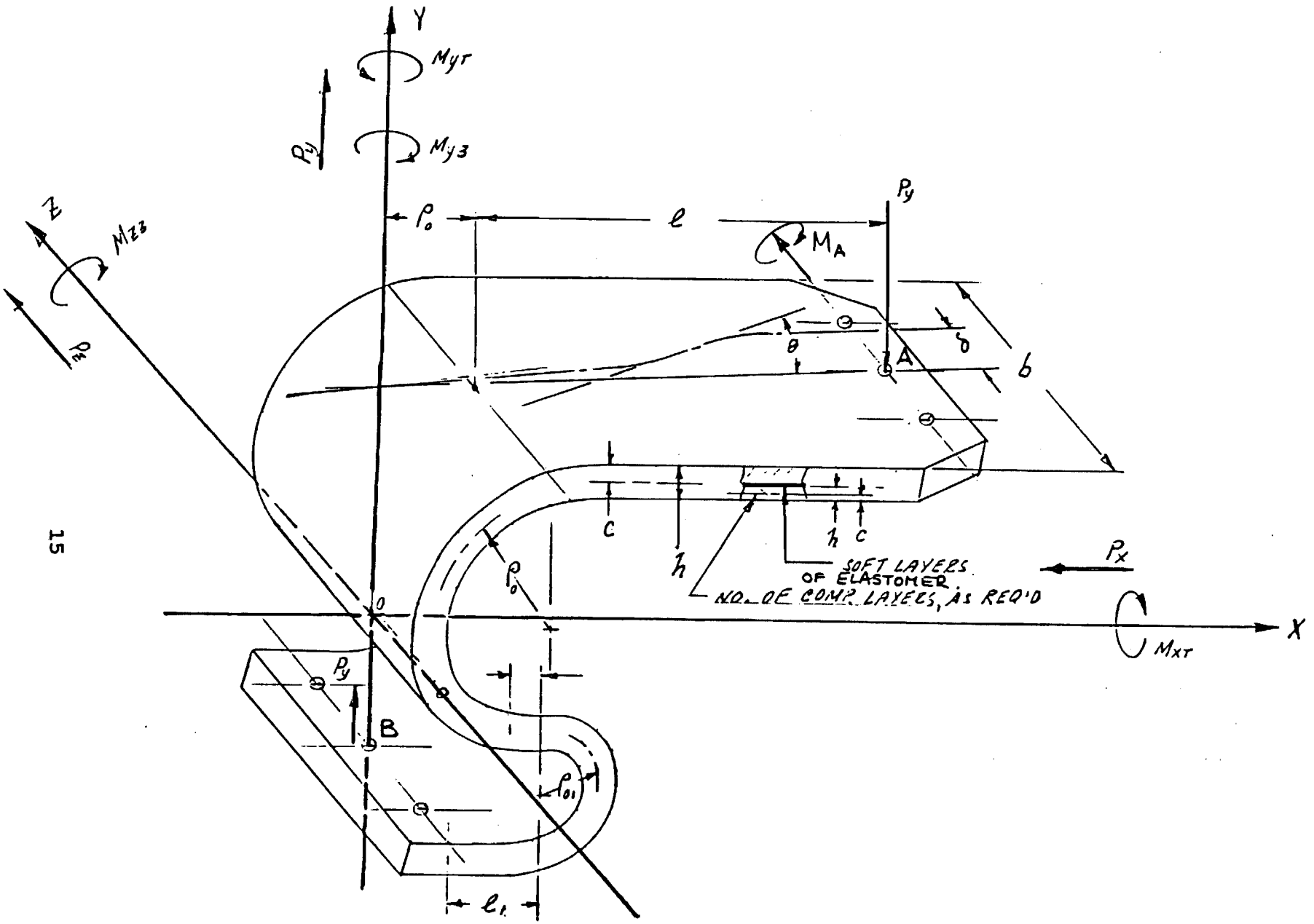

Figure 8. Soft Hub Torque Drive Flex Element

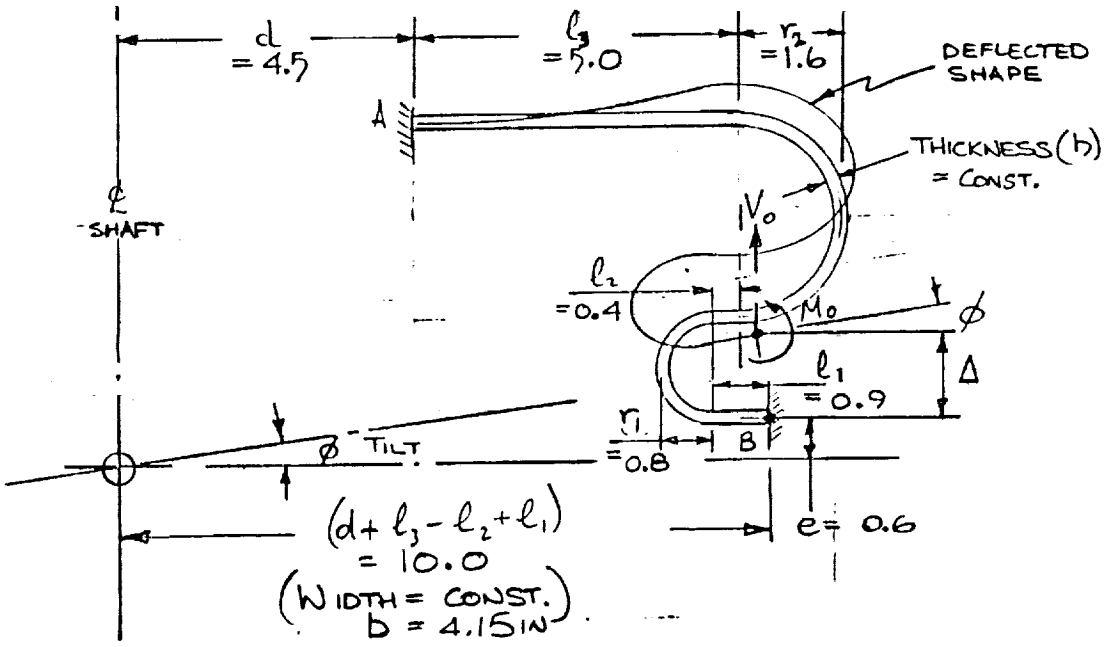

Figure 9. Torque Flexure Dimensions

3.3.1 Flexure Deflection (Δ) Due to Hub Tilt (ø)

Using the strain energy method of Appendix 4, the displacements at B due to applied shear (V_o) and end moment (M_o) have been determined.

FOR CONSTANT (WIDTH, EI) FLEXURE FROM APPENDIX 4

DEFLECTION $\Delta = (d + \ell_3 - \ell_2 + \ell_1)\sin\phi$. and $\ell = (\ell_1 - \ell_2) = 0.5$

$$= \frac{M_o}{EI}\left[\frac{\ell_1^2 - \ell_2^2 + \ell_3^2}{2} + 2(r_1^2 - r_2^2) + \pi(\ell_1 r_1 + \ell r_2) + \ell_1\ell_2 + \ell\ell_3\right]$$

$$+ \frac{V_o}{EI}\left[\frac{\ell_1^3 + \ell_2^3 + \ell_3^3}{3} + \pi\left(\frac{r_1^3 + r_2^3}{2}\right) + \pi(\ell_1^2 r_1 + \ell^2 r_2) + 4(\ell_1 r_1^2 - \ell r_2^2) + \ell_1^2\ell_2 + \ell^2\ell_3 - \ell_1\ell_2^2 + \ell\ell_3^2\right].$$

$$\Delta = \frac{1}{EI}\left[16.58\,M_o + 50.72\,V_o\right] = 10.\phi \qquad \text{——— (1)}$$

and SLOPE ϕ

$$= \frac{M_o}{EI}\left[(\ell_1 + \ell_2 + \ell_3) + \pi(r_1 + r_2)\right]$$

$$+ \frac{V_o}{EI}\left[\left(\frac{\ell_1^2 - \ell_2^2 + \ell_3^2}{2}\right) + \pi(\ell_1 r_1 + \ell r_2) + 2(r_1^2 - r_2^2) + \ell_1\ell_2 + \ell\ell_3\right]$$

$$\phi = \frac{1}{EI}\left[13.83\,M_o + 16.58\,V_o\right] \qquad \text{——— (2)}$$

FOR SMALL DEFLECTIONS, WHERE $\phi = \sin\phi$

By EQUATING (1) & (2).

(a) $M_o = .27 * EI * \phi$ (b) $V_o = .28 * EI * \phi$

3.3.2 Maximum Bending Moment

This will occur at the fixed end A or B

At A, Bending Moment = $5.5 * V_o + M_o = 1.27\ EI * \phi$
At B, Bending Moment = $M_o = -.27\ EI * \phi$

The maximum stress must occur at attachment A where the bending moment is

(c) $M_A = 1.27 * EI * \phi$ or $M_A/EI = 1.27\phi$

3.3.3 Maximum Stress

The prime function of these flexures is the transmittal of the shaft torque to the rotor hub. the design fatigue bending endurance limit stress is selected at $\sigma_e = \pm 2600$ psi to leave enough torque (shear) carrying capacity.

3.3.4 Maximum Thickness of Each Laminate

These flexures will likely be fabricated from ±45° biased 1002S fiberglass reinforced epoxy which has a modulus of $E = 1.6 * 10^6$ psi.

For a laminate thickness (h) = $2 * EI/M_A * \sigma_e/E$

(d) $$h_{max} = \frac{2 * e}{1.27} * \frac{1}{E * \phi} = \frac{.00255}{\phi} \text{ ins./RADIAN}$$

For $\phi = \pm 8°$ ($\pm .14$ RADS) $h_{max} = .018$ ins.

3.3.5 Number of Laminates Required to Carry Drive Torque (My_t)

Maximum shear stress in the flexure due to drive torque will occur where radius (d) is a minimum (i.e., at end A). If N_T is the total number of drive torque flexures, of which one half is above and the other below the blade attachment ring, then the shear load (P_Z) carried by one flexure is given by

(e) $$P_Z = \frac{My_T}{d * N_T} \text{ lb } (d = 4.5 \text{ in})$$

If the steady allowable shear stress in ±45° S2 F/G = 17,000 psi, then the number of laminates required in the flexure is

(f) $$n = \frac{P_Z}{17000 * b * h_{max}}$$ where (b) is flexure width (4.15")

For the BO-105 with 800 S.H.P. at 425 rpm, Design Torque (My_T) at 90% rpm is 11000 ft. lb.

Then from (e) and (f)

$$P_Z = \frac{29333}{N_T} \text{ lb} \quad \text{and} \quad n = \frac{23}{N_T} \text{ laminates}$$

If N_T = 8 flexures are used (i.e., four upper and four lower), then at least three laminates of .018 thickness are required in each flexure to transmit the shaft drive torque.

3.3.6 Finite Element Analysis of the Torque Drive Flexure

The torque drive flexure capabilities have been analyzed using MSC.PAL No. 2 software on an IBM-PC AT. Figure 10 shows the model with 21 nodes, node 21 is attached to the tilting blade attachment ring and node 1 is fixed to the rotor shaft ground. In Table I, Case 1 presents the results for zero horizontal restraint (H_o = 0) at node 21 which roughly confirms the previous strain energy analysis, and Case 2 presents the more exact case where the horizontal displacement is controlled by the hub tilt.

TABLE I. TORQUE DRIVE FLEXURE ANALYSIS

LOAD	S.E. METHOD	MSC.PAL No. 2 ANALYSIS	
		CASE 1	CASE 2
$Vo/EI * \phi_{(21)}$	.28	.201	.265
$Ho/EI * \phi_{(21)}$	0	0	-.179
$Mo/EI * \phi_{(21)}$	-.27	-.167	.307
$V/EI * \phi_{(1)}$	-.28	-.201	-.265
$H/EI * \phi_{(1)}$	0	0	.179
$M/EI * \phi_{(1)}$	-1.27	-.936	-.908

(xx) Node

A comparison of the end moments at node 21 for Case 1 and 2 indicates that the horizontal restrain (translational shear rigidity) is very significant in the derivation of the stress distribution, however, it has not affected the critical moment at Node 1.

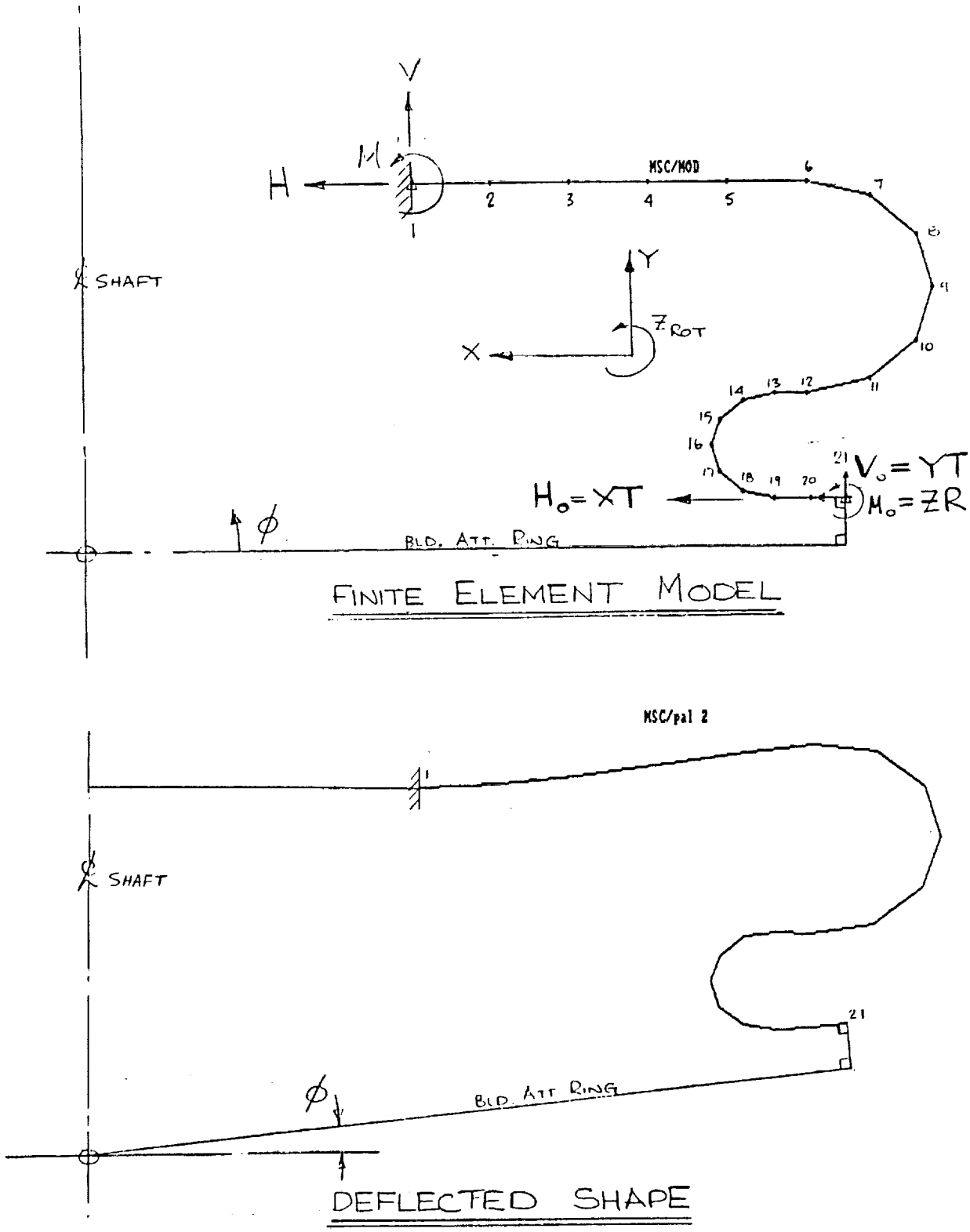

Figure 10. Finite Element Analysis of the Torque Drive Flexure

3.3.7 Conclusion

This method of transmitting drive torque from the rotor shaft to the hub is feasible, however, a more rigorous structural analysis is required which includes

(a) the effects of the separating layers of elastomer

(b) clamping each laminate together at the end attachments

(c) flexure stability.

Discussions with the elastomeric bearing experts (e.g., Lord Corporation) must be made to define the best fabrication procedure and confirm the feasibility of the application.

3.4 ELASTOMERIC MOUNTINGS

The elastomeric mountings at the flexure end have to provide two(2) degrees of rotation as shown in Figure 11.

(1) To accommodate a flexure end rotation due to end slope due to bending

(2) Rotation about a vertical axis normal to the axis defined in (1) due to the horizontal translation of the flexure end (Δh) due to its attachment to the hub drive plate being offset vertically by a dimension (μ).

3.4.1 Radial Bearing

The radial elastomeric journal for rotation (1) above can be sized according to the "LORD" design manual as follows:

With reference to Figure 11 which shows

Flexure thickness (h) = .156 in

Selected end diameter = 3 * (h) = .468 in

With a vertical offset u = 1.25 in sufficient to preclude flexure bottoming for ø = 8° of hub tilt; from Figure 11, the resulting flexure rotation in mounting = 1.63 * ø. For a bearing life of 2000 hours and rotor rpm of 425, the allowable shear strain in the rubber,

$e_s = 1100/\sqrt[5]{2000 * 60 * 425}$ cycles

$= 31.6\%$

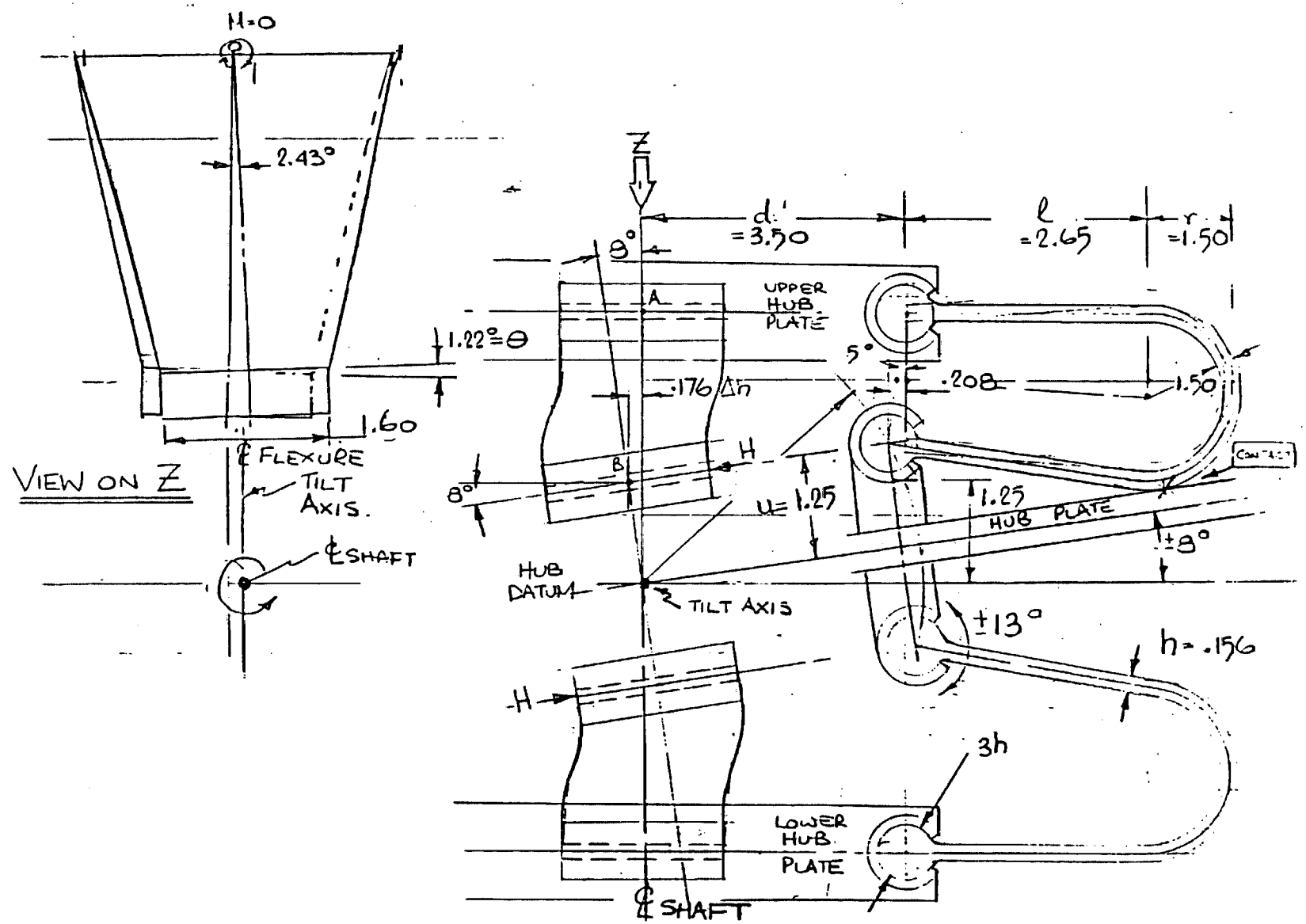

Figure 11. Bending and Lateral Displacement of Hub Stiffening Flexures Due to Hub Tilt

The minimum radial thickness of the elastomer (T_R) becomes

$$T_R = Do * \phi/2 * 3_s$$

$$= (\phi * Di)/(2 * (e_s - \phi))$$

$$= (3 * h * \phi)/(4 * (e_s - \phi))$$

$$T_R = .10 \text{ in.}$$

3.4.2 Shear Pad

To allow for the rotation of (2) the rubber of the elastomeric bearing to accommodate (1) must be able to compress and extend radially to allow for the cocking. The "LORD" handbook limits the compressive fatigue strain to 1%.

For a 1.6 inch wide bearing and a cocking of $\pm 1.22°$ shown in Figure 11, the minimum thickness of elastomer in the radial bearing must be

$$T_{R_{min}} = \frac{1.22}{57.3} * \frac{1.6}{2} * \frac{1}{.01} = 1.70 \text{ in}$$

This thickness of elastomer would make the size of the radial bearing impractical, therefore, another solution has to be found for the cocking rotation.

The most promising is to sandwich the radial bearing between flat elastomeric pads which will allow the cocking rotation as illustrated in Figure 12.

For shear pad dimensions of 1.6 inch * 3h, a displacement $\theta = \pm 1.22°$, and a fatigue life of 2000 hours as before, we can determine the minimum shear pad elastomer thickness (T_S).

$$T_S = \theta * R/e_s \text{ where } R^2 = (1.6/2)^2 + (3/2 * h)^2 = .833 \text{ in.}$$

$$T_S = .06 \text{ inch}$$

3.4.3 Conclusion

The elastomeric mounting is a feasible solution to the problem of supporting the flexure ends and allowing the rotation from flexure cocking. Total depth of the bearing, which includes upper and lower base plates (2 * 0.10 in.), shear pads (2 * .06 in.), radial bearing housing (2 * 0.05 in.), and elastomer (2 * .10 in.). The flexure socket (2 * .06) and flexures (3 * .156 in.) for this particular application would be 1.208 in. which is compatible with the hub stiffening flexure end radius and also the mounting offset (μ) from the hub center plane.

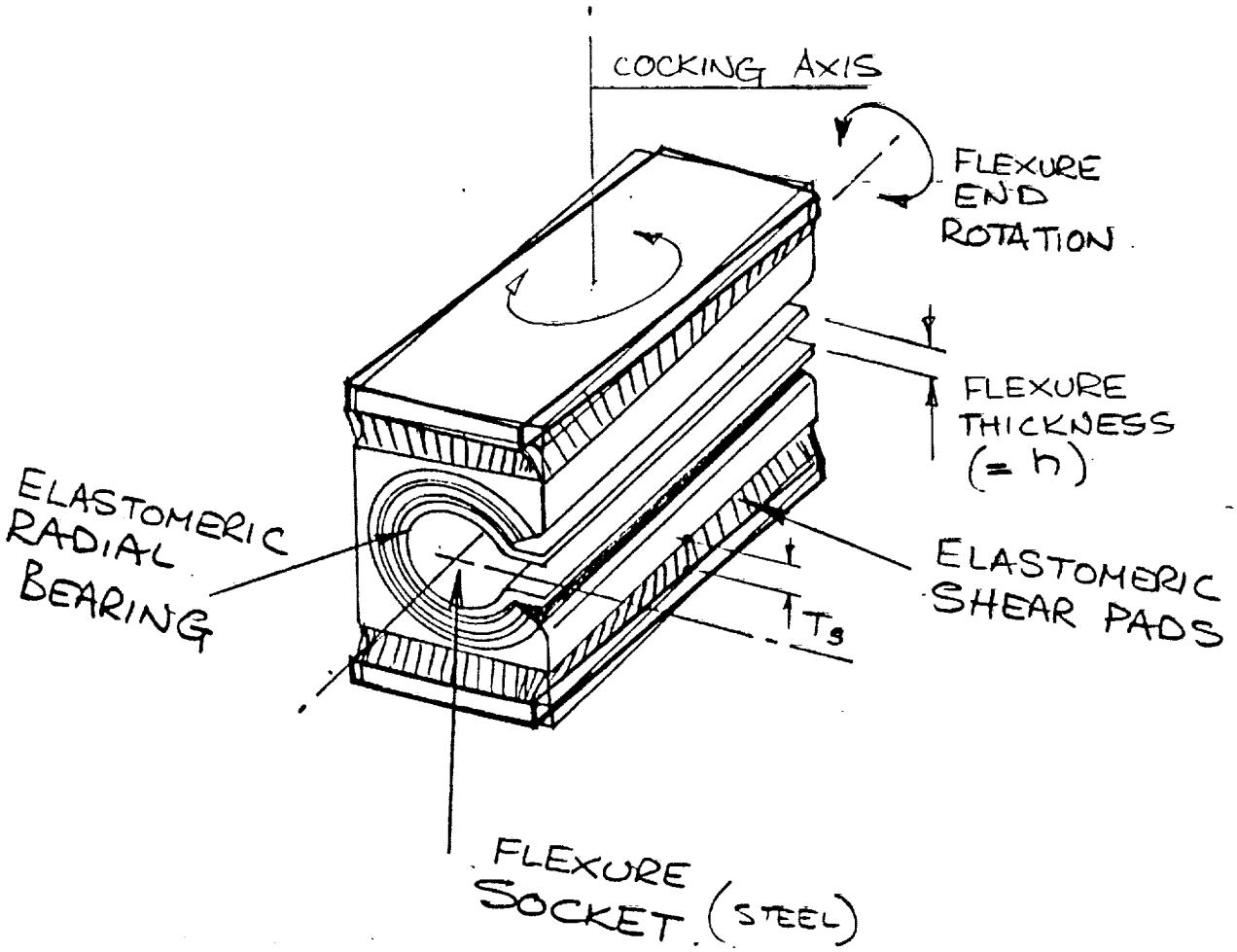

Figure 12. Elastomeric Mountings

3.5 WEIGHT, DRAG, AND VULNERABILITY

Estimates of these characteristics have been based upon the hub only above the shaft attachment and exclusive of the rotor blades, root flexures, and pitch control system

3.5.1 Weight

A component breakdown of this concept is as follows:

Item	Qty.	Wt. Ea. (lb. est.)	Total (lb. est.)
Upper Drive Shaft	1	34.5	34.5
Drive Torque Flexures	8	.55	4.4
Attachment Hardware	16	.11	1.8
Hub Stiffening Flexures	12	.35	4.2
Elastomeric Mountings	24	.44	10.6
Univ. Elast. Bearing	2	14.30	28.6
Blade Attachment Ring (T_L)	1	95.27	95.3
Lower Drive Adapter	1	19.40	19.4
Lower Nut and Washer	1	1.80	2.8
			200.6

Total weight is estimated as 200.6 lb.

3.5.2 Drag

Flat plate area is estimated at 2.43 ft^2.

3.5.3 Vulnerability (and Fail Safety)

With the exclusion of the Drive Shaft and Blade Attachment Ring, no single component failure or damage will result in loss of the aircraft. The Upper Drive Shaft and Blade Attachment Ring could be damaged by an armor piercing projectile but are of a size that, if struck, could survive through mission completion and return to base.

Area of these components is .96 ft^2 of 39% of the total projected area.

3.6 COST, RELIABILITY AND MAINTAINABILITY

3.6.1 Cost

A rough order of magnitude cost for quantity production has been derived as follows:

Item	Qty.	$ Each (est.)	$ Total (est.)
Upper Drive Shaft	1	4,000	4,000
Drive Torque Flexures	8	1,000	8,000
Attachment Hardware	16	25	400
Hub Stiffening Flexures	12	1,000	12,000
Elastomeric Mountings	24	2,500	60,000
Univ. Elast. Bearing	2	10,000	20,000
Blade Attachment Ring (T_L)	1	25,000	25,000
Lower Drive Adapter	1	300	300
Lower Nut and Washer	1	50	50
			129,750

3.6.2 Reliability

Fatigue life goal of the elastomeric bearings is 2000 hours but all other components have been designed for a safe life in excess of 10,000 hours. The elastomeric mountings for the Hub Stiffening Flexures are expected to be the least reliable followed by the Torque Drive Flexures since these are the most complex components to design and fabricate.

3.6.3 Maintainability

Negligible maintenance is required since there are no rolling element bearings. NDT of the flexures should be conducted every 500 hours to detect composite and/or elastomeric delamination. Distress of the elastomer bearings can be noticed by visual inspection, as required. All critical components can be visually inspected without disassembly of the hub.

4.0 A SOFT HUB WITH TORQUE DRIVE BELLOWS FLEXURE

4.1 GENERAL DESCRIPTION

Figure 13 shows a gymballed hub concept which utilizes a horizontal blade attachment ring centered about the rotor shaft through a fibroid lined spherical ball bearing. Rotor thrust is transmitted from the blade attachment ring to the rotor shaft through a single universal spherical elastomeric bearing which provides some elastic restraint against the tilting motion of the hub around the spherical ball. Drive torque is transmitted from the shaft to the blade attachment ring through a fiber reinforced polymer bellows which, due to its bending flexibility, allows the hub to tilt without incurring excessive flexural stresses.

A most important feature of this system is that the bellows is centered about the hub gymbal bearing which allows the bellows to tilt freely with minimum strain. Appendix 2 explains the logic behind this approach. Bellows wall thickness is sized to

accommodate the rotor torque and convolute diameter and number is sized by allowable material strain under the hub tilting motions. The resulting tilting resistance of the bellows is complemented by the cocking stiffness of the elastomeric bearing, to produce the target hub stiffness required by the Design Criteria and Specifications in Appendix 1.

The concept shown in Figure 13 requires (a) sizing of the elastomeric bearing to accommodate the rotor thrust, (b) sizing of the bellows wall thickness to take the rotor drive torque, (c) determining the number of bellows elements required to allow hub tilt without exceeding the material flexural strength, and (d) ensuring that the wall thickness and bellows element end radius is such that interlaminar tension failure in the laminated composite material does not occur.

Other features that need to be added are (e) a pre-compressing arrangement around the elastomeric bearing that will maintain an interlaminar compressive stress under negative thrust conditions, AND (f) mechanical tilting stops that do not result in shearing of the elastomeric bearing.

The additions (a) through (f) have been illustrated in Figure 13.

4.2 THE ELASTOMERIC BEARING

Figure 14 shows the schematic of a universal elastomeric thrust bearing. The inside diameter (1/D) is essentially sized by the shaft diameter which, in turn, is sized by the required hub moment. The Design Criteria and Specifications of Appendix 2 requires a hub stiffness of 700 ft. lb/deg and a design tilt of $\pm$ 8°. Design hub moment is therefore 5,600 ft. lbs (67,200 in. lbs).

The shaft minimum diameter is sized in high grade steel (ftu 180,000 psi). With a fatigue design allowable of $\pm$25,000 psi and K_T = 3, minimum shaft diameter (1/D) and corresponding inside diameter of the bearing is:

$$\text{Minimum I/D} = \left(\frac{32*67,200*3}{*25,000}\right)^{1/3} = 4.4 \text{ inches}$$

Using a 2g thrust of 10,000 lb and a bearing stress of 5,000 psi, the outside diameter (O/D) is

$$\text{Minimum O/D} = \left(\frac{4x10,000}{*5,000} + 4.4^2\right)^{1/2} = 4.7 \text{ inches}$$

Thrust capacity is not very influential in sizing this bearing. The bearing annular width will be sized for stability but could be increased to provide hub stiffness.

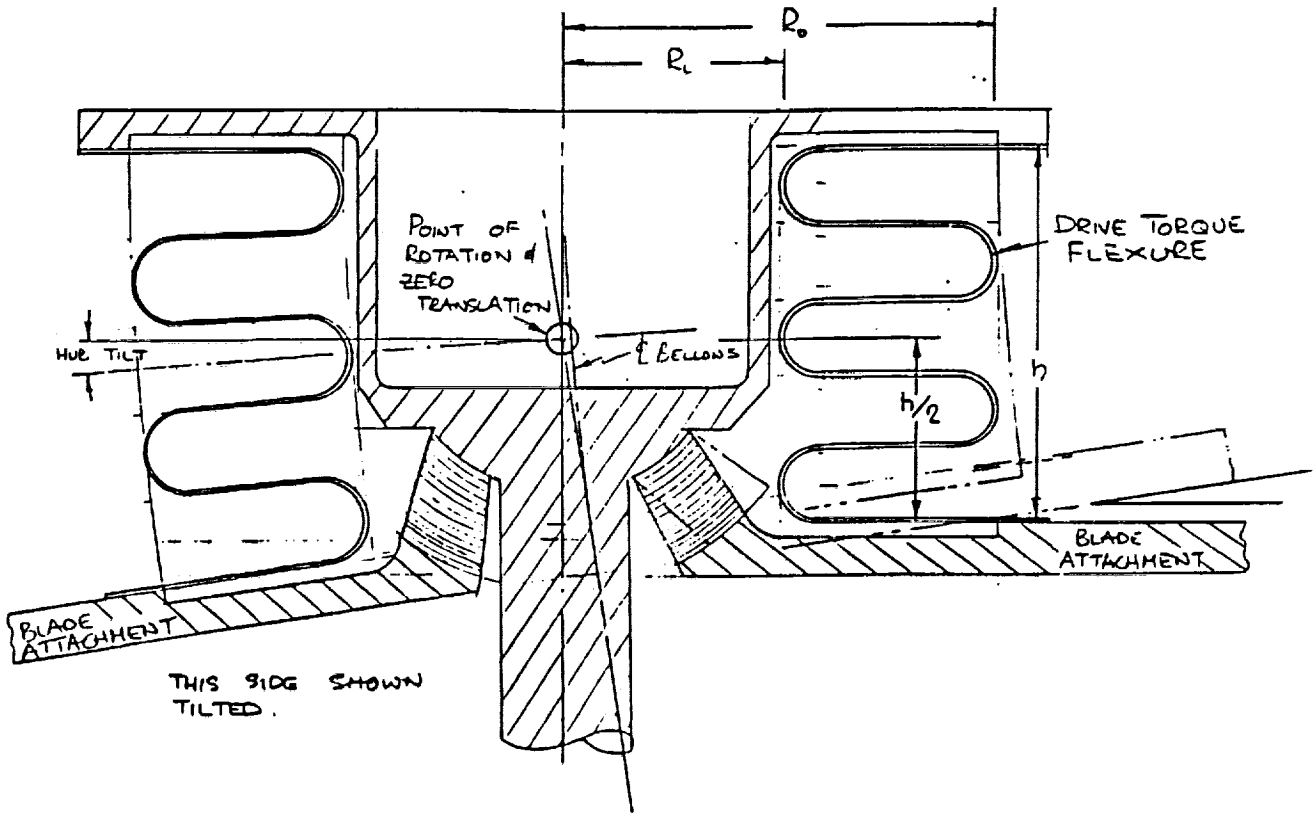

Figure 13. Soft Hub Concept with Torque Drive Bellows

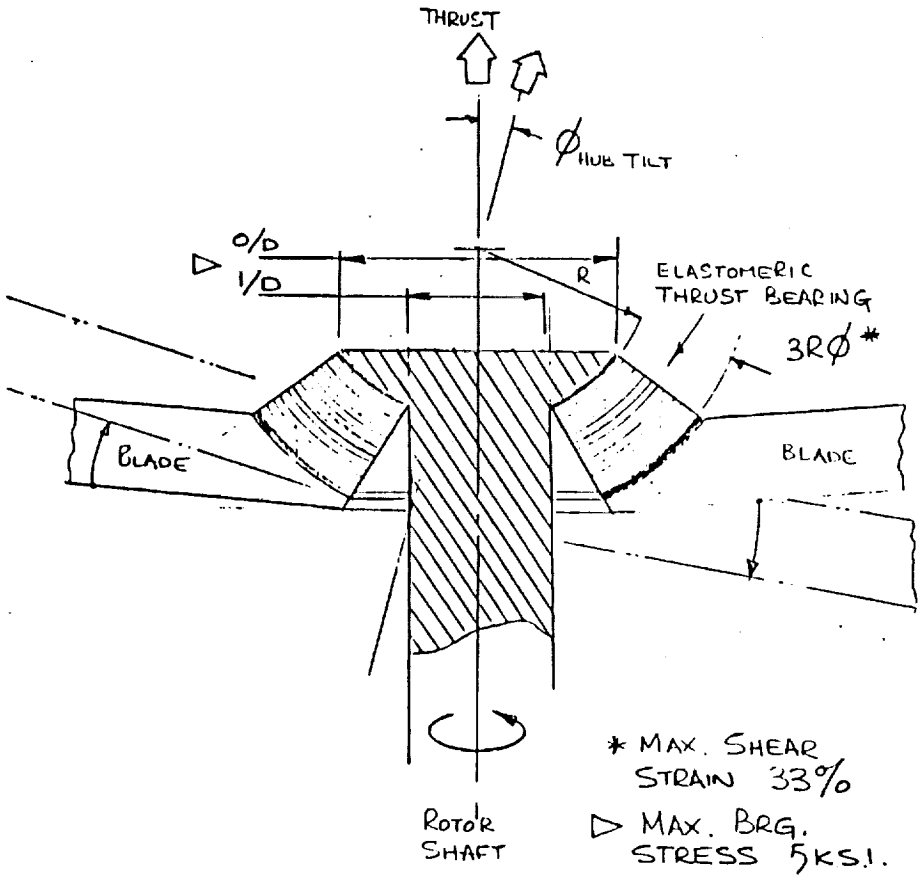

Figure 14. The Elastomeric Bearing

Thickness of the bearing laminate stackup is determined by the allowable shear strain in the elastomer.

Typically, the allowable strain is greater than 33% and allowable shear stress is greater than 300 psi. At the 6-inch spherical radius strain in Figure 5, the shear area is 44 in^2 which can result in (300*44=) 13,200 lb of shear force. The resultant limited moment is, therefore, (13,200*6 in=) 79,200 in. lb or 6,600 ft. lb. If the limited tilt angle is 8°, then the hub stiffness can be as high as 825 ft. lb/deg.

This exceeds the goal of 700 ft. lb/deg and suggests that an auxiliary hub stiffening device is not required. See item (g) in the previous section.

4.3 THE TORQUE DRIVE BELLOWS

The primary function of the bellows is to transmit the rotor shaft drive torque to the rotor hub without imposing undue restraint to the hub teetering freedom about the universal elastomeric bearing. The overall geometry is dictated by the size of the elastomeric thrust bearing on the inside and the element radial length required to accommodate the deflections due to hub tilt.

The radial length of a single straight flexure is excessive to fit inside a normal hub envelope. However, this straight element can be folded into a series of stacked hairpin flexures which begins the bellows concept. The number of convolutes (or bellows elements) required depends upon a practical outside diameter chosen and the total radial length of the wall.

To avoid interlaminar tension failure in the composite (if used) at the fold there will be a minimum fold radius which will, together with the number of folds (or convolutes) define the bellows height.

The following studies have been made to facilitate preliminary sizing and parametric variation analysis.

4.3.1 Minimum Wall Thickness

Shear Stress in Bellows (σ_s) under Drive Torque (Q)

Let Minimum radius of bellows/flexure = R_i
Minimum Thickness of bellows/flexure = t.

For a complete circumference, $S = 2 * \pi * R_i$

Shear Flow $$q = \frac{Q}{2A} = \frac{Q}{2 * \pi * R_i^2}$$

$$\text{Shear Stress} = \frac{q}{t} = \frac{1}{2 * \pi} * \frac{Q}{R_i^2 * t} \quad \text{(Figure 15)}$$

Shear stress variation with bellows inside radius and thickness is compared with material allowables in Figure 15.

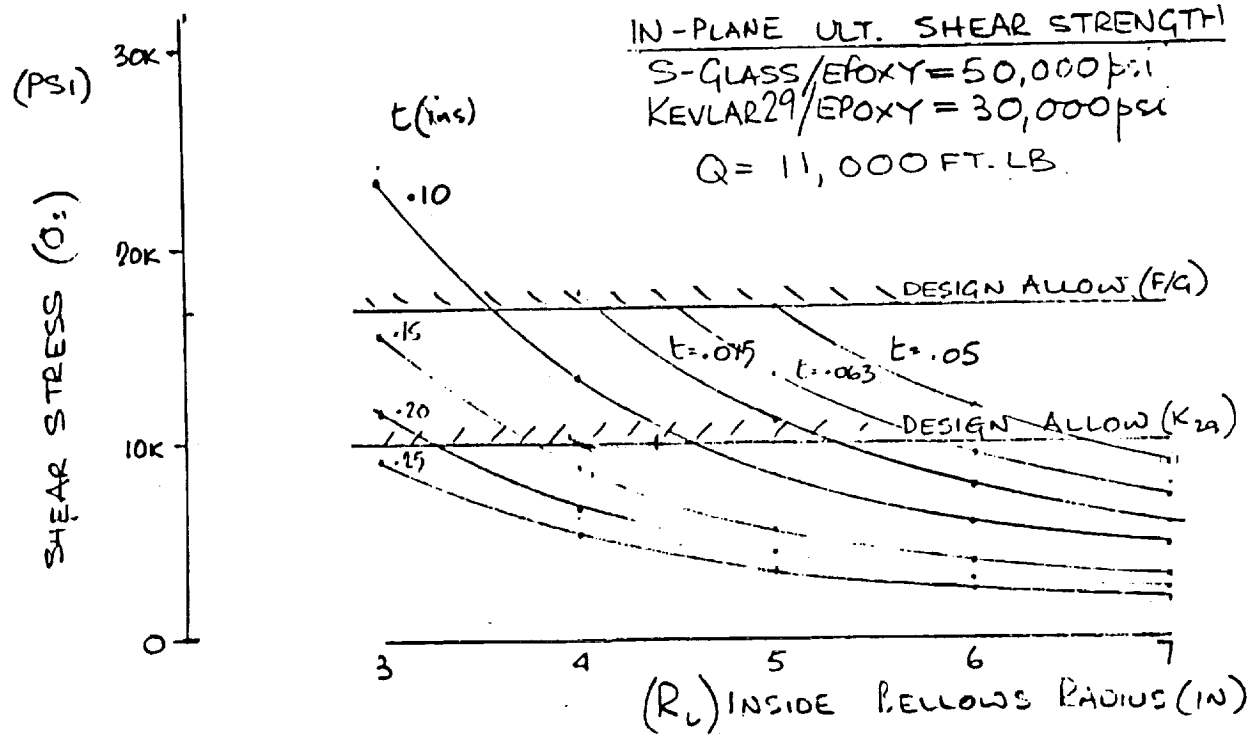

Figure 15. Effect of Bellows Inside Diameter and Wall Thickness on Shear Stress

Minimum bellows wall thickness required is graphed in Figure 16.

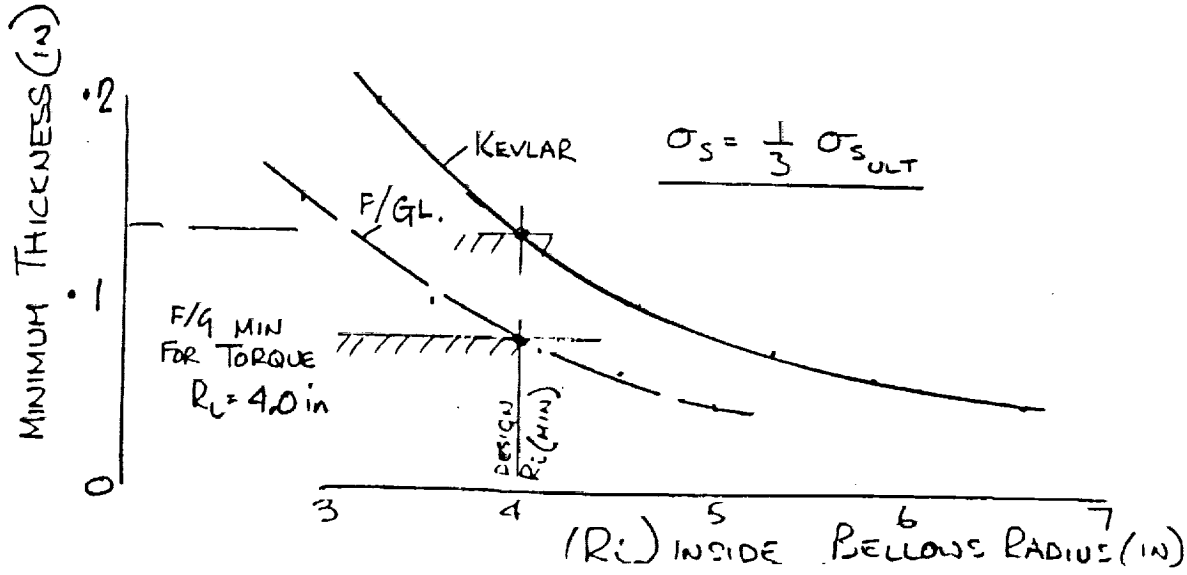

Figure 16. Minimum Wall Thickness

4.3.2 Bending Strain Due to Tilt (Approximation)

Considering a radial slice of the bellows of unit width and having the following dimensions (see Figure below):

Wall Thickness	t	Outside Radius	R_o
Inside Radius	R_i	Number of 1/2 Convolutes	N

If hub tilt = $\pm\ \phi_T$, Then each 1/2 convolute beam will experience an end slope change $\phi = \pm\phi_T/N$ and an end deflection of $\Delta = \phi * R_i$.

With reference to Appendix 3, from Case 1, Equations I, (Fixed Ended)

$$M_o = M_{max} = \frac{EI}{\ell} * \left(4 + 6 * \left(\frac{R_i}{\ell}\right)\right) * \phi \qquad (\phi \text{ in Radians})$$

or

$$\frac{M}{EI} = \frac{1}{\ell} * \left(4 + 6 * \left(\frac{R_i}{\ell}\right)\right) * \phi$$

and bending strain $\epsilon_t = \frac{M*t/2}{EI}$

Bending Strain $\epsilon_t = \frac{t}{2*\ell} * \left(4 + 6 * \left(\frac{R_i}{\ell}\right)\right) * \frac{\phi_T}{N}$

or

$$\epsilon_t = \frac{t}{2} * \left(4 + 6 * \left(\frac{R_i}{\ell}\right)\right) * \frac{\varnothing}{\ell}$$

In fiberglass/epoxy, $S_{e_t} = \pm 2{,}400\ \mu$ in/in (10^8 cycles)

In Kevlar 29/epoxy, $S_{e_c} = \pm 4{,}300\ \mu$ in/in (10^8 cycles)

Therefore, at best in Kevlar 29

$$\frac{t}{n} < \frac{.004300}{\left(4 + 6 * \left(\frac{R_i}{\ell}\right)\right) * \frac{\varnothing}{2*\ell}}$$

If R_i = 4.0" and l = 4.85", for $\varnothing_T = \pm 8°$ then the limiting thickness to avoid bending failure is given by Figure 17.

NOTE: Minimum number of whole convolutes = 3.

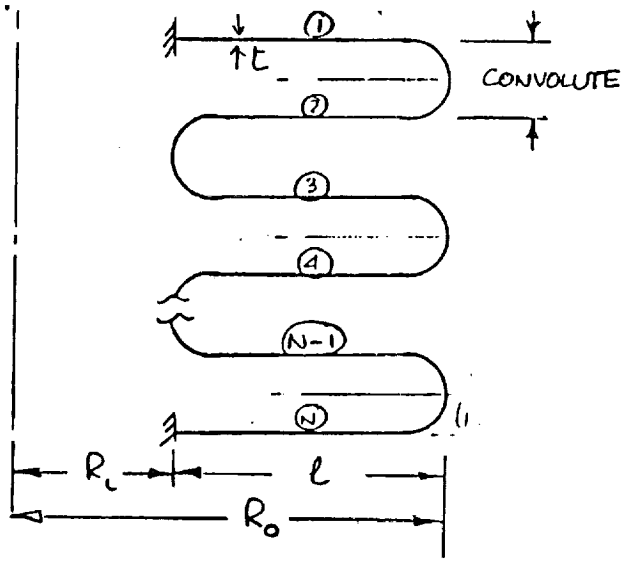

4.3.3 Thickness Limitation from Interlaminar Tension in the Radius

As shown in Figure 18, the radiused inboard and outboard ends of the convolutes experience a bending moment (M) in the wall. Due to the curvature (r), the laminated material will attempt to split apart under interlaminar tensile loads if the wall thickness exceeds the critical value derived in the following:

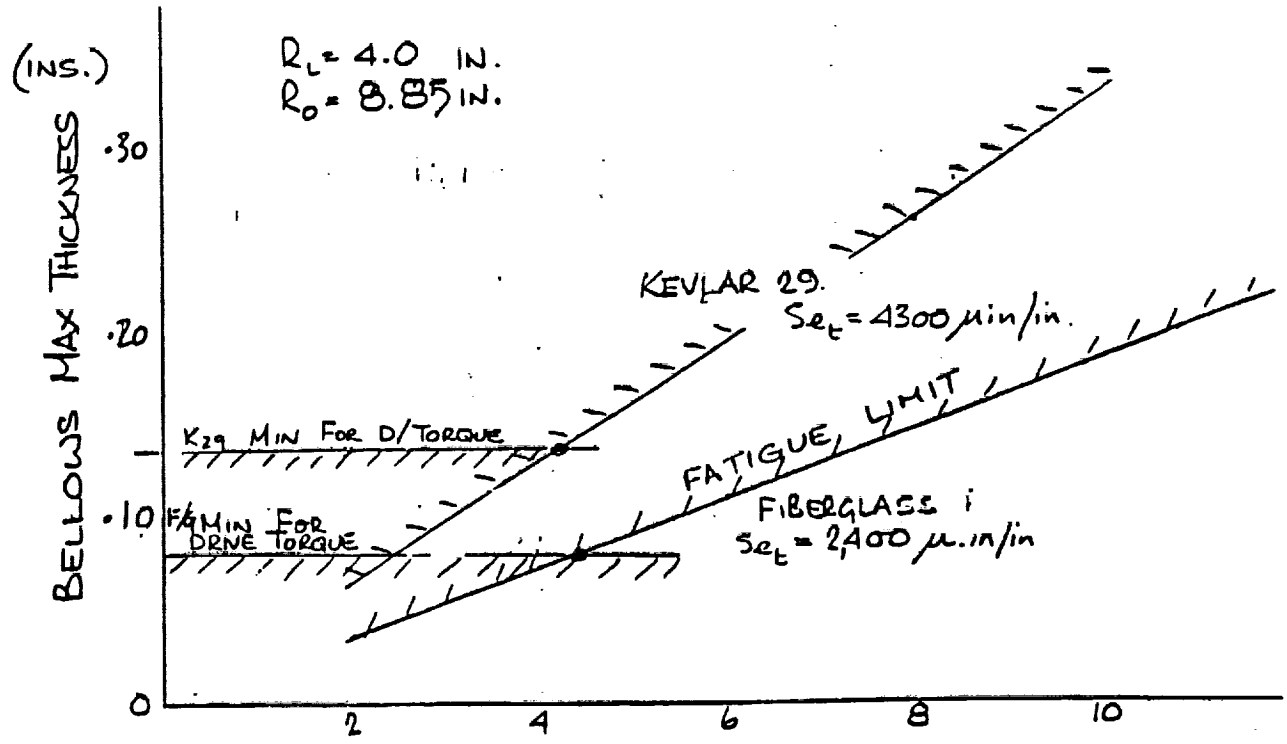

Figure 17. Number of 1/2 Convolutes

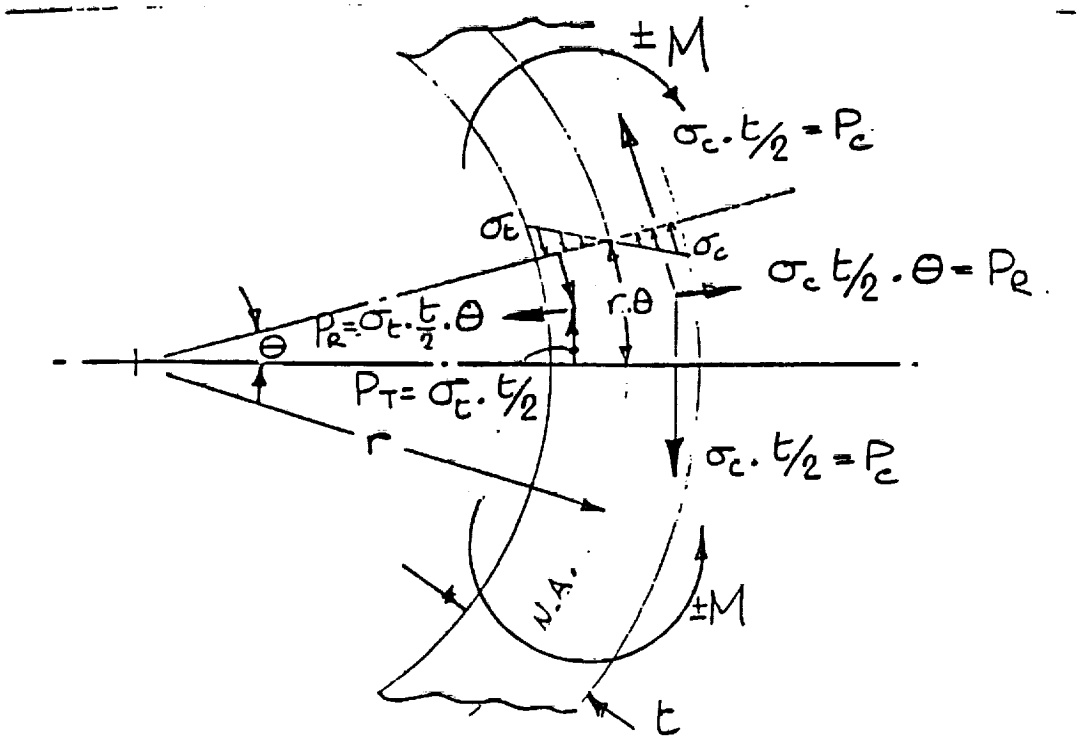

Figure 18. Interlaminar Normal Stress in a Curved Beam in Bending

The outer half of the wall under compressive stress (σ_c) will experience a compressive load (P^{2e}) and the inside, a tensile load (P_T).

In a wall segment, length ($r*\theta$), these tangential components resolve into radial components (P_R) in opposite directions resulting in a tensile stress (σ_n):

$$\sigma_n = \frac{P_R}{r*\theta} = \frac{\sigma_t * t/2*\theta}{r*\theta} = \frac{\sigma_t * t}{2*r}$$

If $\sigma_1 = S_{e_{t_1}}$ (endurance limit of the material in tension)

$\sigma_3 = S_{e_{t_3}}$ (endurance limit of the matrix in tension)

Then $t_{max} = 2 * \frac{Set_3}{Set_1} * r$

	P.S.I.		
MATERIAL	Set_1	Set_3*	t/r max
FIBERGLASS	15,600	1575	.20
KEVLAR 29	30,000	595	.04

* STATIC STRENGTH x .35

WHERE $.35 = \left(\frac{Set_3}{Stu}\right)$ GR/EP

If the material is used up to its tensile E.L., if r = 1.25" then in fiberglass, interlaminar tension failure may occur if the thickness is greater than .25"

and

In Kevlar, interlaminar tension failure may occur if the thickness is greater than .05" (see Figure 19).

The low interlaminar tensile strength of Kevlar may eliminate it as a potential bellows material.

If the minimum number of whole convolutes is three, then the minimum bellows height in fiberglass is (2*.4*3) = 2.4" and in Kevlar 29, the minimum bellows height is (.135/.05*1.25*3) = 10.1".

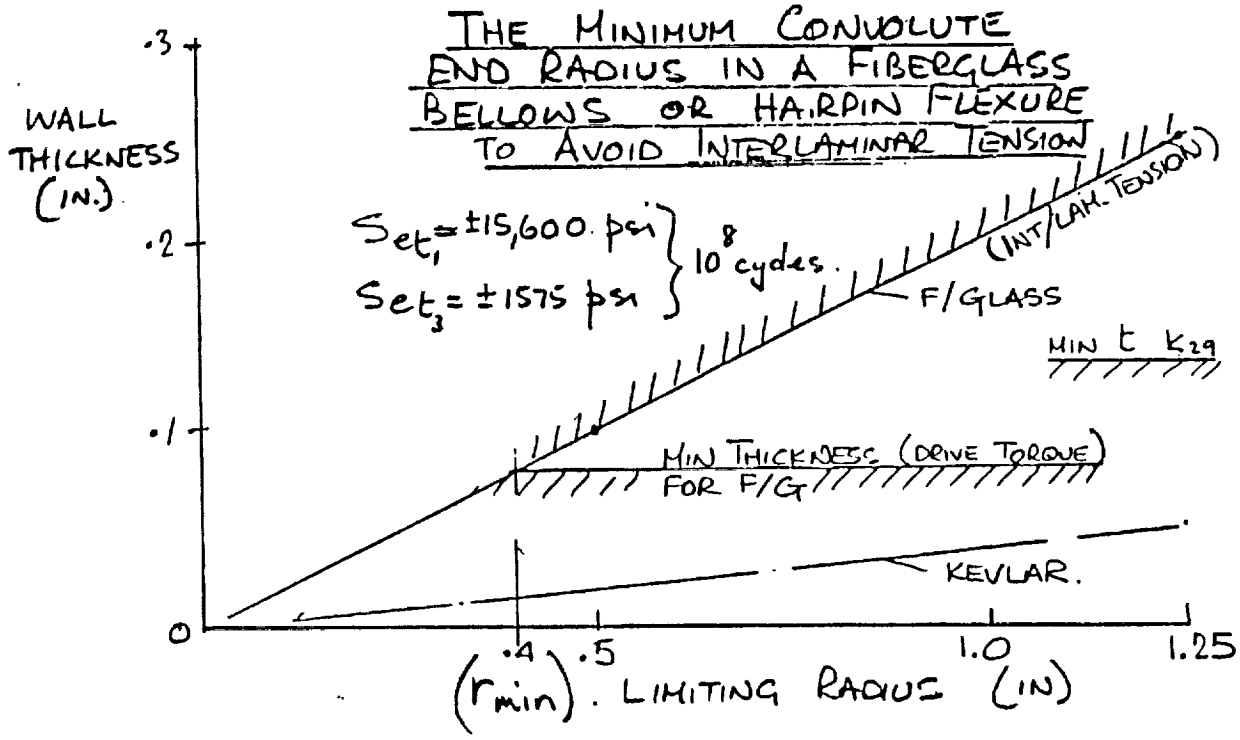

Figure 19. Minimum End Radius as Limited by Interlaminar Tension

4.3.4 Conclusion

In conclusion:

(a) the minimum bellows wall thickness required to carry the specified drive torque is 0.08".

(b) the maximum wall thickness that will not result in interlaminar tension failure is proportional to the fold radius.

(c) at 0.08" wall thickness, the allowable minimum number of whole bellows convolutes is three. However, if the wall thickness is increased to 0.25", then the minimum number of whole convolutes increases to 14.0.

(d) for minimum size and weight, a nominal thickness of .10 should be chosen. The bellows should have three whole convolutes with an end radius greater than 0.5" as shown in Figure 5.

4.4 BELLOWS FABRICATION

4.4.1 Material Form

Single element bellows drive shaft couplings have been molded successfully using resin transfer into braided preforms. Braiding results in a natural thickening of the wall towards the inside where torsional shears are high and thinning on the outside where torsional shears are lowest. Additionally, the fiber orientation can be optimized for torsion on the inside with a high winding angle which decreases radially towards the optimum required for flexure at the outside perimeter.

Pre-impregnated woven or tape broadgoods do not drape and conform to compound contours and has been rejected as a candidate.

4.4.2 Material Selection

For high flexural strength, fiberglass S2 and Kevlar 29 reinforcing fibers have been considered and both have been successfully braided and have excellent impact damage resistance. Kevlar 29, however, has a low transverse tensile strength and has been rejected.

Resins should be chosen for their flexural properties and their strength retention under exposure to the environmental conditions that rotor systems experience. A minimum glass transition temperature drop with moisture content is a desirable characteristic.

For resin transfer molding, a system with low viscosity characteristics is required to ensure complete impregnation of the dry glass preforms prior to cure. For hand impregnation, a long pot-life of the resin would be required.

4.4.3 Braiding

Various braiding machines are available and capable of braiding the hub bellows with no modifications required. A 96 carrier system

would have sufficient capacity. Figure 20 shows a typical braiding set up.

Braiding would be conducted over a soluble salt mandrel which is pre-formed in a metal die or turned to shape from a billet of material supported by a central mandrel. After cure, the salt mandrel is dissolved from the part by hot water or steam.

4.4.4 Attachment Reinforcements

At the ends of the bellows, broadgoods material cut into flat circular patterns will be interleaved with the braided layers in the discrete orientation required to transmit torsion and bending loads at the bolted attachments. Figure 21 shows a detail of the proposed interleaving. A goal of a pseudo-isotropic distribution of fibers should be set.

4.4.5 Resin Transfer Molding

The pre-form, together the with internal mandrel, is then inserted into a close fitting, multi-piece, female mold, sealed at the ends and all joints against resin squeeze-out. The cavity is then evacuated of air. After mixing and degassing, the resin is injected into the heated tool cavity, thus impregnating the fiber pre-form. The injection ports are then capped and the part is heated with the tool until cured.

Trimming and hole drilling are then completed and finally the salt mandrel is washed away, leaving the finished part.

4.4.6 Hand Impregnation

Prototype bellows can be made by hand impregnating the material by brushing wet resin into the fibers as they are being braided. Care must be exercised to obtain 100 percent wetting and completed removal of entrapped air. Squeezing out of excess resin and entrapped air occurs naturally in the braiding process due to the fiber tension. If these processes are satisfactorily achieved then the part can be cured without autoclave pressure but under atmospheric pressure requiring vacuum bagging only.

4.4.7 Vacuum Bagging

After braiding and impregnation, the bellows surface should be covered with pieces of peel-ply to absorb excess resin and to impart surface smoothness. A high elongation silicone rubber vacuum bag should be made by applying uncured material to a male wood pattern and curing under vacuum. The bagging material for this operation can be common nylon or FEP sheeting sealed against itself with zinc chromate tape since exterior surface finish of this silicone rubber bag is not important.

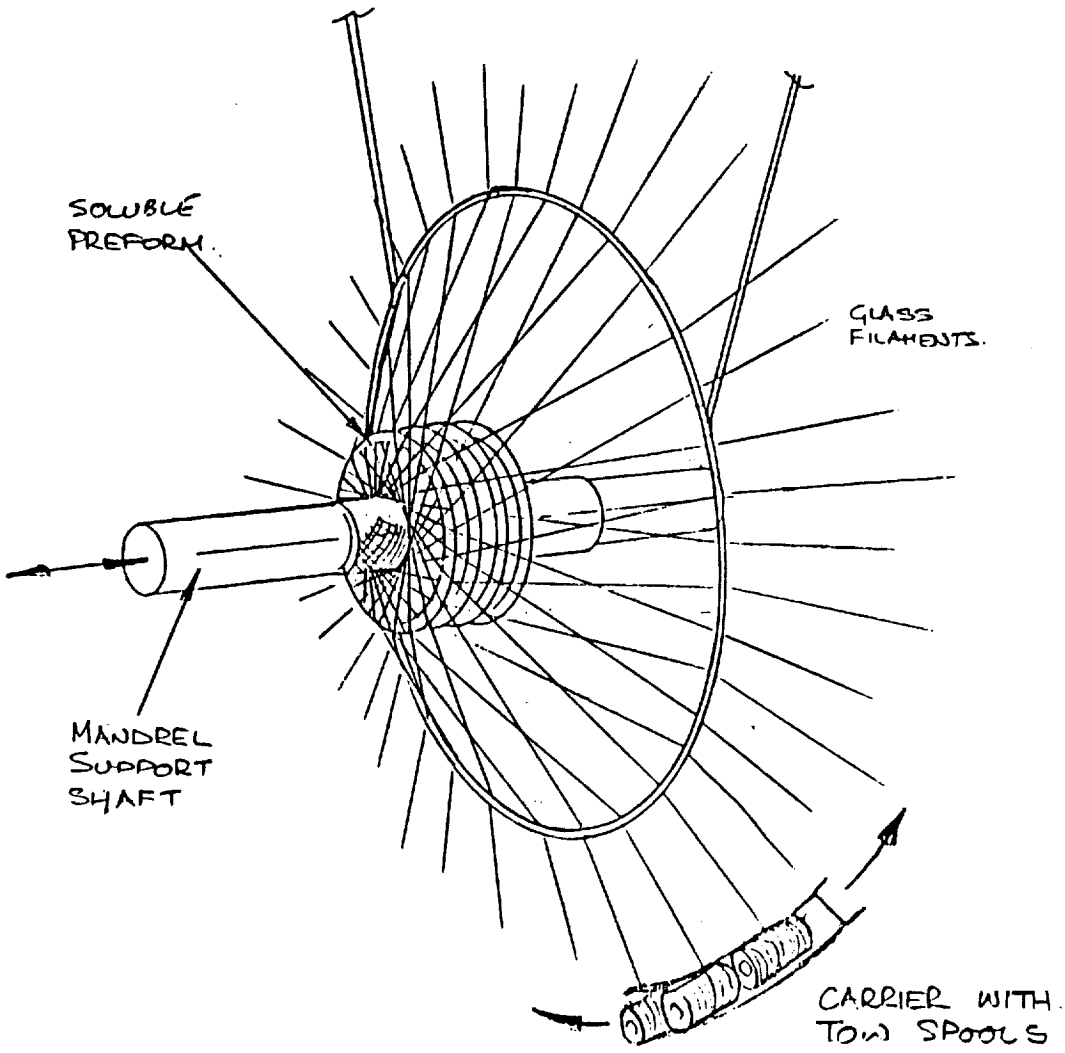

Figure 20. Braiding Machine Set Up for Composite Bellows

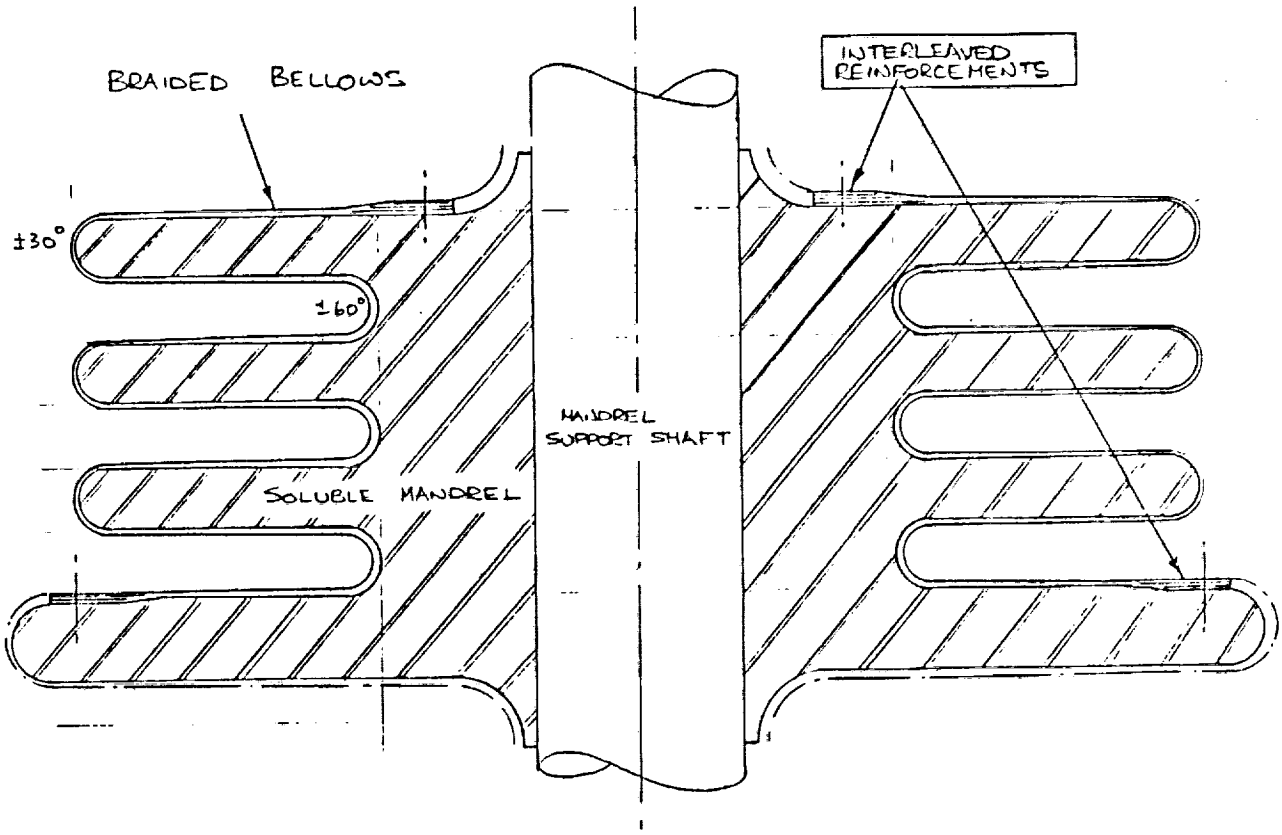

Figure 21. Proposed Interleaving

The silicone rubber bag can be reinforced down each side with additional thickness of rubber which can be slit after cure to produce a sealable joint to facilitate application and removal from the bellows.

4.4.8 Cure Process

The bellows, braided on the mandrel and impregnated with resin, encapsulated in peel ply and custom made vacuum bag can be oven cured.

4.5 WEIGHT, DRAG, AND VULNERABILITY

Rough order of magnitude estimates have been made for the hub only above the rotor shaft joint and out to the blade attachment. Blade root flexure and pitch control mechanism are excluded.

4.5.1 Weight

A component breakdown is as follows:

Item	Qty.	Wt. Ea. (lb. est.)	Total (lb. est.)
Hub Nut	1	.68	.7
Drive Collar	1	6.29	6.3
Centralizing Ball Brg.	1	5.78	5.8
Support Center	1	6.20	6.2
Bellows	1	14.92	14.9
Blade Attachment Ring (T_1)	1	76.64	76.6
Support, Lower	1	16.01	16.0
Univ. Elast. Brg.	1	32.61	32.6
Shaft Extension	1	34.50	34.5
			193.6

4.5.2 Drag

Frontal area has been estimated as 1.31 ft^2.

4.5.3 Vulnerability

Failure of any single component is not expected to result in loss of the aircraft. A hit by an armor piercing projectile (12.7 mm) will not result in catastrophic damage. Each component, if damaged, is large enough to retain enough integrity to allow the aircraft to complete its mission.

4.6 COST, RELIABILITY, AND MAINTAINABILITY

4.6.1 Cost

A rough order of magnitude cost has been estimated for each component in the quantity production as follows:

Item	Qty.	$ Each (est.)	$ Total (est.)
Hub Nut	1	50	50
Drive Collar	1	1,000	1,000
Centralizing Ball Brg.	1	3,000	3,000
Support Center	1	2,000	2,000
Bellows	1	8,000	8,000
Blade Attachment Ring	1	23,000	23,000
Support, Lower	1	2,000	2,000
Univ. Elast. Brg.	1	15,000	15,000
Shaft Extension	1	4,000	4,000
			58,050

4.6.2 Reliability

A 2000 hours life at $\pm 8^{\circ}$ of tilt can be expected of the universal elastomeric bearing and the spherical centralizing ball. All other components are designed to infinite life and should be good for 10,000 hours.

4.6.3 Maintainability

No lubrication is required. The safe life designed elastomeric and ball bearing are accessed for visual inspection by removal of the rotor from the hub by detaching the upper hub nut and the lower support to elastomeric bearing joint and disconnection of the pitch links. This procedure should not be required at intervals less than 500 hours.

APPENDIX 1

Design Criteria and Specifications for the Soft Hub for Bearingless Rotors

1.0 BACKGROUND AND SUMMARY

Current and past configurations of bearingless rotors are limited in their capabilities to flap and/or provide rotor disc path plane tilt without incurring fatigue damage to their (usually composite) flexures. These flexures provide the means of articulating and pitching the rotor blade by bending and twisting which results in straining of the composite materials.

Highly maneuverable single and tandem rotor helicopters need to flap (or tilt the rotor disc) to levels of $\pm$ 8° and $\pm$ 12° respectively without generating high shaft bending loads in the process (due to hub and flexure stiffness).

The soft hub concepts being studies under this effort are devices which provide rotor disc tilt without generating excessive hub moments and reduce the need for the blade flexures to bend beyond their endurance limit.

This document describes those criteria for loads, deflections, and material allowables to which the soft hub concepts will be constrained to result in infinite life and optimum capability.

The Messerschmidt-Bolkow-Blohm 105 helicopter is presented as a typical helicopter.

2.0 DESIGN CRITERIA

The fundamental criteria to be used in designing the soft hubs for the BO-105 are:

a. No flap, lag, or blade pitch bearings will be used.

b. The BO-105 ground and air stability will be maintained.

c. At 425 rpm (normal BO-105 rotor speed) the rotor frequencies shall be within the following ranges.

1st flap (cyclic mode)	< 1.05 per rev.
1st chord (cyclic mode)	< .64 per rev.
1st torsion	> 3.2 per rev.

d. All soft hub and blade components will be designed to a minimum fatigue life goal of > 10,000 hours following the flight profile of Table 1.

e. The design test vehicle will be the MBB BO-105 shown in Figure 1 and whose general characteristics are presented in Table 2.

Table 1. Load Profile

Time at g per 10,000 Hours (sec)

n_z → / V_c ↓	3.5	3.25	3.00	2.75	2.50	2.25	2.0	1.9	1.8	1.7	1.6	1.5	1.4	1.3	1.2	1.1 Level Flight	1.1 Climb	1.0 Descent	0.9	0.7	0.6	0.5	0.4	0.3	0.2	0
110										72	250	694	986	2,178	3,525	818,056			352							
100							44	78	156	367	797	1,917	3,600	8,828	15,725	2.66×10^{5}		136,800	1,331	283	50	25				
90						39	244	431	622	1,100	1,822	5,583	16,650	34,514	219,600	4.39×10^{5}	34,167	308,333	3,500	1,356	283	139	39			
80					85.6	171	500	849	2,333	3,667	6,833	11,888	64,381	124,475	269,314	2.78×10^{5}	205,154	513,000	12,349	4,294	456	258	147	131		
70				23.3	51.9	249	1,544	2,755	3,889	8,250	20,500	75,694	107,239	815,244	240,500	5.57×10^{5}	1.06×10^{5}	1.38×10^{5}	33,108	8,667	1,506	878	216	81	44	
60	5.6	6.7	26.7	20.8	47.2	264	2,489	4,333	8,928	14,667	34,167	104,139	176,444	229,906	483,731	34,194	171,111	171,111	56,808	16,981	2,253	1,447	216	64	44	111
50				23.3	51.9	249	1,644	3,289	11,900	58,300	150,806	403,800	528,106	539,567	895,108	34,194	68,333	102,500	341,189	18,782	1,808	939	216	81	44	
40						78	89	808	1,244	24,567	102,500	358,333	$514,886$	$1,056,381$	$888,464$	34,194	68,333	68,333	137,583	2,289	456	44	69			
30							44	361	1,183	3,667	15,945	90,083	569,306	$1,823,881$	$2,064,850$	5.42×10^{5}	68,333	136,800	21,358	1,664	144	25				
Sideward																$11,944$										
Rearward																$11,944$										
Total	5.6	6.7	26.7	66.6	236.6	1,050	6,590	12,804	30,255	114,657	341,620	732,832	$1,841,906$	$3,134,284$	$5,062,826$	1.17×10^{6}	1.71×10^{5}	2.73×10^{5}	507,427	54,326	6,994	3,755	903	357	132	111

Exceedance in 10,000 Hours

n_z → / V_c ↓	3.5	3.25	3.00	2.75	2.50	2.25	2.0	1.9	1.8	1.7	1.6	1.5	1.4	1.3	1.2	Level Flight	Climb	Descent	0.9	0.7	0.6	0.5	0.4	0.3	0.2	0
110										11	42	111	208	386	675				75							
100							11	27	56	111	208	400	725	1,411	2,700				375	92	22	8				
90						14	75	167	278	444	667	1,225	2,325	5,675	23,675				1,200	456	125	58	14			
80					58	111	236	417	833	1,389	2,222	3,411	9,211	18,858	41,925				4,000	1,364	317	186	103	50		
70				18	58	139	525	1,111	1,806	3,056	5,556	13,125	22,786	32,636	52,358				10,000	2,956	842	411	128	50	19	
60	11	22	56	72	108	194	817	1,738	3,333	5,556	9,722	20,136	36,058	55,708	85,358				17,503	5,458	1,317	644	178	100	75	56
50				18	58	139	558	1,250	3,375	12,208	31,575	71,875	118,461	165,588	238,358				56,844	5,528	844	431	128	50	19	
40						27	58	222	444	4,167	16,667	56,500	102,886	193,175	266,008				30,003	728	169	39	25			
30							11	67	278	833	3,778	11,786	63,875	158,586	328,008				5,000	456	25	8				
Sideward																										
Rearward																										
Total	11	22	56	110	258	624	2,275	5,000	10,483	27,775	68,437	178,568	357,118	634,899	1,041,625				125,000	17,038	3,761	1,705	576	250	93	56

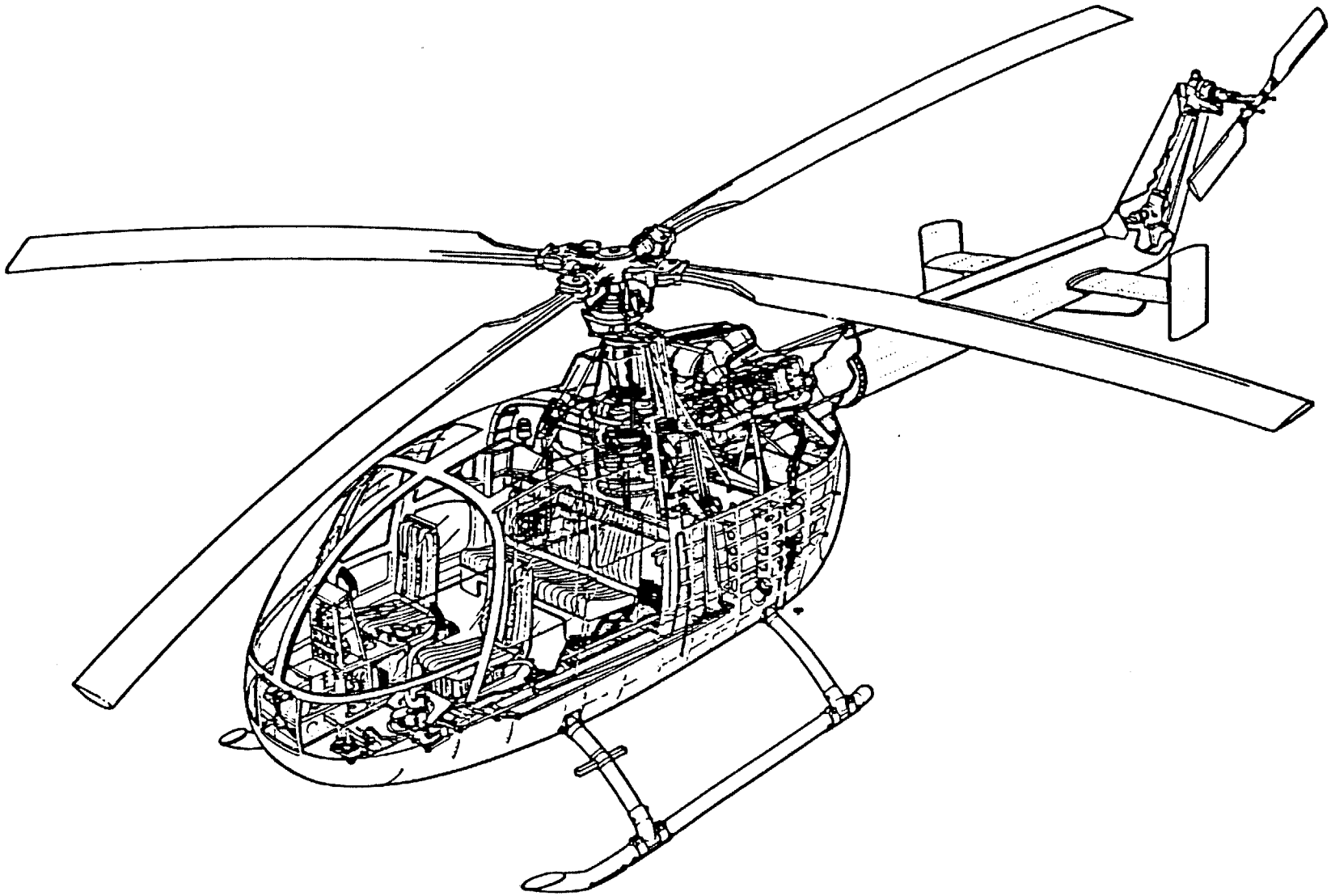

Figure 1. BO-105 General Arrangement Illustration

TABLE 2. BO-105 Dimensions and General Data

Overall Dimensions	
Length (Tail Rotor Horizontal)	38 ft 10.1 in.
Width (Rotor Diameter)	32 ft 2.6 in.
Height (Tail Rotor Vertical)	12 ft 5.6 in.
Height (Tail Rotor Horizontal)	10 ft 1.3 in.
Fuselage	
Length (Tail Rotor Vertical)	28 ft 0.6 in.
Width	5 ft 3.0 in.
Height (including Landing Gear)	9 ft 8.1 in.
Fuselage Ground Clearance	1 ft 1.8 in.
Tail Boom Ground Clearance	4 ft 5.2 in.
Landing Gear	
Track (Unloaded)	8 ft 2.4 in.
Track (Loaded)	8 ft 4.4 in.
Length of Landing Skids	8 ft 10.3 in.
Tail Boom with Vertical Fin and Stabilizer Assy	
Length	13 ft 0.7 in.
Width	6 ft 10.6 in.
Height	4 ft 9.0 in.
Cargo Compartment Volume	45.0 cu ft
Allison 250-C20 Engine Data	
Design Power Output	400 shp
Design Speeds:	
Gas Producer	100% (50,970 rpm)
Power Turbine	100% (33,290 rpm)
Power Output Shaft	6016 rpm
Fuel Specification	
Primary	MIL-T-5624, Grade JP-4 and JP-5 ASTM D-1655, Jet B ASTM D-1655, Jet A
Main Rotor	
Number of Blades	Four
Diameter	32 ft 2.6 in.
Blade Chord	10.63 in.
Tail Rotor	
Number of Blades	Two
Diameter	6 ft 2.8 in.
Blade Chord	7.05 in.

2.1 STRENGTH CRITERIA

As a reference, Table 3 presents the strength characteristics of the current BO-105 rotor hub.

Composite materials design data is presented in Table 4.

The soft hub concepts will be designed within these materials and aircraft strength constraints.

2.2 LOADS DATA

The endurance limit flapping (10^8 cycles) of the current BO-105 rotor has been estimated at $\pm$ 2°.

Measured BO-105 loads data is presented in Figures 2 through 10.

The soft hub will be designed to $\pm$ 8° and the blade root flexure to $\pm$ 4° of endurance limit flapping resulting in $\pm$ 12° of endurance limit rotor disc tilt.

The blade root flexure will be designed to an endurance limit lag angle of 1/4 of the hub tilt or $\pm$ 3°. These displacements are assumed to be out of phase with flap by 90° and therefore do not occur concurrently.

2.3 REQUIRED HUB SPRING STIFFNESS FOR THE SOFT HUB

Single Rotor Helio (at 5,000 lb DGW)

Hub spring stiffness is required for control ability of the aircraft at low thrust conditions where rotors with zero hinge offset have to rely on thrust vector offset to provide hub moment.

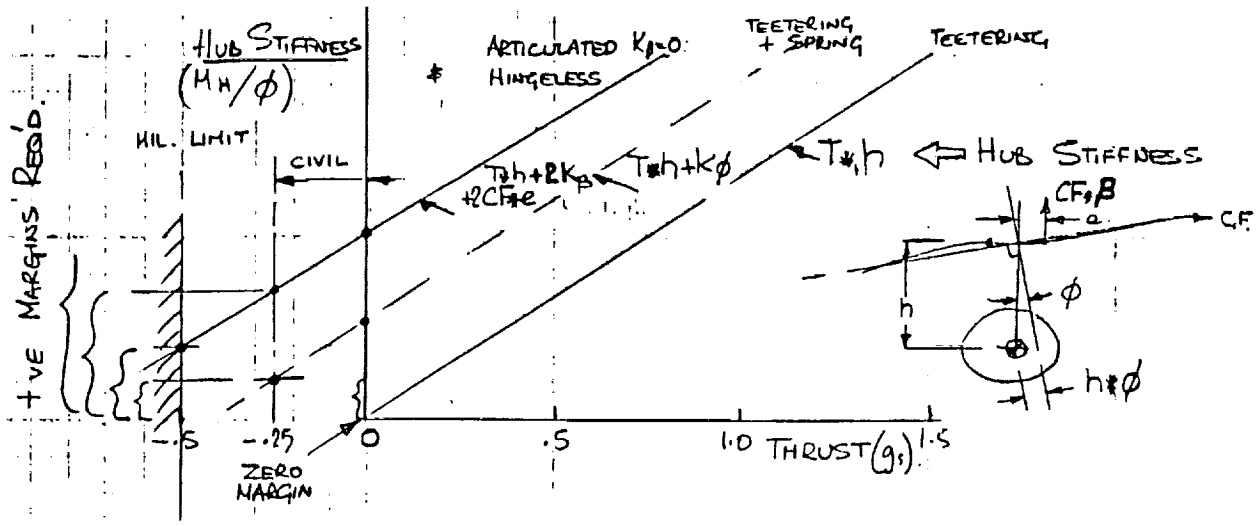

Figure 2. Hub Stiffness (A/C Control Moment)

TABLE 3. BO-105 Rotor Strength Summary

Component Description Note 2	Part Number	Predominant Loading	Max Measured Level-Flight Load		BO-105 Endurance Limit (M – 3σ) @ 10^7 Cyc	Fatigue Life (hr)
			Basic Aircraft	Units		BO-105
Rotor Blade	105-15103	CF, flap, & chord bending	± 6,315	in.-lb	± 21,800	10,000
Primary Blade Mount Bolt	105-14101.31	CF, flap bending	± 5,243	in.-lb	± 18,200	600
Secondary Blade Mount Bolt	105-14101.35	Chord bending	± 3,520	in.-lb	± 17,750	2,400
Blade Root Attachment	105-14181	CF, flap	± 5,143	in.-lb	± 21,600	UNLIMITED
Bendix Tension-Torsion Strap	2602559	CF, torsion	33,370	lb	Note 1	1,200
Tension-Torsion Strap Retention Pins	105-14101 .22 & .23	CF	33,370	lb	Note 1	2,400
Tension-Torsion Strap Center Plates	105-14101.19 & .20	CF	33,370	lb	Note 1	2,400
Rotor Hub	105-14101.12	Flap & chord bending	± 21,000	in.-lb	± 88,760	6,000
Rotor Shaft (Mast)	4619-305-032	Flap bending	± 21,000	in.-lb	± 58,900	2,400
Pitch Arm	105-14201	Pitch-link load	± 47	lb	± 290	UNLIMITED

NOTES:

1. Life based on ground-air-ground cycles
2. Critical components shown for each system

Table 4. A Selection of Material Design Characteristics

Material	Style	Bias	Density ρ (lb/in.³)	Modulus: Tensile lb/in.²	Modulus: Shear lb/in.²	Static Strength: u.t.s. lb/in.²	Static Strength: l.t.s. lb/in.²	Static Strength: Shear Ult lb/in.²	Fatigue Strain: Tensile μin./in.	Fatigue Strain: Shear μin./in.	Impact: Notched IZOD ft lb/in.	Resist. To Temp. & Humidity	Remarks
E Glass /Epoxy	Uni	0°	0.067	6.5×10^6	0.8×10^6	160×10^3	11×10^3	14×10^3	2300	2900	60	High	(1) Large data bank
	Uni	± 45°	0.067	1.8×10^6	1.8×10^6	23×10^3	11×10^3	46×10^3	1400	3250	–	Medium	
	Woven	0°/90°	0.066	3.1×10^6	0.8×10^6	45×10^3	–	14×10^3	2540	2330	11	High/Med	
	Woven	± 45°	0.066	1.8×10^6	1.35×10^6	27×10^3	–	26×10^3	1600	3300	–	Medium	
Kevlar /Epoxy	Uni	0°	0.050	11×10^6	0.3×10^6	120×10^3	8×10^3	8.7×10^3	2720	–	25	Medium	(1) Low fiber/matrix bondstr
	Uni –	± 45°	0.050	1.1×10^6	1.8×10^6	18×10^3	6×10^3	27×10^3	–		–	Med/low	(2) Low moisture resistance
	Woven	0°/90°	0.048	4×10^6	0.3×10^6	70×10^3	4×10^3	4×10^3	2620	–	10	Medium	(1) Adequate data bank
	Woven	± 45°	0.048	1.1×10^6	2.0×10^6	20×10^3	4×10^3	26×10^3	2550	2400	–	Low	
Graphite /Epoxy	Uni	0°	0.056	20×10^6	0.8×10^6	164×10^3	9×10^3	11.4×10^3	2100	900	8	High	(1) Low damage tolerance
	Uni	± 45°	0.056	2.25×10^6	4×10^6	25×10^3	3×10^3	45×10^3	1700	1150	–	Medium	(2) Adequate data bank
	Woven	0°/90°	0.056	9×10^6	0.6×10^6	60×10^3	9×10^3	10×10^3	2100	–	–	High/Med	
	Woven	± 45°	0.056	2×10^6	3.5×10^6	20×10^3	3×10^3	36×10^3	2100	–	–	Medium	
Graphite /P1700	Uni	0°	0.056	16.3×10^6	0.56×10^6	192×10^3	14×10^3	16×10^3	2782	–	20	High	(1) Toughest matrix
	Uni	± 45°	0.056	2.2×10^6	4.0×10^6	21×10^3	11×10^3	35×10^3	–	–	11.	High/Med	(2) High Temp Reinst
	Woven	0°/90°	0.055	10.2×10^6	–	77×10^3	9×10^3	15×10^3	–	–	14	High/Med	(3) Small data bank
	Woven	± 45°	0.055	–	4.0×10^6	–	–	35×10^3	–	2400	–	High/Med	
Desired Characteristics			Low	High	Low	High	High	High	High	High	High	High	

Tandem Rotor Helio (at 34,000 lb DGW) (REFERENCE ONLY)

For this transport type of helicopter, hub moment is used for roll maneuvers only since differential collective is used for pitch control. High roll rates are not required. However, the hover turn requirements dictate ± 15° of left and right tilt of the thrust vectors to provide a yawing couple.

Besides providing a rolling moment, the typical 2% radius flap hinge offset provides a fuselage twisting torque during the yaw maneuver which has to be accommodated structurally.

The hub spring required in a soft gymbaled hub for tandem rotors must be equated to hinge offset only.

Design Goal for the Soft Hub Program

Table 5 presents Hub Stiffness Characteristic Data for typical types of helicopters. The analysis gives the hub stiffness contribution from flap hinge offset for a tandem rotor helicopter at 34,000 lb and for a typical single rotor helicopter at 5,000 lb gross weight and 3% radius flap hinge offset.

The design goal for the soft hub, applied to a BO-105 size of helicopter, is therefore set at 700 ft. lb/degree of hub tilt.

2.4 VIBRATION

It is essential that the kinematics of the soft hub do not result in vibrations in excess of those experienced with the conventional hub system. In the case of the BO-105, the rotor system is bearingless with the flap and lag articulations provided through blade root flexures. The pitch motions are within a hub spider rigidly attached to the shaft. Articulated rotors generally have their flap and chord hinges offset radially from the center of rotation.

Flapping of the rotor, or tilting of the rotor disc, in these cases results in in-plane coriolis loading of the rotor blades due to the radial velocity of rotor components in a plane normal to the axis of rotation. These vibratory loads are manageable in the current systems and must not be aggravated by adverse changes in kinematics. A most important consideration is cyclic variation of rotor velocity (rpm) with hub tilt and azimuth, produced by orthogonally hinged blades offset from the rotor shaft. A safe approach for the soft hub would be to have a constant velocity drive torque transmittal from the vertical shaft to the tilted axis of the tilted (flapping) rotor disc. This is illustrated in Figure 1(b) which concludes that the bellows type of drive torque flexible coupling is a constant velocity joint and can be used for the soft hub.

Table 5. Hub Stiffness Characteristics

Hub Type	Helicopter	R. (ft) Rotor Rad	e/R (%) Hinge,Offst	h. (ft.) Hub to C.G.	T (lbs) ① Thrust	(lbs) Blade C.F.	Kβ (ft.lb/deg) Flap Spring	K_H (ft.lb/deg) ① Hub Stiffness	K_H (normalized) ③ $K_H * T^{-3/2}$
Teetering	AH-1	NR	0.00	6.5	8,500	N.R.	0	964	.0011
Articulated	UH-60	26.8	4.70	5.5	16,000	67,800	0	4,517	.00223
Articulated	CH-46	25.5	1.67	8.5	17,000	59,000	0	3,407	.00153
Articulated	CH-47	30.0	2.22	9.5	27,000	100,000	0	6,800	.00153
Hingeless	YUH-61	24.5	② 15.00	4.0	16,000	66,000	515	10,624	.00525
Hingeless	BO105	16.1	② 13.40	5.1	5,050	35,000	144	2,898	.00810
Bearingless	BMR-BO 05	16.1	11.38	5.1	5,150	40,000	144	3,304	.00894

NOTES:

1 @ 1 g - DGW

2 Equivalent (Flap Frequency Based)

3 $T^{3/2}$: Force = $T = L^2$, $L = T^{1/2}$
Moment = $T.L = L^3 = T^{3/2}$

(K_H) GYMBALLED HUB WITH SPRING

FOR A TYPICAL TANDEM ROTOR HELICOPTER. R=300 in

THRUST/ROTOR = 34000/2

T = 17000 LB

h = 80 in., $K_\phi = 0$

e = 2%R = 6 in, CF = 60,000 LB

(ARTICULATED) $T*h + 2CF*e = T*h + K_\phi$ (GYMBALED)

AGAIN, $K_\phi = 2CF*e$ OR $2*CF*(e/R)*R$.

$(= 6\times10^4$ FT.LB/RAD = 1050 FT.LB/DEG)

FOR A TYPICAL SINGLE ROTOR HELICOPTER WITHOUT A HUB SPRING ($K_\phi = 0$) R = 200 IN.

T = 5000 LB, h = 60 in

e = 3%R = 6 IN., CF = 40,000 LB

HUB STIFFNESS = 5000 * 60 + 2 * 40,000 * 6

$= (30*10^4 + 48*10^4)$ IN.LB/RAD.

$= (2.5*10^4 + 4.0*10^4)$ FT.LB/RAD

IT SHOULD BE NOTED THAT HINGE OFFSET CONTRIBUTES MORE THAN 1/2 OF THE TOTAL HUB STIFFNESS IN A TYPICAL HELICOPTER.

TO REPLACE THIS OFFSET HUB WITH A SPRUNG GYMBALED OR TEETERING SYSTEM WITH EQUAL HUB STIFFNESS:

$T*h + K_\phi = T*h + 2CF*e$

THEN THE REQUIRED HUB SPRING STIFFNESS

$K_\phi = 2CF*e$. OR $2*CF*(e/R)*R$.

$(= 4*10^4$ FT.LB/RAD = 700 FT.LB/DEG.)

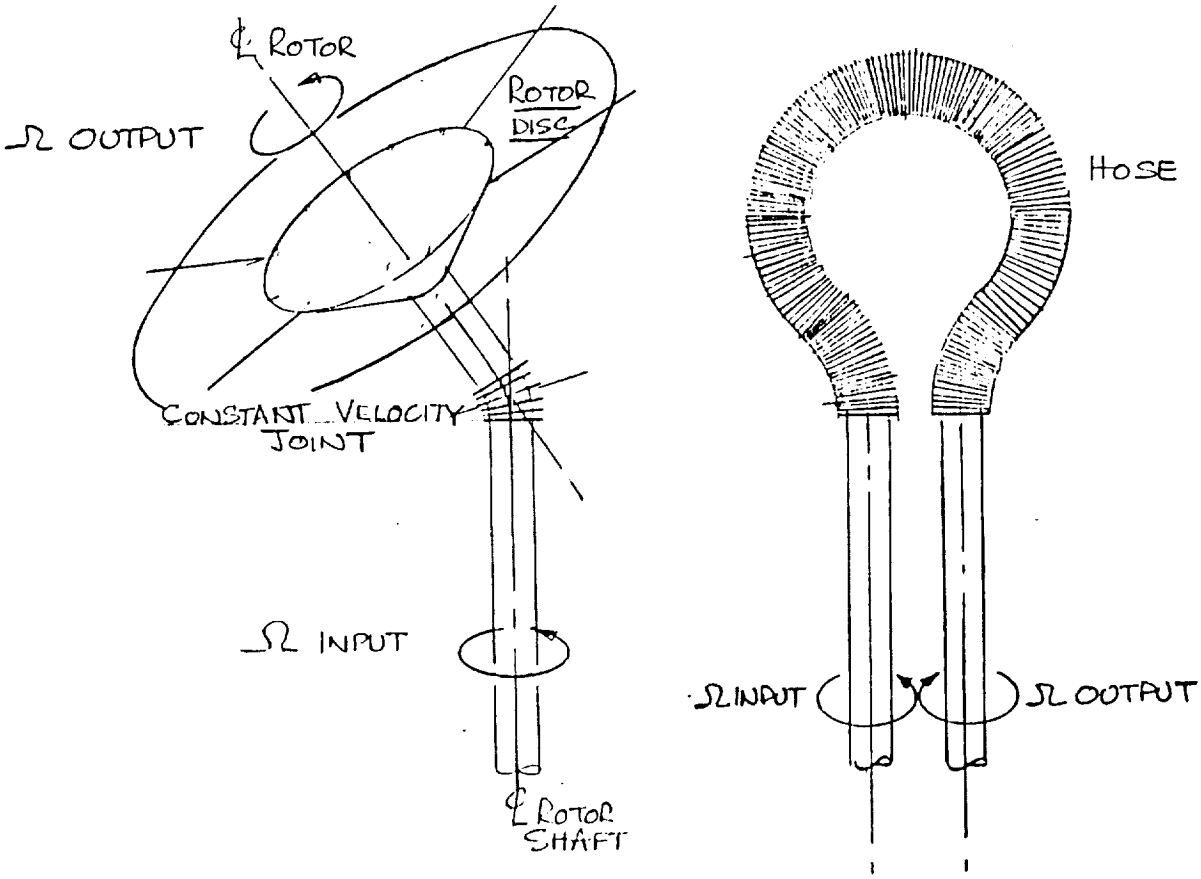

1(b)

TILTED ROTOR DISC. DRIVEN BY CONSTANT VELOCITY JOINT.

1(c).

A BELLOWS IS A CONSTANT VELOCITY JOINT

Figure 1b. The Bellows/Corrugated Hose as a Constant Velocity Joint

REFERENCE (3)

USAAMRDL TR75-50, Validation of Rotorcraft Flight Simulation Program Through Correlation with Flight Data for Soft-in-Plane Hingeless Rotors

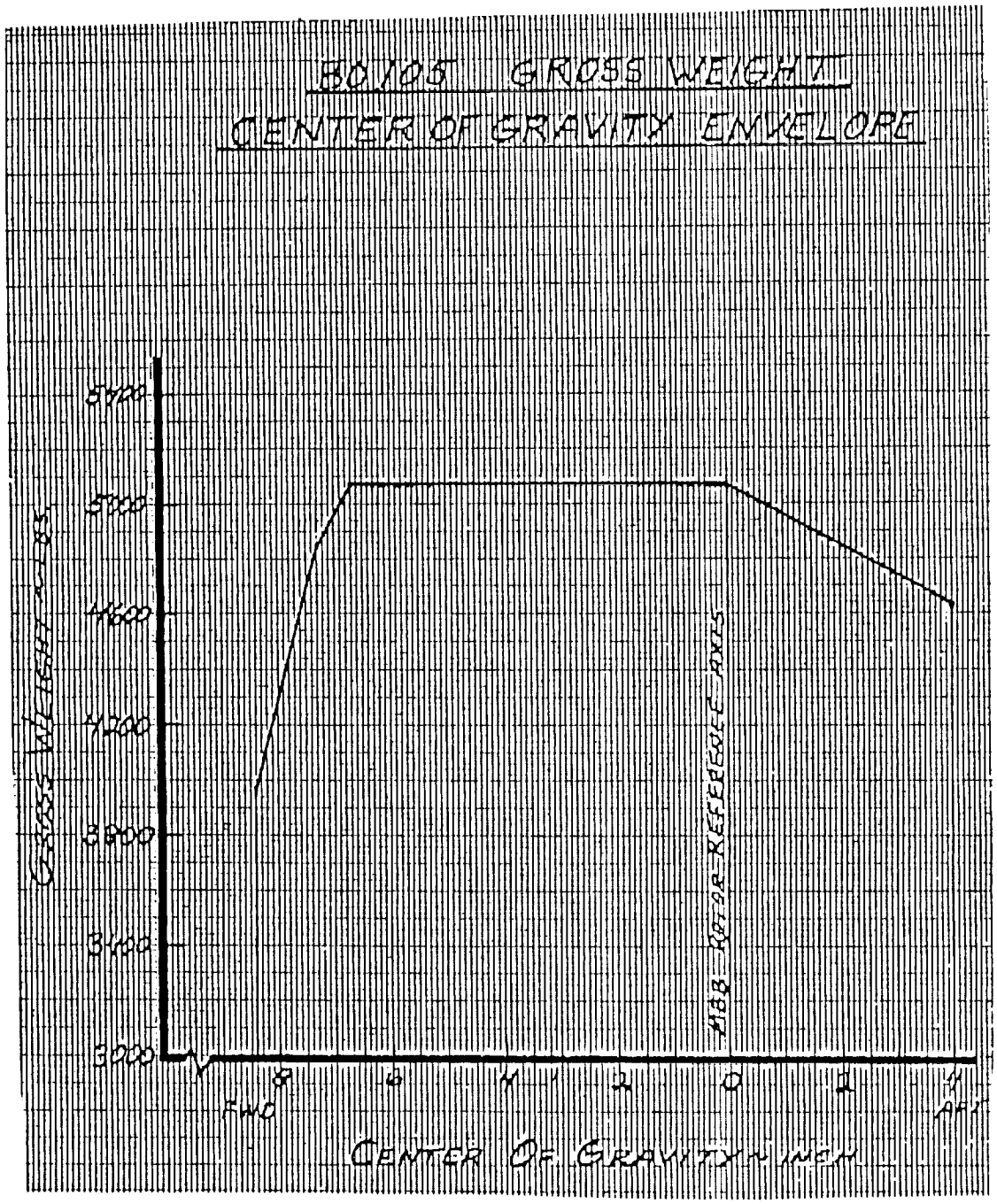

Figure 3. BO-105 Gross Weight Center of Gravity Envelope

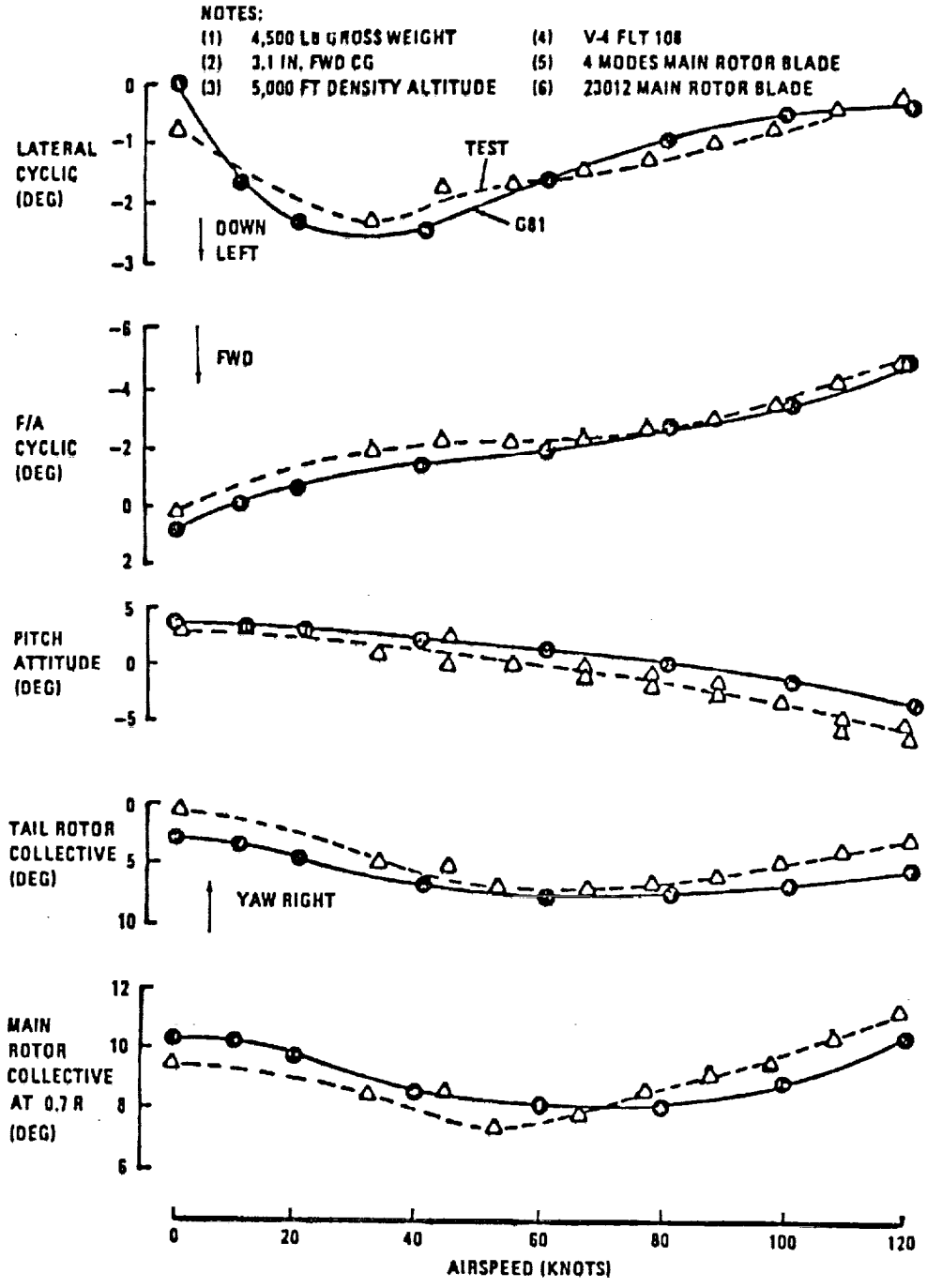

Figure 4. Trim Angles vs. Speed

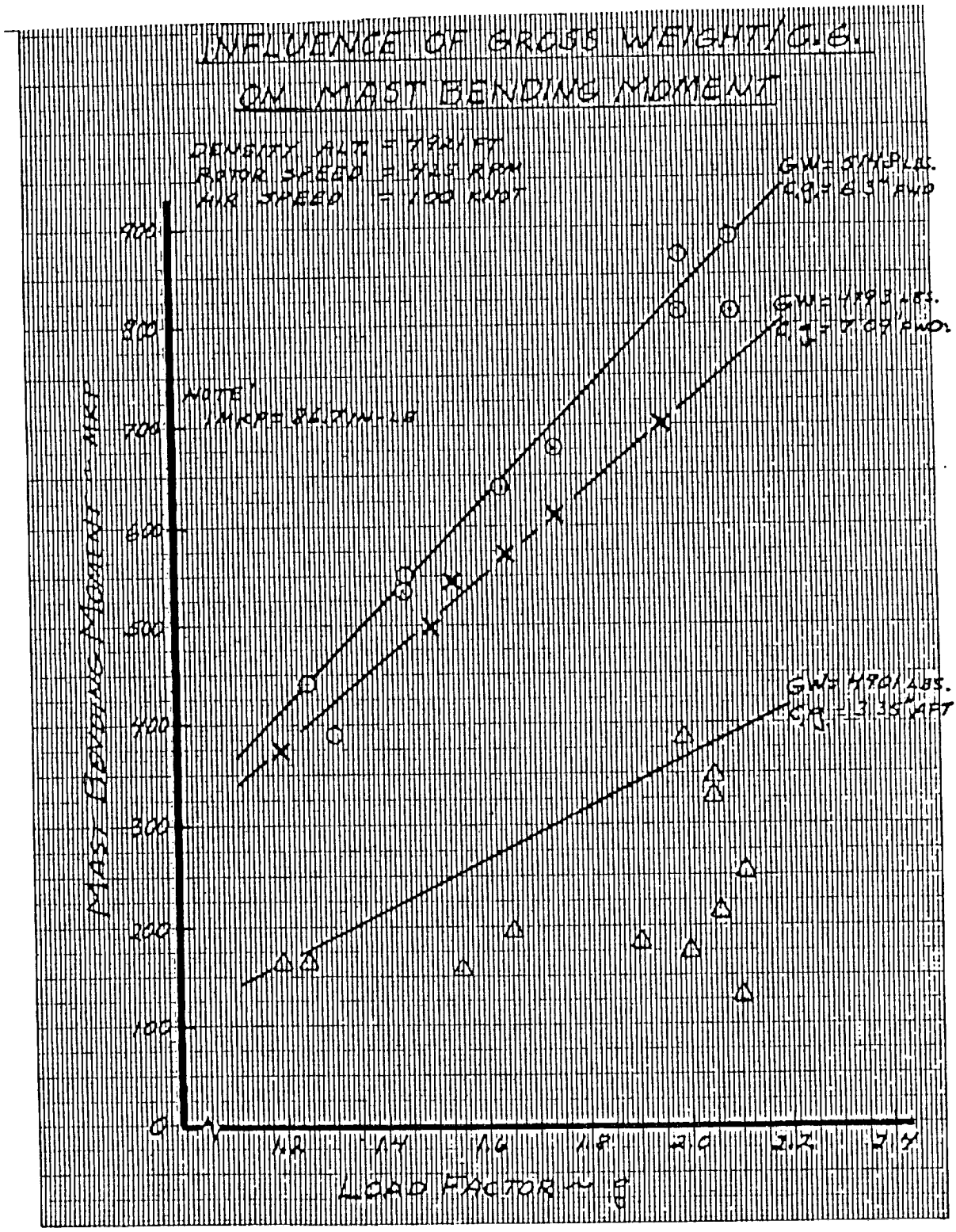

Figure 5. Influence of Gross Weight/C.G. on Mast Bending Moment

Figure 6. Measured Mast Bending Moment of BO-105

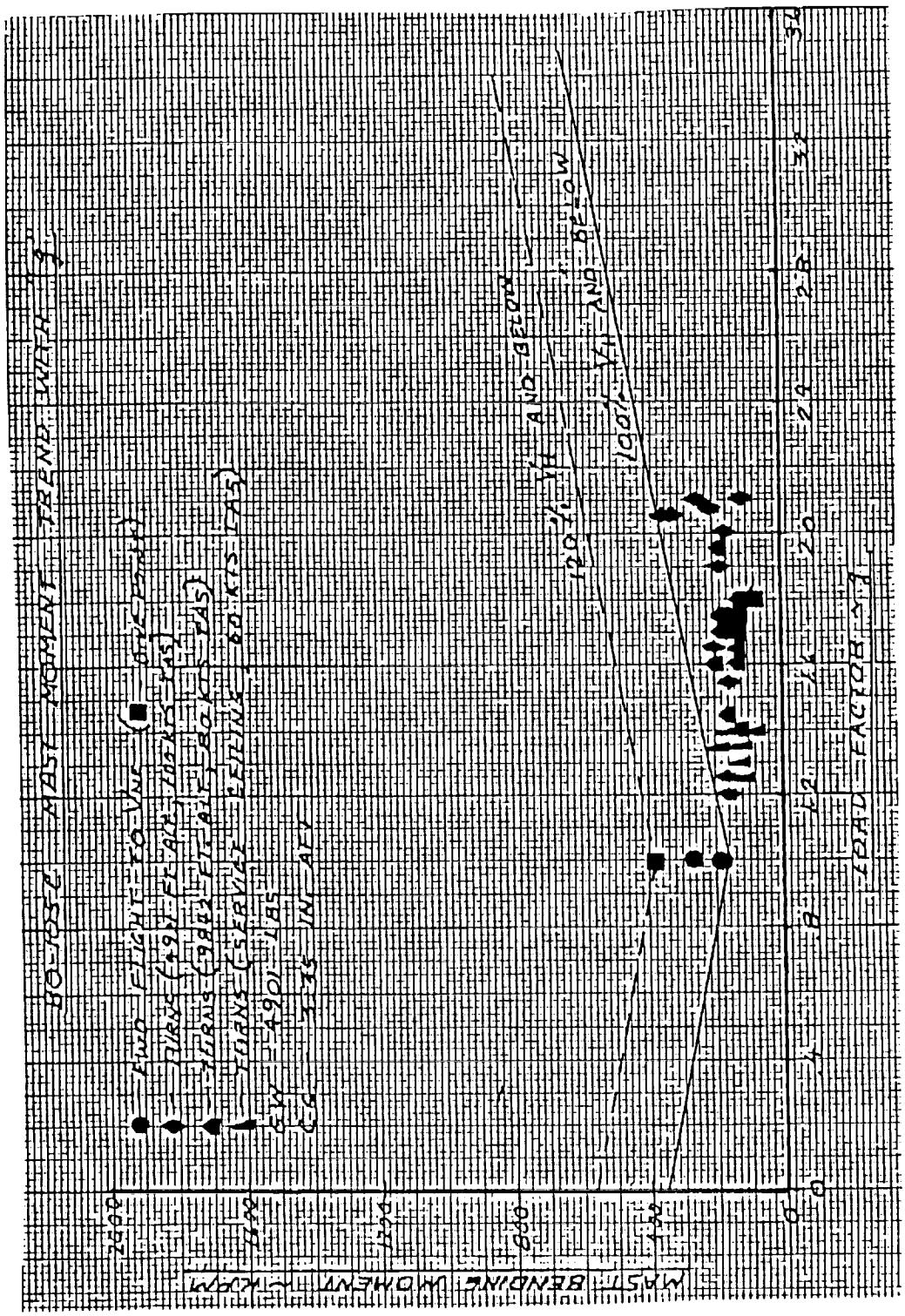

Figure 7. BO-105C Mast Moment Trend with "g"

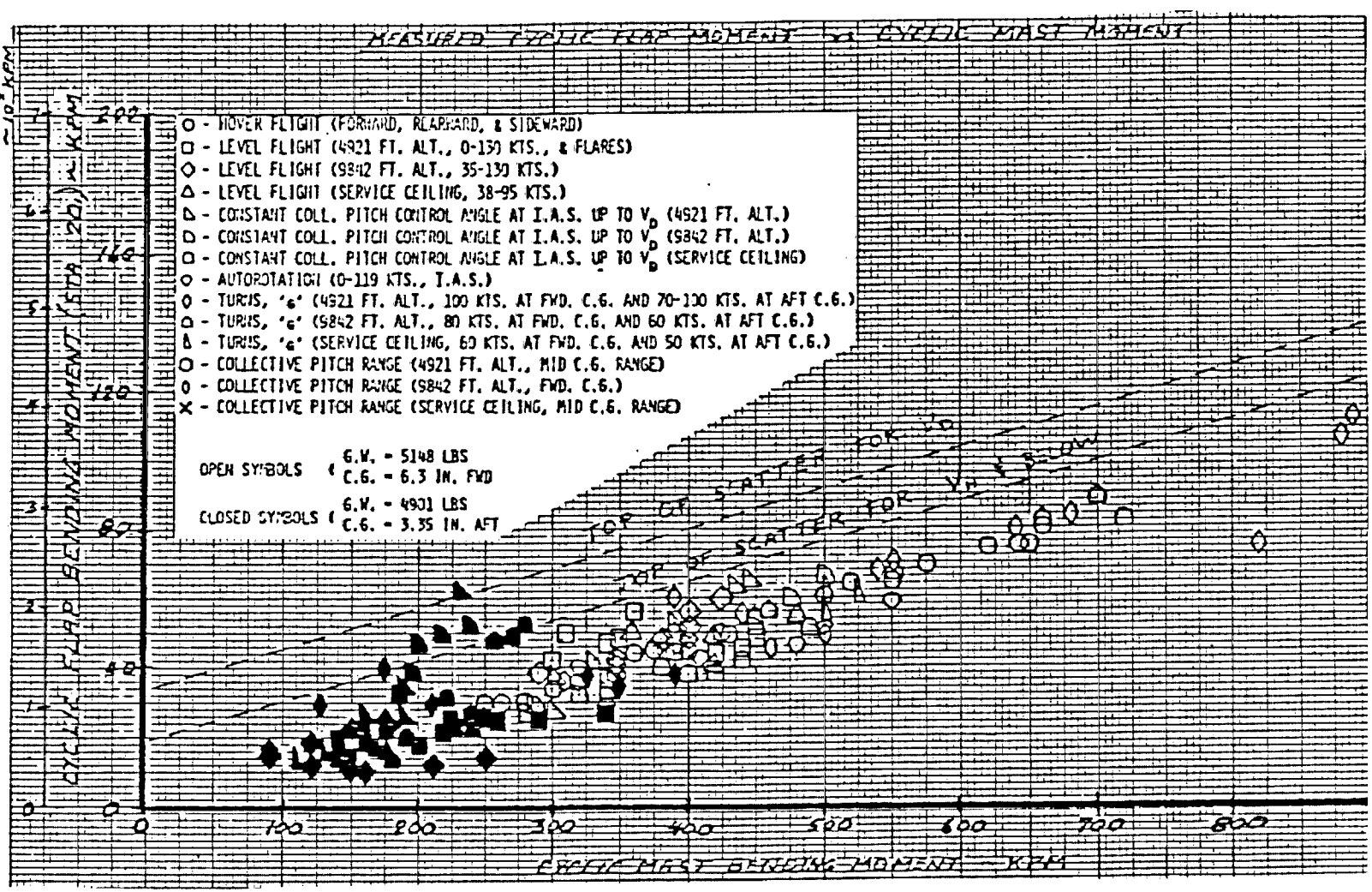

Figure 8. Measured Cyclic Flap Moment vs. Cyclic Mast Moment

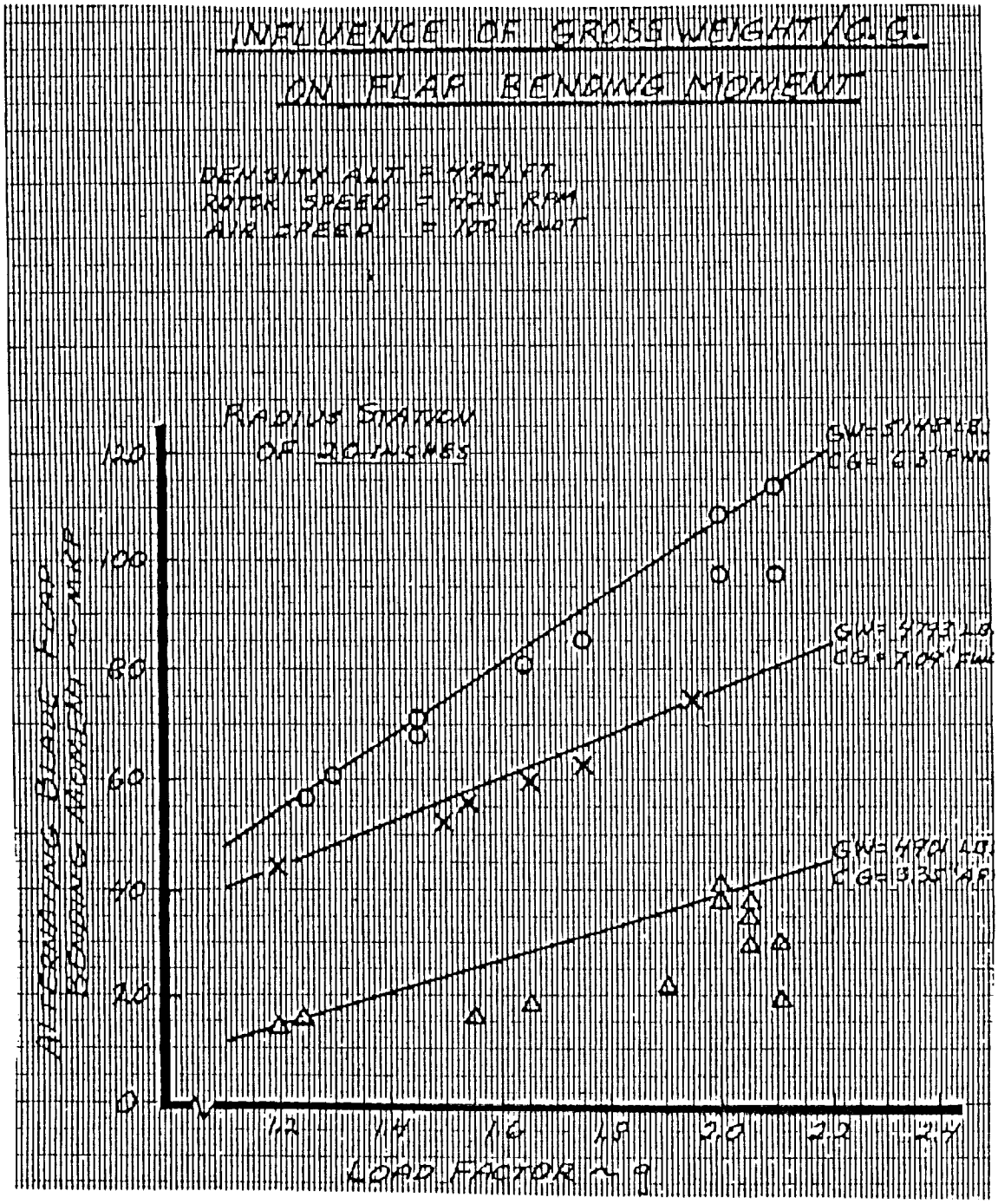

Figure 9. Influence of Gross Weight/C.G. on Flap Bending Moment

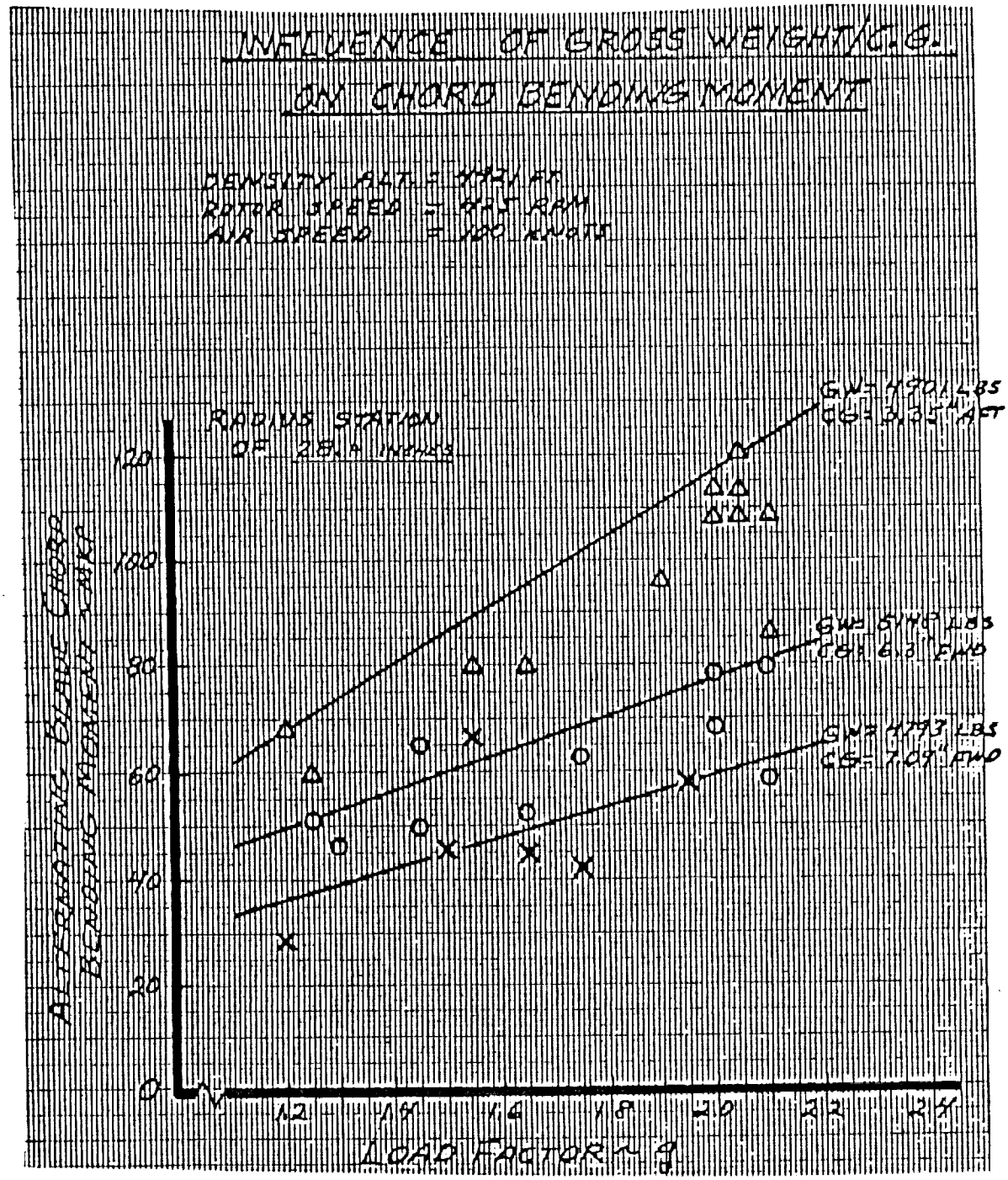

Figure 10. Influence of Gross Weight/C.G. on Chord Bending Moment

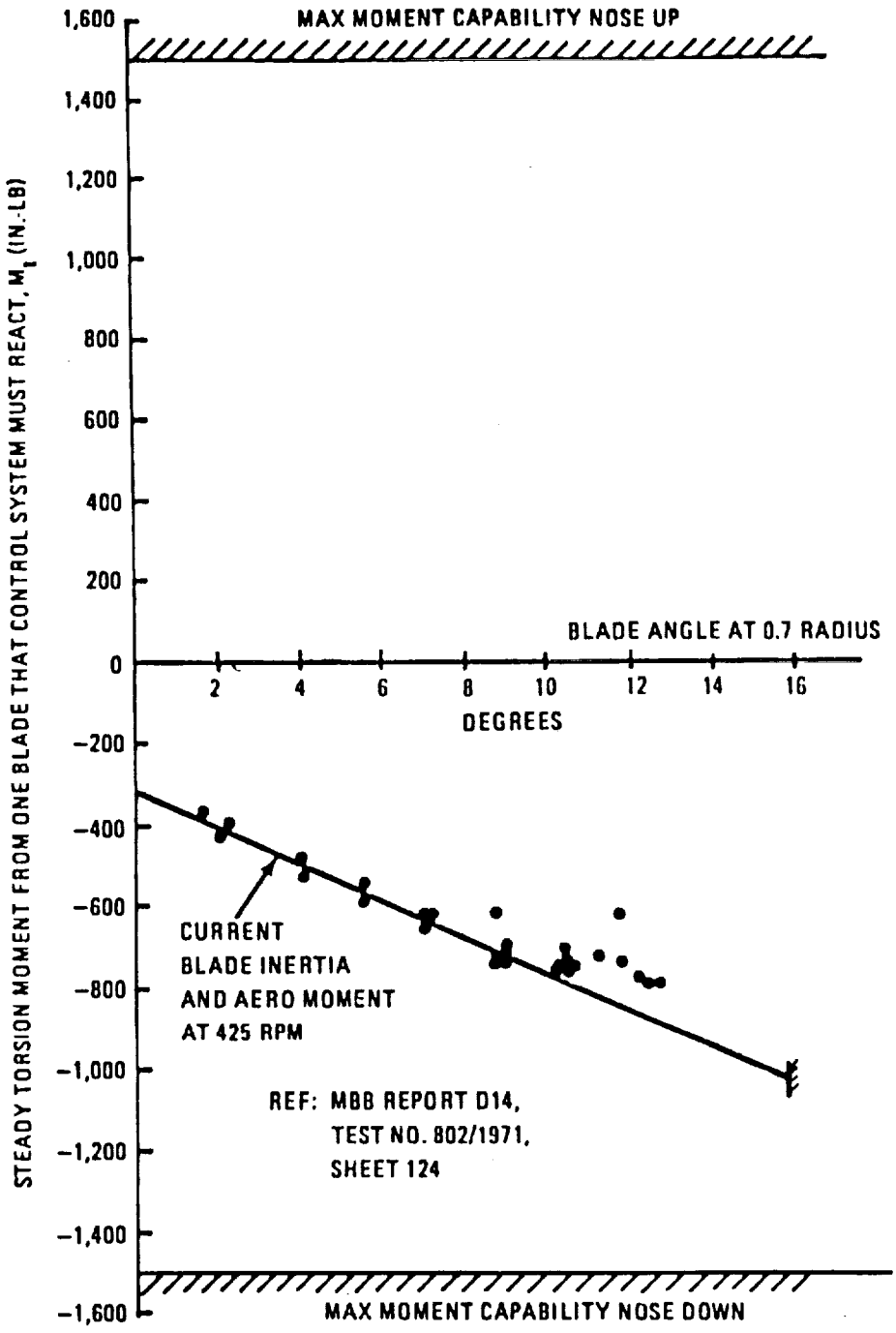

Figure 11. Steady Torsion Moment that Current BO-105 Control System Sees from One Blade with Pitch Bearings

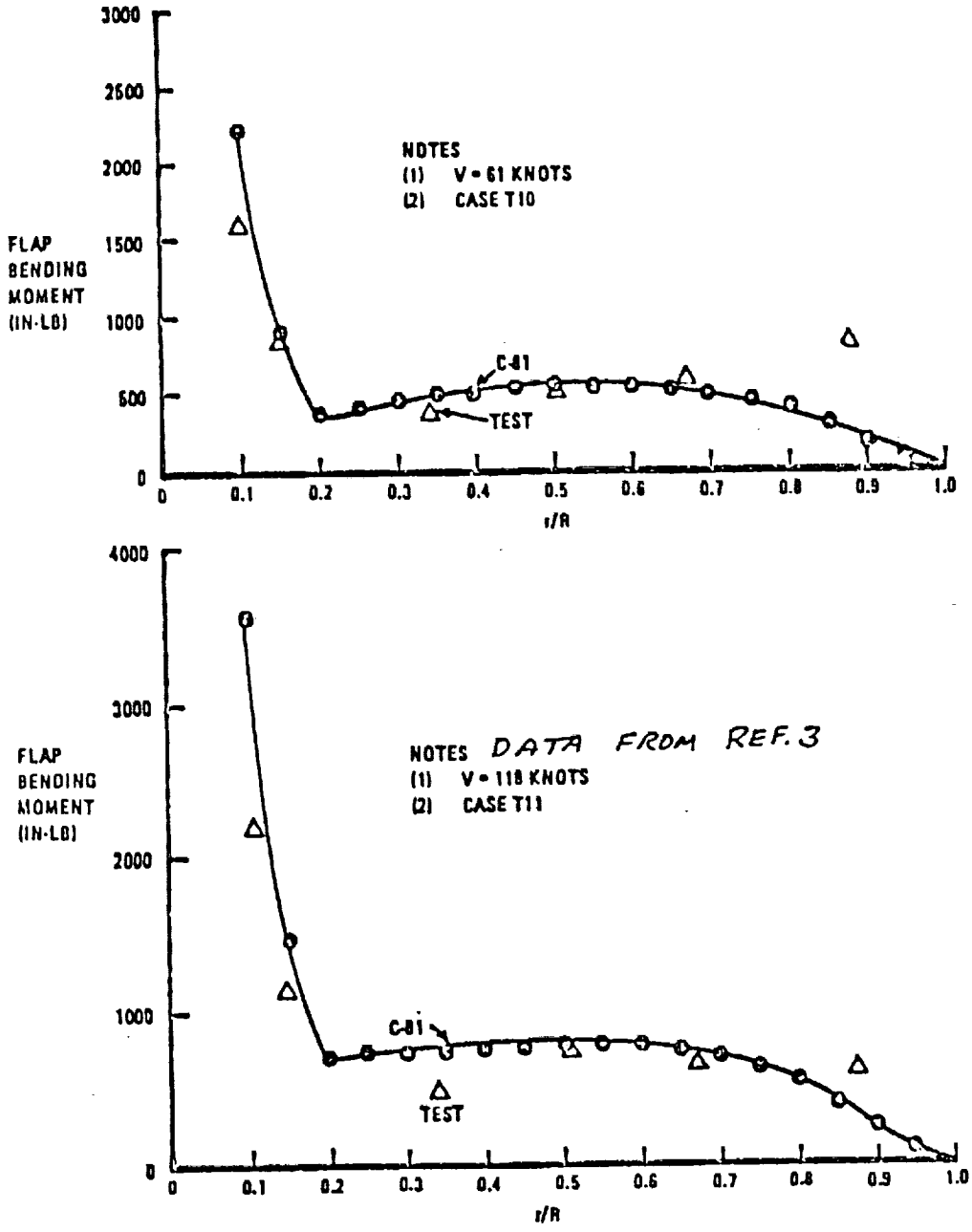

Figure 12. Alternating Flap Bending Moment vs. Blade Radius at 61 and 110 Knots

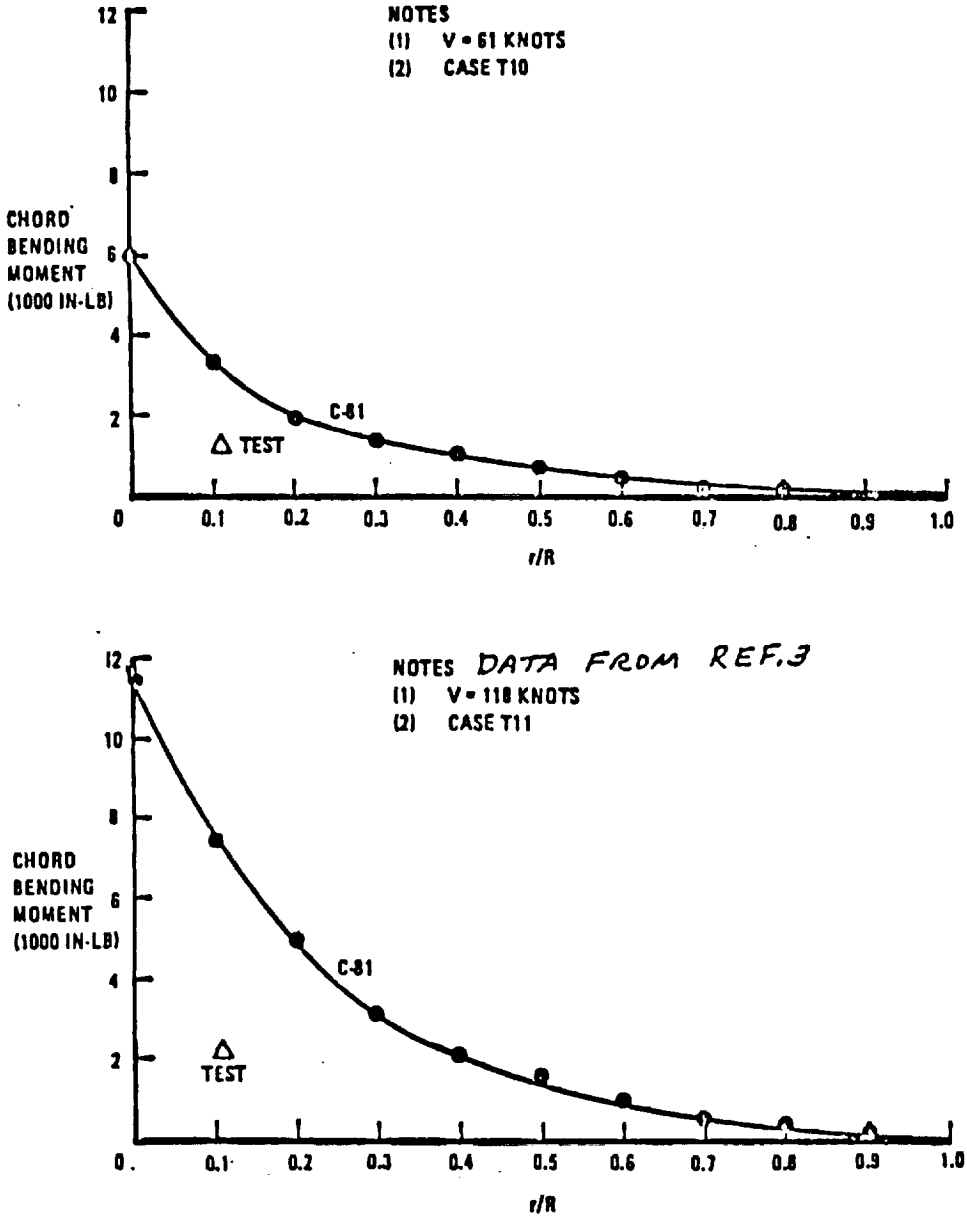

Figure 13. 1/Rev Chord Bending Moment Amplitude vs. Radius at 61 and 118 Knots

APPENDIX 2

Discussion on Torsional and Bending Strains
(Single vs. Dual Bellows)

1.0 Laminate Thickness and Radius of Curvature

2.0 Torsion

3.0 Flexural and Bending Strains Due to Tilt

4.0 Conclusions

1.0 LAMINATE THICKNESS AND RADIUS OF CURVATURE

When the bellows is used to transmit rotor torque, the thickness of the laminate is proportioned to the torque and shear strength of the material. In flexure, the surface strains are also proportional to the laminate thickness as well as the radius of bending curvature.

For maximum life (minimum surface strain), it follows that the laminate thickness should be minimized and the bellows radius of bending curvature should be maximized.

2.0 TORSION

If torque is shared between two bellows as shown in Figures 2 and 3 of the main text, the laminate thickness can be reduced to one-half of that required in the single bellows shown in Figure 4 of the main text. This favors a dual bellows system.

3.0 FLEXURAL AND BENDING STRAINS DUE TO TILT

In studying the natural deflection of a bellows structure (such as corrugated hose or "Sealol" bellows type flexible shaft coupling), it can be seen that the tilt at the end produces a constant radius of curvature (R) as shown in Figure 1(a). This radius of curvature is proportional to the tilt (ø) and the bellows length (h).

For bending, therefore, it follows that the bellows length (h) should be maximized if the radius of curvature is to be maximized for a fixed value of hub tilt (ø), thus minimizing bending strains due to tilt. This suggests that a single bellows may be better with regard to bending strains if overall hub height is to be minimized.

It must also be noted that the point of rotation with zero lateral translation for the single bellows is at the intersection of the normal axes of the tilted end planes which occurs at one-half the bellows length from each end. This is important since it is necessary for the flexures to maintain coincidence of the attachments to the tilted hub disc as shown in Figures 1(b) and 2.

When comparing the single and dual bellows arrangement for radius of curvature, Figure 2 shows that each of the dual bellows must inflex; but the single bellows shown in Figure 1(a) will not inflex if the center of the hub tilt is at the point of rotation with zero translation as in the single bellows concept of Figure 4 in the main text.

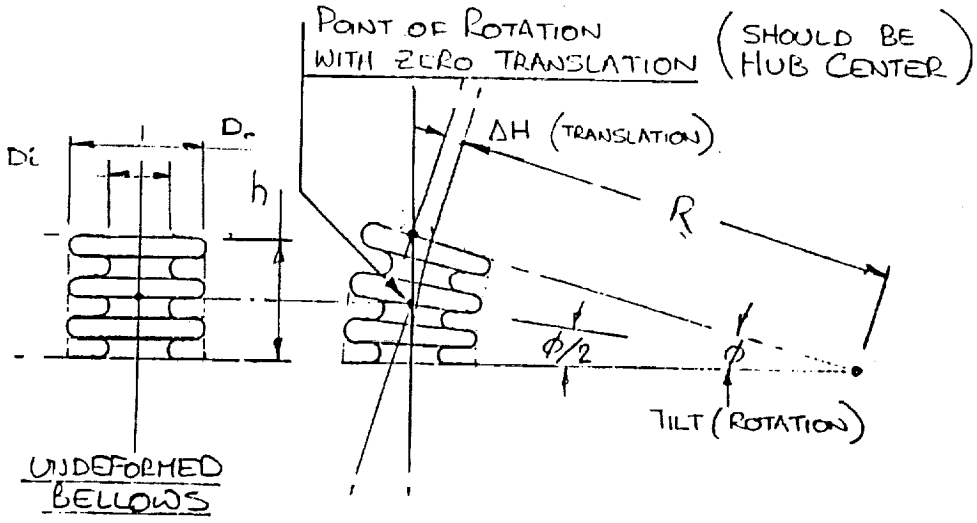

Figure 1a. Natural Tilt of a Bellows

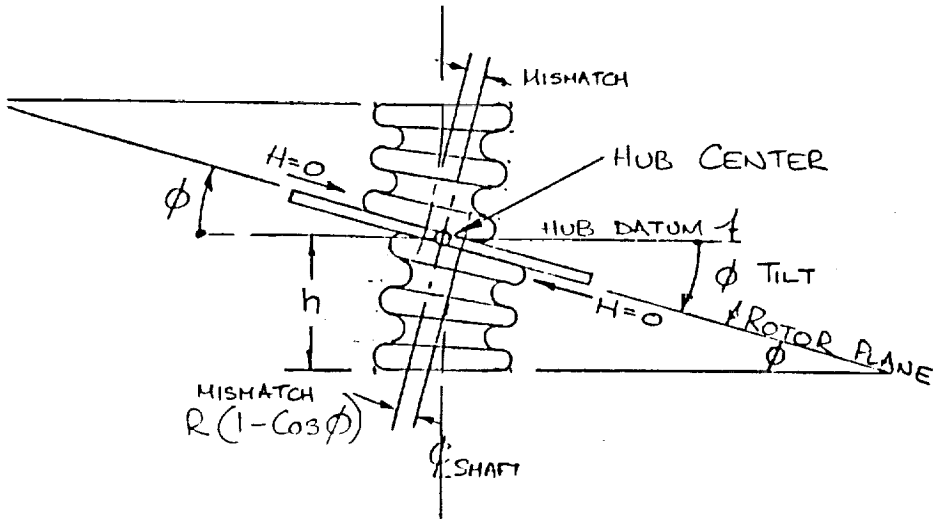

Figure 1b. Natural Deflection of a Bellows Structure

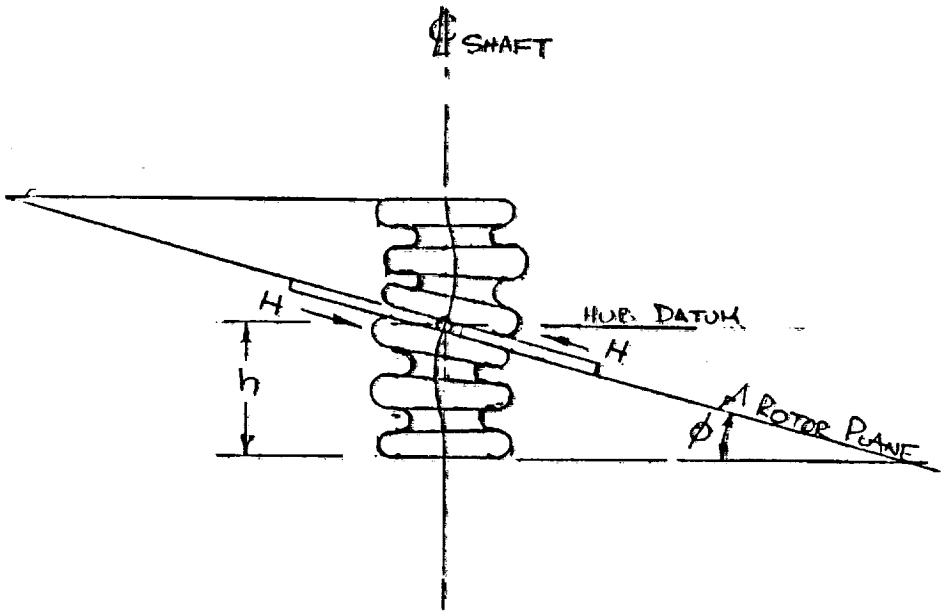

Figure 2. Forced Deflection of a Bellows Structure

4.0 CONCLUSIONS

An analysis of the radii of curvature is as shown in Figure 3 which concludes that the radius of curvature for the dual bellows is four times that in the single which suggests that for the same laminate thickness, the flexural stress in the dual bellows is higher by the same proportion, however, if the credit of one-half the laminate thickness is taken due to torque sharing, the dual bellows will have only twice the flexural stress levels experienced by the single bellows.

RADIUS OF CURVATURE = RADIUS OF BENDING + RADIUS OF INFLEXION.

FOR A DUAL BELLOWS

RADIUS OF BENDING = R

RADIUS OF INFLEXION = $\pm R/2$

MINIMUM RADIUS OF CURVATURE = $R/2$

FOR A SINGLE BELLOWS

RADIUS OF BENDING = 2R

RADIUS OF INFLEXION = 0

MINIMUM RADIUS OF CURVATURE = 2R

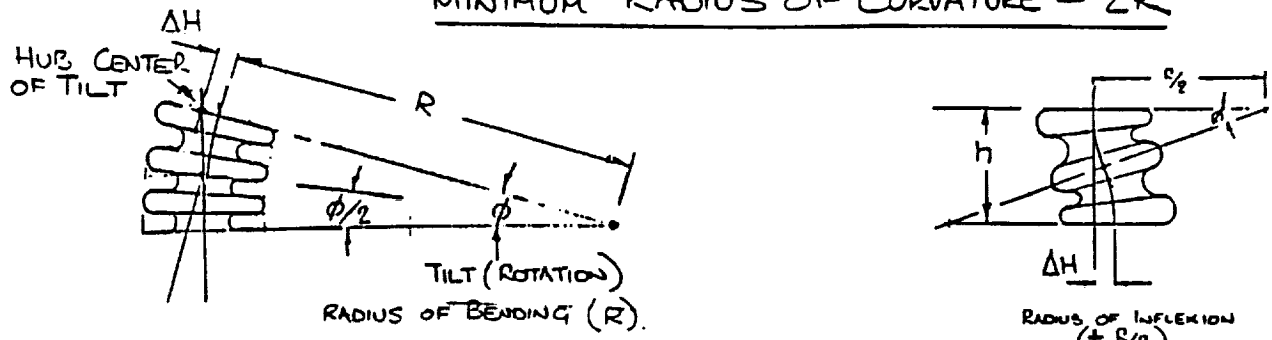

FLEXURE MODES – DUAL

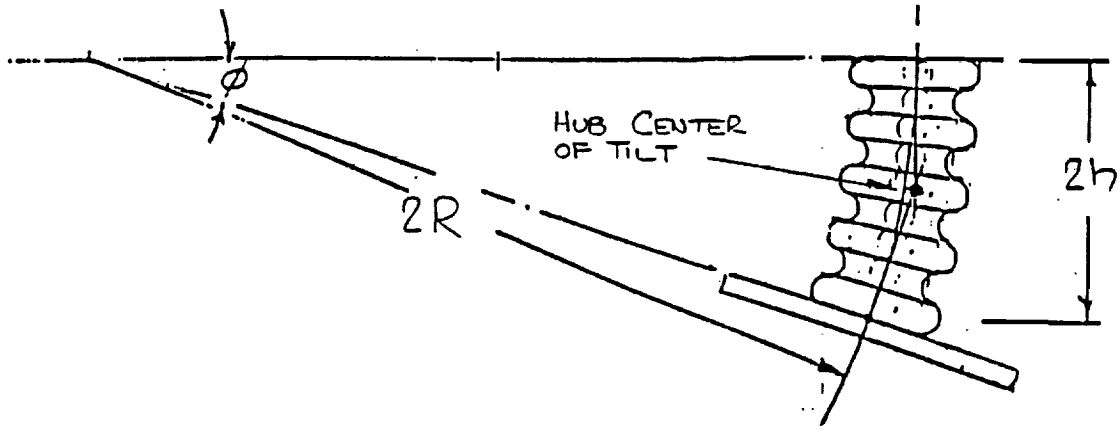

FLEXURE MODE – SINGLE

Figure 3. Flexure Modes

APPENDIX 3

Derivation of Approximate Stiffness and Stress Distribution Analysis Methodology for the Preliminary Sizing of the Bellows or Hairpin Flexures being Considered for the Soft Hub Concept.

(See Appendix 4 for a more rigorous analysis)

1.0 Flexure Attachment Options

2.0 Fixed Ended Flexures
- 2.1 Flexure Loads
- 2.2 Bending Moment Distributions
- 2.3 Contribution to Hub Stiffness

3.0 Pinned/Fixed Flexures

4.0 Hub Stiffness

1.0 FLEXURE ATTACHMENT OPTIONS

For the attachment of the drive torque bellows to the shaft and to the rotor, there were the four variations illustrated below in Figure 1. The objective of this appendix is to decide which of the options provides the required stiffneess to the Soft Hub for the least penalty in flexure stress level.

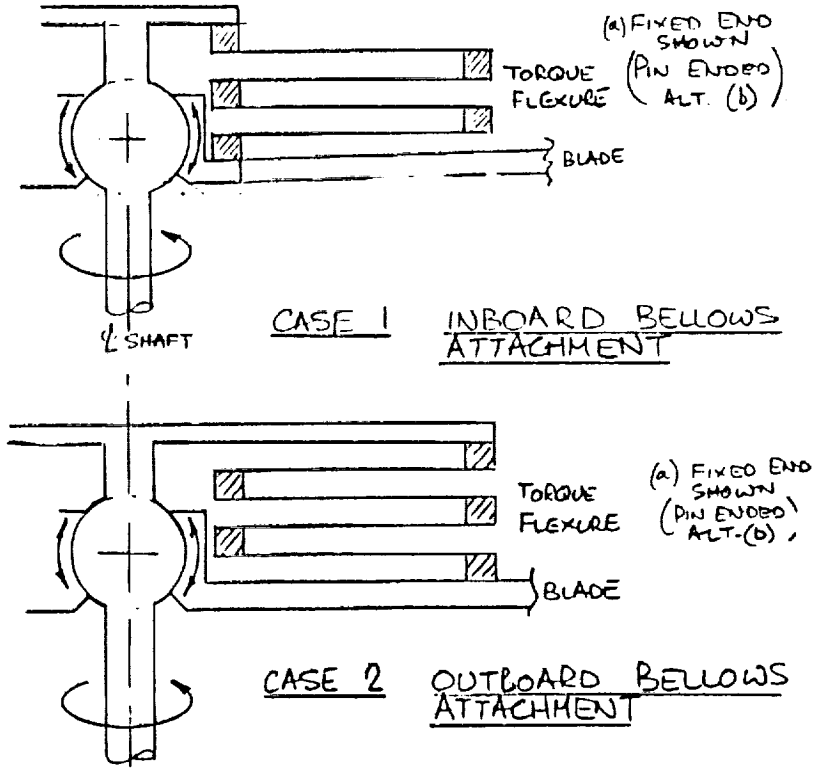

Figure 1. Bellows Attachment Options

These options are graphically simplified in Figure 2 which shows that Case 2 may have an advantage over Case 1 since the end of the cantilevered flexure is already sloping down, due to the vertical shear V_o, in the direction of the hub tilt.

2.0 FIXED ENDED FLEXURES

Normal or Reversed Elements?

The tilting motion of the hub will introduce both deflection and end moment in the torque flexure. There are two choices of installation, one of which may be better than the other in strength and stiffness. Both options compared in this study are shwon in Figure 2.

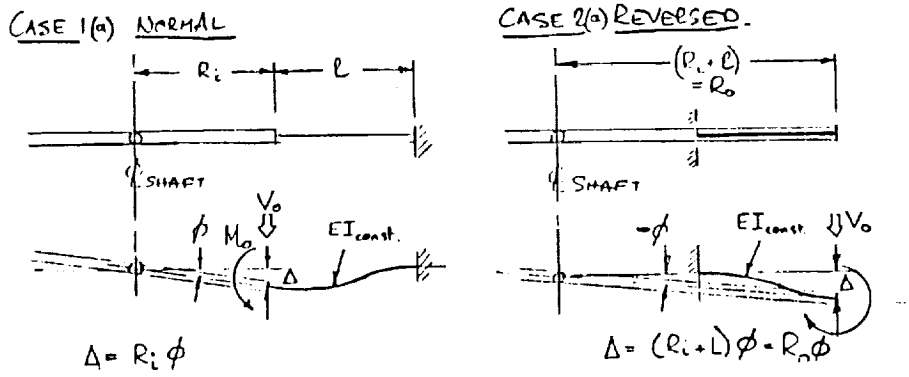

Figure 2. Installation Options

Cantilevered Flexure

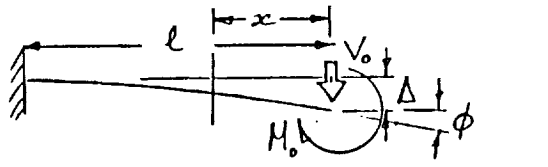

CASE 1: $\frac{\Delta}{R_i} = \phi$ CASE 2: $\frac{\Delta}{R_o} = -\phi$

$$\Delta = \frac{V_o \ell^3}{3EI} + \frac{M_o \ell^2}{2EI} \quad \text{(1)}$$

$$\phi = -\frac{V_o \ell^2}{2EI} - \frac{M_o \ell}{EI} \quad \text{(2)}$$

$$M_x = M_o + V_o x \quad \text{(3)}$$

2.1 FLEXURE LOADS

FLEXURE LOADS

CASE 1: VERT. DEFLN $\Delta = R_L \cdot \phi$

$$\phi = \frac{\Delta}{R_L}$$

FROM ① $$\phi = \frac{1}{3}\cdot\frac{V_0 \ell^2}{EI}\left(\frac{\ell}{R_1}\right) + \frac{1}{2}\frac{M_0 \ell}{EI}\left(\frac{\ell}{R_1}\right) \quad \text{——③}$$

FROM ② $$\phi = -\frac{1}{2}\frac{V_0 \ell^2}{EI} - \frac{M_0 \ell}{EI}$$

OR $$\frac{\phi}{2}\left(\frac{\ell}{R_1}\right) = -\frac{1}{4}\frac{V_0 \ell^2}{EI}\left(\frac{\ell}{R_1}\right) - \frac{1}{2}\frac{M_0 \ell}{EI}\left(\frac{\ell}{R_1}\right) \quad \text{——④}$$

$$V_0 = 2\frac{EI}{\ell^2}\cdot\left(3+6\left(\frac{R_1}{\ell}\right)\right)\cdot\phi$$

$$M_0 = -\frac{EI}{\ell}\left(4+6\left(\frac{R_1}{\ell}\right)\right)\cdot\phi \quad \text{——I}$$

CASE 2: VERT. DEFLN $\Delta = R_0 \cdot \phi$

$$\phi = \frac{\Delta}{R_0}$$

FROM ① $$\phi = -\frac{1}{3}\frac{V_0 \ell^2}{EI}\left(\frac{\ell}{R_0}\right) - \frac{1}{2}\frac{M_0 \ell}{EI}\left(\frac{\ell}{R_0}\right)$$

FROM ② $$\phi = -\frac{1}{2}\frac{V_0 \ell^2}{EI} - \frac{M_0 \ell}{EI}$$

OR $$\frac{\phi}{2}\left(\frac{\ell}{R_0}\right) = -\frac{1}{4}\frac{V_0 \ell^2}{EI}\left(\frac{\ell}{R_0}\right) - \frac{1}{2}\frac{M_0 \ell}{EI}\left(\frac{\ell}{R_0}\right)$$

$$V_0 = 2\frac{EI}{\ell^2}\left(3-6\left(\frac{R_0}{\ell}\right)\right)\cdot\phi$$

$$M_0 = -\frac{EI}{\ell}\left(4-6\left(\frac{R_0}{\ell}\right)\right)\cdot\phi \quad \text{——II}$$

2.2 BENDING MOMENT DISTRIBUTIONS

CASE 1: FROM I, $M_0\left[\frac{\ell}{EI}\cdot\frac{1}{\phi}\right] = -\left(4+6\left(\frac{R_L}{\ell}\right)\right)$

FROM EQ. (3), $\frac{M_x}{\phi} = \left[-\frac{EI}{\ell}\left(4+6\left(\frac{R_L}{\ell}\right)\right) + \frac{2EI}{\ell^2}\left(3+6\left(\frac{R_L}{\ell}\right)\cdot x\right)\right]$

OR $M\left[\frac{\ell}{EI}\cdot\frac{1}{\phi}\right] = \left[2\left(3+6\left(\frac{R_L}{\ell}\right)\right)\cdot\frac{x}{\ell} - \left(4+6\left(\frac{R_L}{\ell}\right)\right)\right]$ (15.9, 2.94, 2 i L)

THE INFLEXION POINT ($M=0$) IS WHERE $\frac{x}{\ell} = \frac{2+3\left(\frac{R_L}{\ell}\right)}{3+6\left(\frac{R_L}{\ell}\right)}$

CASE 2: FROM II, $M_0\left[\frac{\ell}{EI}\cdot\frac{1}{\phi}\right] = \left(4-6\left(\frac{R_0}{\ell}\right)\right)$

FROM EQ. 3. $\frac{M_x}{\phi} = \left[\frac{EI}{\ell}\left(4-6\left(\frac{R_0}{\ell}\right)\right) - \frac{2EI}{\ell^2}\left(3-6\left(\frac{R_0}{\ell}\right)\right)\cdot x\right]$

OR $M\left[\frac{\ell}{EI}\cdot\frac{1}{\phi}\right] = \left[-2\left(3-6\left(\frac{R_0}{\ell}\right)\right)\frac{x}{\ell} + \left(4-6\left(\frac{R_0}{\ell}\right)\right)\right]$ (-6.94)

THE INFLEXION POINT ($M=0$) IS WHERE $\frac{x}{\ell} = \frac{2-3\left(\frac{R_0}{\ell}\right)}{3-6\left(\frac{R_0}{\ell}\right)}$

IF, FOR EXAMPLE, $R_L = 4.0$ IN, $R_0 = 8.85$ IN, $\ell = 4.85$ (OR WHEN $R_0 = (R_L + \ell)$)
THEN THE MOMENT DISTRIBUTIONS FOR CASES 1 & 2 WOULD BE

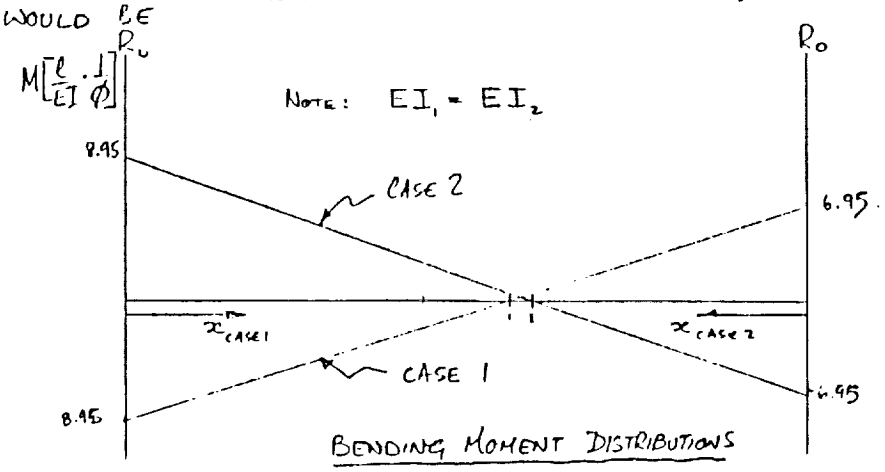

BENDING MOMENT DISTRIBUTIONS

CONCLUSION: The normal and reversed flexures have the same strengths.

2.3 CONTRIBUTION TO HUB STIFFNESS

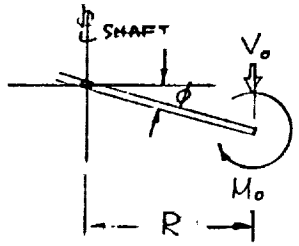

HUB MOMENT = $V_o R + M_o$

HUB STIFFNESS = HUB MOMENT / ϕ

CASE 1.

$$\text{HUB STIFFNESS} = \frac{EI}{\rho}\left[\left(4+6\left(\frac{\rho_i}{\ell}\right)\right)+\left(6+12\left(\frac{\rho_i}{\ell}\right)\right)\frac{\rho_i}{\ell}\right]$$

CASE 2

$$\text{HUB STIFFNESS} = \frac{EI}{\rho}\left[\left(4-6\left(\frac{\rho_o}{\ell}\right)\right)-\left(6-12\left(\frac{\rho_o}{\ell}\right)\right)\frac{\rho_o}{\ell}\right]$$

WHEN $R_o = (R_L + \ell)$ IT HAS BEEN SHOWN THAT BOTH HUB STIFFNESS HAVE THE SAME VALUE

CONCLUSION: The normal and reversed flexures produce the same hub stiffness.

3.0 PINNED/FIXED FLEXURES

Do pinned/fixed flexures offer any advantage of fixed/fixed flexures?

CASE 1(b) NORMAL

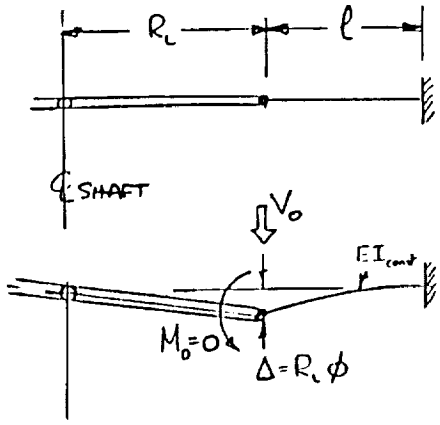

CASE 2(b) REVERSED

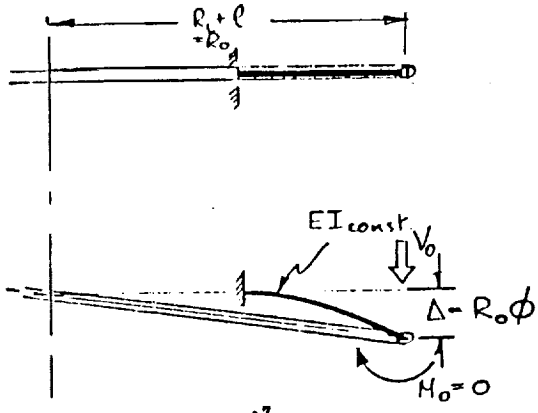

FLEXURE DEFLECTION:

$$\Delta = R_i \cdot \phi \qquad \Delta = \frac{V_o \ell^3}{3EI} \qquad \Delta = R_o \cdot \phi$$

FLEXURE END LOAD:

$$V_o = \frac{3EI \cdot R_i \cdot \phi}{\ell^3} \qquad V_o = \frac{3EI \cdot R_o \cdot \phi}{\ell^3}$$

HUB STIFFNESS

$$K_H = V_o R_i / \phi \qquad K_H = V_o R_o / \phi$$

$$K_H = \frac{3EI_1 R_L^2}{\ell^3} \qquad K_H = \frac{3EI_2 R_o^2}{\ell^3}$$

FLEXURE MOMENT ($= V_o \ell$)

$$M_{max} = \frac{3EI_1 R_L \cdot \phi}{\ell^2} \qquad M_{max} = \frac{3EI_2 R_o}{\ell^2}$$

FLEXURE STRESS

$$\sigma = \frac{Mc_1}{EI_1} = \frac{3R_i \cdot c_1 \cdot \phi}{\ell^2} \qquad \sigma = \frac{Mc_2}{EI_2} = \frac{3R_o c_2 \cdot \phi}{\ell^2}$$

FOR THE SAME STRESS ALLOWABLE

$$c_1 \cdot R_1 = c_2 R_o \quad \text{or} \quad c_2 = c_1 \frac{R_i}{R_o}$$

$$\text{or} \quad EI_2 = EI_1 \left(\frac{R_i}{R_o}\right)^3$$

4.0 HUB STIFFNESS

NORMAL

$$K_{H①} = \left(\frac{3EI_1}{\ell^3}\right) R_i^2$$

REVERSED

$$K_{H②} = \frac{3EI_2}{\ell^3} R_o^2$$

$$= \frac{3EI_1}{\ell^3} R_o^2 \left(\frac{R_i}{R_o}\right)^3$$

$$= \left(\frac{3EI_1}{\ell^3}\right) R_i^3 \left(\frac{R_i}{R_o}\right)$$

$$K_{H②} = K_{H①} * \left(\frac{R_i}{R_o}\right)$$

CONCLUSION: At the same strength, the reversed flexure produces less hub stiffness than the normal.

APPENDIX 4

A Rigorous Analysis for the Stiffness and Bending Moment Distribution of a Folded, Cantilevered Flexure Subjected to Vertical, Radial, and Sloping End Displacements

(Lateral displacements and torsional rotations are not included.)

1.0 Deflection of a Curved 1/2 U-Shaped Beam of Constant EI

2.0 Deflection of a Curved U-Shaped Beam

3.0 Bellows Analysis

1.0 DEFLECTION OF A CURVED 1/2 U-SHAPED BEAM OF CONSTANT EI

By Castigliano,

$$\Delta_A = \frac{1}{EI}\int_{S=A\to C} M\frac{\partial M}{\partial V_o}\,ds$$

and

$$\alpha_A = \frac{1}{EI}\int_{S=A\to C} M\frac{\partial M}{\partial M_o}\,ds$$

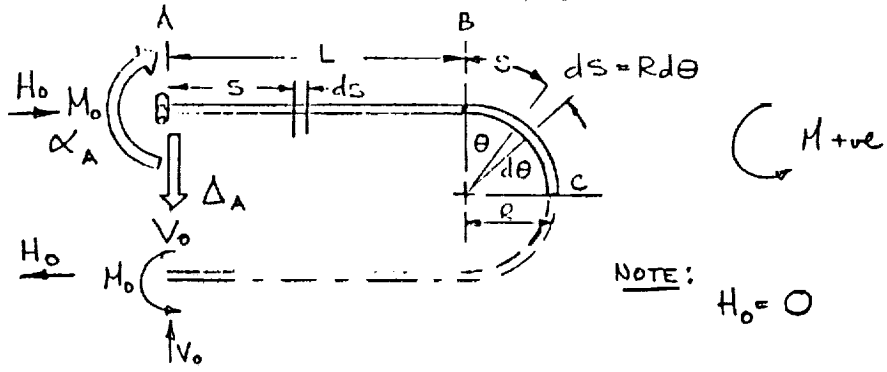

ELEMENT	M =	$\frac{\partial M}{\partial V_o}$ =	$\frac{\partial M}{\partial M_o}$ =
A → B	$V_o.S - M_o$	S	-1
B → C	$V_o(L+RSin\theta) - M_o$	$(L+RSin\theta)$	-1

VERTICAL DEFLECTION

For A → B $\quad M\frac{\partial M}{\partial V_o} = V_o S^2 - M_o.S$

$$I_{V_o} = \frac{1}{EI}\int_0^L (V_o S^2 - M_o S)\,ds = \frac{1}{EI}\left[\frac{1}{3}V_o L^3 - \frac{1}{2}M_o L^2\right]$$

For B → C

$$M\frac{\partial M}{\partial V_o} = V_o(L+RSin\theta)^2 - M_o(L+RSin\theta)$$

$$I_{V_o} = \frac{1}{EI}\left[\int_0^{\pi/2} V_o.R(L+RSin\theta)^2.d\theta - \int_0^{\pi/2} M_o R(L+RSin\theta)\,d\theta\right]$$

$$= \frac{1}{EI}\left[V_o\left(\frac{\pi}{2}RL^2 + \frac{\pi}{4}R^3 + 2R^2L\right) - M_o\left(R^2 - \frac{\pi}{2}RL\right)\right]$$

End Rotation

For $A \rightarrow B$,

$$M\frac{\partial M}{\partial M_0} = -(V_0 S - M_0)$$

$$I_{M_0} = -\frac{1}{EI}\int_0^L (V_0 S - M_0)\,ds = -\frac{1}{EI}\left[\frac{1}{2}V_0 L^2 - M_0 L\right]$$

For $B \rightarrow C$:

$$M\frac{\partial M}{\partial M_0} = -\frac{R}{EI}\int_0^{\pi/2} (V_0 L + V_0 R\sin\theta - M_0)\,d\theta$$

$$= -\frac{R}{EI}\left[V_0 L\frac{\pi}{2} + V_0 R - M_0\frac{\pi}{2}\right]$$

SUMMARY.

$$\Delta_A = V_0 \cdot \frac{1}{EI}\left[\frac{L^3}{3} + \frac{\pi}{2}L^2 R + 2LR^2 + \frac{\pi}{4}R^3\right] - M_0 \cdot \frac{1}{EI}\left[\frac{L^2}{2} - \frac{\pi}{2}R \cdot L + R^2\right]$$

$$\alpha_A = -V_0 \cdot \frac{1}{EI}\left[\frac{L^2}{2} + \frac{\pi}{2}LR + R^2\right] + M_0 \cdot \frac{1}{EI}\left[\frac{\pi}{2} + L\right]$$

2.0 DEFLECTION OF A CURVED U-SHAPED BEAM

Deflections and slopes are twice 1/2 beam values.

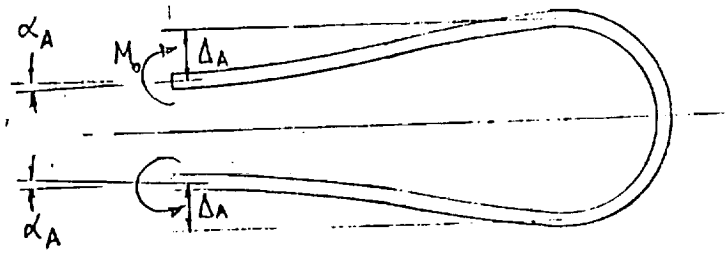

3.0 BELLOWS ANALYSIS

Unit Perimeter Length (DP = 1)

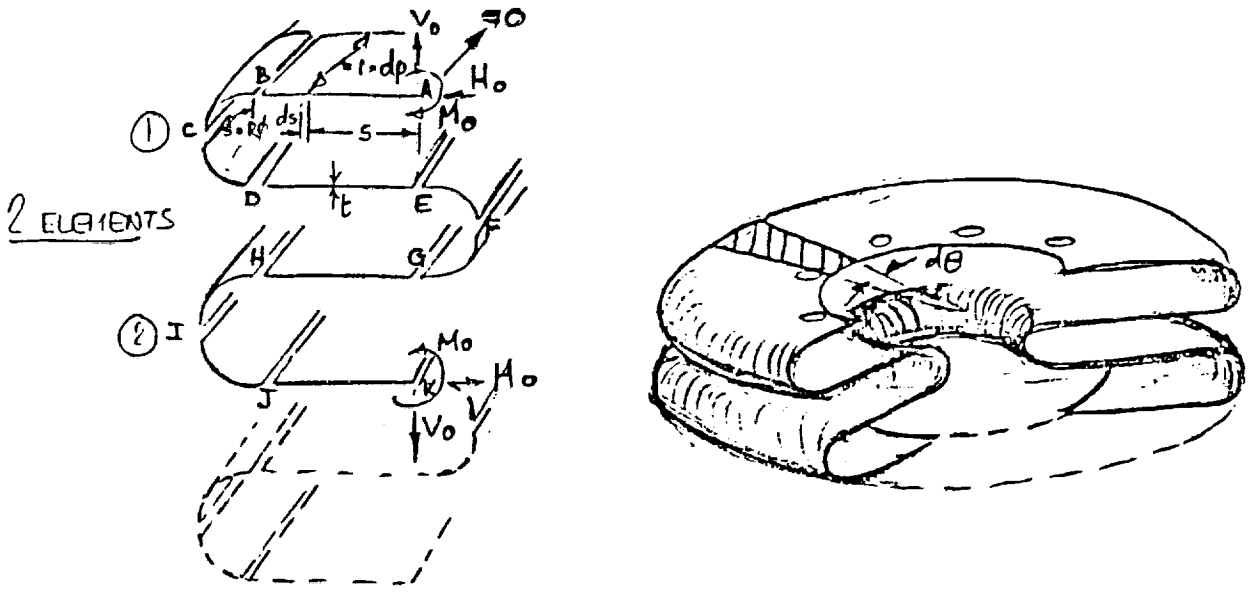

Figure 1. Radial Slice From a Bellows Flexure

Figure 1 shows a two-element bellows structure and a loads diagram showing how a radial slice (flexure) of the structure is sectioned into elements for analysis purposes.

The following sheets present a simplified analysis of each flexural slice. For a constant $EI_{Bending}$, using Castigliano's theorem,

$$\theta_{M_o} = \int_0^{\ell} \frac{M_s}{EI} \cdot \frac{\partial M_s}{\partial M_o} \cdot ds \,, \quad \Delta_{V_o} = \int_0^{\ell} \frac{M_s}{EI} \cdot \frac{\partial M_s}{\partial V_o} \cdot ds \,, \quad \Delta_{H_o} = \int_0^{\ell} \frac{M_s}{EI} \cdot \frac{\partial M}{\partial H_o} \cdot ds$$

By formulating the above 3 equations and simultaneously solving them for the unknowns M_o, V_o, and H_o (since θ_{M_o}, Δ_{V_o}, and Δ_{H_o} are known functions of the bellows geometry), the normal bending moment distribution in the slice of constant width can be determined.

The rotation and in-plane (transverse, sideways, lateral) displacements of the slice, caused by hub tilt about the orthogonal axis, can also be resolved in terms of the lateral bending moment distribution and slice element (flexure) rotation as shown in Figure 2.

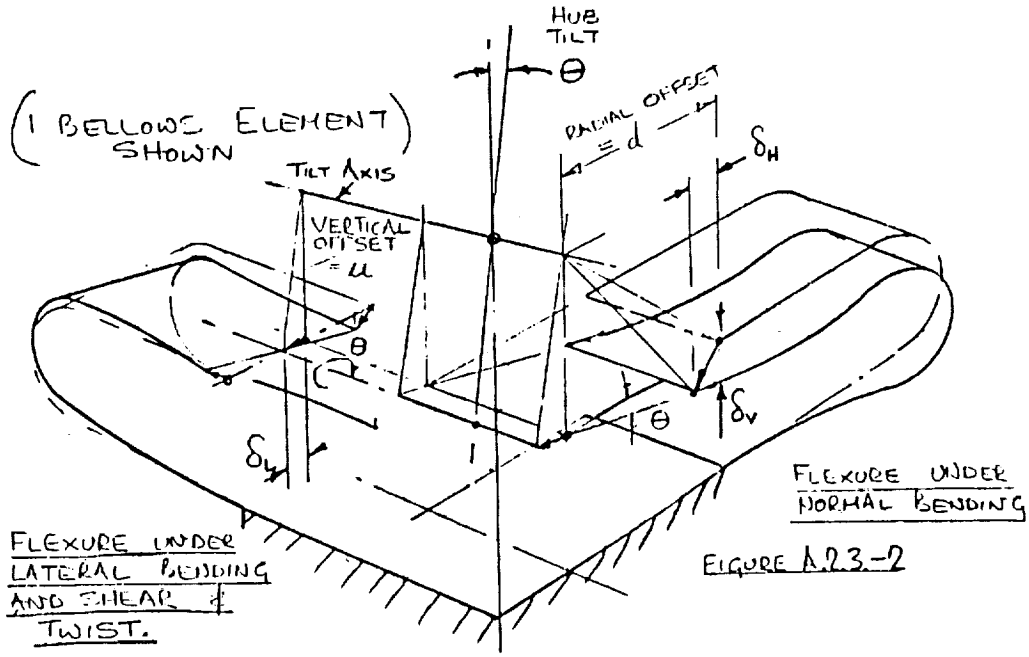

FIGURE A.2.3-2

TILT Θ RESULTS IN: → FLEXURE TORSION & NORMAL BENDING

LINEAR DISPLACEMENTS:

$\delta_V = -u(1-\cos\theta) + d\sin\theta$ → FLXR. NORMAL BENDING

$\delta_{H1} = u\sin\theta + d(1-\cos\theta)$ → FLXR. NORMAL BENDING

$\delta_L = u\sin\theta$ → FLXR. LATERAL BENDING & SHEAR.

Figure 2. Flexure Displacements

This analysis considers the vertical and radial deflections of the flexure together with the end rotations due to hub tilt. Flexure twist and lateral displacements can be considered independently.

MOMENT EQUATION FOR ELEMENTS

With reference to figure 1.,

ELEMENT	BENDING MOMENT (H_s) AT S	
STRAIGHT :-		
A → B	$H_o - V_o.S$	
D → E	$H_o + V_o.S - V_o.L$	$-2H_o.r$
G → H	$H_o - V_o.S$	$-4H_o.r$
J → K	$H_o - V_o.S - V_o.L$	$-6H_o.r$
RADIUS :-	$(S = r.\theta)$	
B → C	H_o	$-V_o.L - V_o.r\,Sin\phi - H_o.r + H_o.r\,Cos\phi$
C → D	H_o	$-V_o.L - V_o.r\,Cos\phi - H_o.r - H_o.r\,Sin\phi$
E → F	H_o	$+V_o.r\,Sin\phi - 3H_o.r + H_o.r\,Cos\phi$
F → G	H_o	$+V_o.r\,Cos\phi - 3H_o.r - H_o.r\,Sin\phi$
H → I	H_o	$-V_o.L + V_o.r\,Sin\phi - 5H_o.r + H_o.r\,Cos\phi$
I → J	H_o	$-V_o.L - V_o.r\,Cos\phi - 5H_o.r - H_o.r\,Sin\phi$

PARTIAL DIFFERENTIALS

ELEMENT	$\frac{\partial M_s}{\partial V_o}$	$\frac{\partial M_s}{\partial H_o}$	$\frac{\partial M_s}{\partial M_o}$
STRAIGHT :-			
A→B	$-S$	0	1
D→E	$+S-L$	$-2r$	1
G→H	$-S$	$-4r$	1
J→K	$-S-L$	$-6r$	1
RADIUS :-			
B→C	$-L-r\sin\phi$	$-r+r\cos\phi$	1
C→D	$-L-r\cos\phi$	$-r-r\sin\phi$	1
E→F	$+r\sin\phi$	$-3r+r\cos\phi$	1
F→G	$+r\cos\phi$	$-3r-r\sin\phi$	1
H→I	$-L-r\sin\phi$	$-5r+r\cos\phi$	1
I→J	$-L-r\cos\phi$	$-5r-r\sin\phi$	1

INTEGRAL FOR VERTICAL END DISPLACEMENT (δ_V)

$$\int M \frac{\partial M_s}{\partial V_0} \cdot ds$$

ELEMENT	
A → B.	$I_{AB} = \int (-S)(M_0 - V_0 \cdot S_\cdot) \cdot ds$
D → E	$I_{DE} = \int (+S - L)(M_0 + V_0 \cdot S - V_0 \cdot L) ds$ $- 2H_0 \cdot r$
G → H	$I_{GH} = \int (-S)(M_0 - V_0 \cdot S) \cdot ds$ $- 4H_0 r$
J → K	$I_{KL} = \int (-S - L)(M_0 - V_0 \cdot S - V_0 \cdot L) \cdot ds$ $- 6H_0 \cdot r$

$$\Sigma I = \int_0^L 2(-S) M_0 ds + \int_0^L 2(-L) M_0 ds + \int_0^L 4(S)^2 V_0 \cdot ds + \int_0^L 2L^2 V_0 \cdot ds + \int_0^L 8(S) H_0 r \cdot ds + \int_0^L 8 L \cdot H_0 r \cdot ds$$

ST. ELEMENTS:

$$\Sigma I_{ST.ELE.} = -L^2 M_0 - 2L^2 M_0 + \frac{4}{3} L^3 V_0 + 2L^3 V_0 + 4L^2 r H_0 + 8L^2 r H_0$$

$$\boxed{\Sigma I_{ST.EL.} = -3M_0 L^2 + \frac{10}{3} L^3 V_0 + 12 L^2 r H_0.}$$

B → C.	$I_{BC} = \int_0^{\pi/2} (-L - r\sin\phi)(-M_0 - V_0 \cdot L - V_0 r \sin\phi - H_0 r + H_0 r \cos\phi) \, r \cdot d$
C → D	$I_{CD} = \int_0^{\pi/2} (-L - r\cos\phi)(-M_0 - V_0 L - V_0 r \cos\phi - H_0 r - H_0 r \sin\phi) \, r \cdot d$
E → F	$I_{EF} = \int_0^{\pi/2} (r\sin\phi)(M_0 + V_0 r \sin\phi - 3H_0 r + H_0 r \cos\phi) r \cdot d$
F → G	$I_{FG} = \int_0^{\pi/2} (r\cos\phi)(M_0 + V_0 r \cos\phi - 3H_0 r - H_0 r \sin\phi) r \cdot d$
H → I	$I_{HJ} = \int_{\pi/2}^{0} (-L - r\sin\phi)(M_0 - V_0 L - V_0 r \sin\phi - 5H_0 r + H_0 r \cos\phi) r \, d\phi.$
I → J	$I_{JL} = \int_0^{\pi/2} (-L - r\cos\phi)(M_0 - V_0 L - V_0 r \cos\phi - 5H_0 r - H_0 r \sin\phi) r \, d\phi.$

$$\Sigma I = \int_0^{\pi/2} -4LM \underbrace{(M_0 - V_0 L)}_{(+3H_0 r)} d\phi + \int_0^{\pi/2} r^2 \underbrace{(4LV_0 + H_0)}_{(+3H_0 r)} (\sin\phi + \cos\phi) d\phi + \int_0^{\pi/2} \beta V_0 r^2 d\phi$$

$$\boxed{\Sigma I_{RAD} = -2\pi r L \underbrace{(M_0 - V_0 L + 3H_0 r)}_{+\frac{3}{4} V_0 r} + 0}$$

$$\delta V_0 = \frac{1}{EI} \left[\Sigma I_{ST.ELEM.} + \Sigma I_{RAD\ ELEM.} \right]$$

INTEGRAL FOR HORIZONTAL END DISPLACEMENT (δ_H)

$$\int M \frac{\partial M_s}{\partial H_0} \cdot ds$$

ELEMENT

$A \to B \qquad I_{AB} = 0$

$D \to E \qquad I_{DE} = \int_0^L 2r(M_0 + V_0 \cdot s - V_0 \cdot L)\, ds$

$G \to H \qquad I_{GH} = \int_0^L 2r(M_0 - V_0 \cdot s - 4H_0 \cdot r)\, ds$

$J \to K \qquad I_{KL} = \int_0^L 2r(M_0 - V_0 \cdot s - V_0 \cdot L - 6H_0 \cdot r)\, ds$

ST. ELEMENTS:

$$\boxed{\Sigma I_{ST.\,ELEM} = 6rH_0 L - 5rV_0 L^2 - 20r^2 H_0 L}$$

$L \to C \qquad I_{AC} = \int_0^{\pi/2} -r^2(1-\cos\phi)(M_0 - V_0 L - V_0 r \sin\phi - H_0 r + H_0 r\cos\phi)\, d\phi$

$C \to D \qquad I_{CD} = \int_0^{\pi/2} -r^2(1+\sin\phi)(M_0 - V_0 L - V_0 r\cos\phi - 1H_0 r - H_0 r\sin\phi)\, d\phi$

$E \to F \qquad I_{EF} = \int_0^{\pi/2} -r^2(3-\cos\phi)(M_0 + V_0 r\sin\phi - 3H_0 r + H_0 r\cos\phi)\, d\phi$

$F \to G \qquad I_{FG} = \int_0^{\pi/2} -r^2(3+\sin\phi)(M_0 + V_0 r\cos\phi - 3H_0 r - H_0 r\sin\phi)\, d\phi$

$H \to I \qquad I_{HJ} = \int_0^{\pi/2} -r^2(5-\cos\phi)(-V_0 L - V_0 r\sin\phi - 5H_0 r + H_0 r\cos\phi)\, d\phi$

$I \to J \qquad I_{JK} = \int_0^{\pi/2} -r^2(5+\cos\phi)(-V_0 L - V_0 r\cos\phi - 5H_0 r - H_0 r\sin\phi)\, d\phi$

RAD. ELEMENTS:

$$\Sigma I = r^2 \int_0^{\pi/2} (18M_0 - 12V_0 L - 18H_0 r)\, d\phi - r^2 \int_0^{\pi/2} (12V_0 r - 6V_0 r\sin\phi + \cos\phi)\, d\phi + r^2 \int_0^{\pi/2} (3H_0 r - 3H_0 r(\sin\phi - \cos\phi))\, d\phi + r^2 \int_0^{\pi/2} 3H_0 r\, d\phi$$

$\lambda = 0$

$$\boxed{\Sigma I_{RAD} = \frac{\pi r^2}{2}(18M_0 - 12V_0 L - 15H_0 r) - 6r^2(V_0 r - V_0 L)}$$

$$\delta_{H_0} = \frac{1}{EI}\left[\Sigma I_{ST.\,ELEM.} + \Sigma I_{RAD.\,ELEM.}\right]$$

INTEGRAL FOR END SLOPE (θ)

$$\int M \frac{\partial M}{\partial M_0} \, ds$$

ELEMENT

$A \to B$. $I_{AB} = \int_0^L (M_0 - V_0 \cdot S)\, ds$

$D \to E$ $I_{DE} = \int_0^L (M_0 + V_0 \cdot S - V_0 \cdot L)\, ds$

$G \to H$ $I_{GH} = \int_0^L (M_0 - V_0 \cdot S)\, ds$

$J \to K$. $I_{KL} = \int_0^L (M_0 - V_0 \cdot S - V_0 \cdot L)\, ds$

$$\Sigma I = \int_0^L (4M_0 - 2V_0 \cdot S - 2V_0 \cdot L)\, ds$$

$$\boxed{\Sigma I_{ST.\,ELEM} = 4M_0 \cdot L - 3V_0 L^2}$$

$B \to C$ $I_{BC} = r \int_0^{\pi/2} (M_0 - V_0 \cdot L - V_0 \cdot r \sin\phi - H_0 r + H_0 r \cos\phi)\, d\phi$.

$C \to D$ $I_{CD} = r \int_0^{\pi/2} (M_0 - V_0 \cdot L - V_0 \cdot r \cos\phi - H_0 \cdot r - H_0 \cdot r \sin\phi)\, d\phi$.

$E \to F$ $I_{EF} = r \int_0^{\pi} (M_0 + V_0 \cdot r \sin\phi - 3H_0 \cdot r + H_0 \cdot r \cos\phi)\, d\phi$

$F \to G$ $I_{FG} = r \int_0^{\pi} (M_0 + V_0 \cdot r \cos\phi - 3H_0 r - H_0 \cdot r \sin\phi)\, d\phi$.

$H \to I$ $I_{HI} = r \int_{\pi/2}^{\pi} (M_0 - V_0 \cdot L - V_0 \cdot r \sin\phi - 5H_0 r + H_0 \cdot r \cos\phi)\, d\phi$

$I \to J$ $I_{JK} = r \int_0^{\pi/2} (M_0 - V_0 \cdot L - V_0 r \cos\phi - 5H_0 \cdot r - H_0 \cdot r \sin\phi)\, d\phi$

$$\Sigma I = r \int_0^{\pi/2} (6M_0 - 4V_0 \cdot L - V_0 \cdot r(\sin\phi + \cos\phi) - 18H_0 r + 3H_0 r(\sin\phi + \cos\phi)$$

$$\boxed{\Sigma I_{RAD} = r \left[(6M_0 - 4V_0 \cdot L - 18H_0 r)\pi/2 \right] \quad - 6H_0 r^2 !}$$

$$\theta_{M_0\,0} = \frac{1}{EI} \left[\Sigma I_{ST.\,ELEM} + \Sigma I_{RAD\ ELEM} \right]$$

Since the displacements are linear functions of the applied loads and if the displacements are known, the solution for the end loadings resulting from those displacements, can be obtained from the inversion of the following and then the bending moment and stress distributions can be derived.

DISPLACEMENTS LOADS COMPLIANCE COEFFICIENTS

$$\begin{bmatrix} \Delta_{V_o} \\ \Delta_{H_o} \\ \theta_{M_o} \end{bmatrix} = \begin{bmatrix} \frac{V_o}{EI} \\ \frac{H_o}{EI} \\ \frac{M_o}{EI} \end{bmatrix} \times \begin{bmatrix} A_{V_{V_o}} & A_{V_{H_o}} & A_{V_{H_o}} \\ A_{H_{V_o}} & A_{H_{H_o}} & A_{H_{H_o}} \\ A_{\theta_{V_o}} & A_{\theta_{H_o}} & A_{\theta_{H_o}} \end{bmatrix}$$

where

$$A_{V_{V_o}} = \frac{10\ell^3}{3} + 2\pi r\ell\left(\ell - \frac{3r}{4}\right)$$

$$A_{H_{V_o}} = -5r\ell^2 - 6r^2\left(\ell(\pi - 1) - r\right)$$

$$A_{\theta_{V_o}} = -3\ell^2 - 2\pi r L$$

$$A_{V_{H_o}} = 12\ell^2 r - 6\pi r^2\ell$$

$$A_{H_{H_o}} = -20r^2\ell - \frac{15}{2}\pi r^3$$

$$A_{\theta_{H_o}} = -3r^2(3\pi + 2)$$

$$A_{V_{H_o}} = -3\ell^2 - 2\pi r\ell$$

$$A_{H_{H_o}} = 6r\ell + 9\pi r^2$$

$$A_{\theta_{M_o}} = 4\ell + 3\pi r$$

APPENDIX 5

Deflection of a Tapered Beam - An Approximate Solution

DEFLECTION OF A TAPERED BEAM

APPROXIMATE SOLUTION

CONSIDER THE 3 SEPARATE BEAMS ①, ② & ②

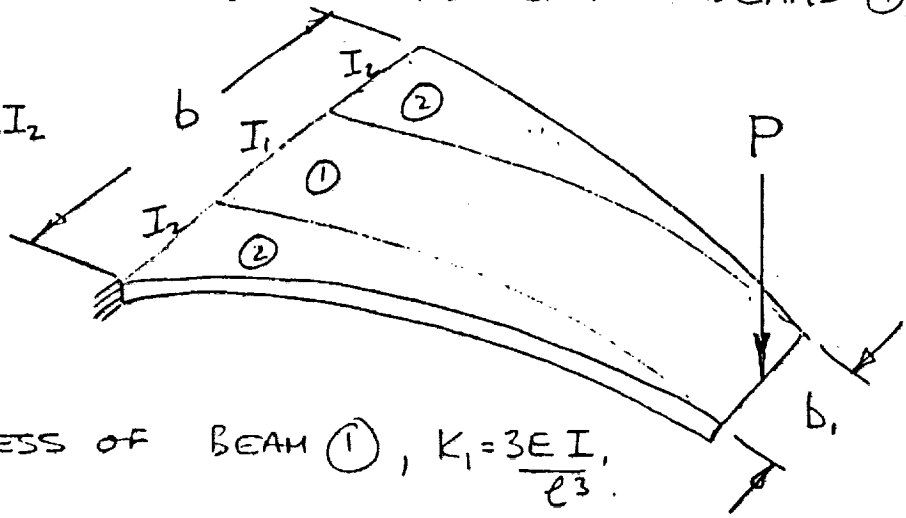

STIFFNESS OF BEAM ①, $K_1 = \frac{3EI_1}{\ell^3}$.

STIFFNESS OF BEAM ②, $K_2 = \frac{2EI_2}{\ell^3}$.

FOR AN APPROXIMATE TOTAL STIFFNESS OF 3 BEAMS JOINED

$$K_{TOT} = K_1 + 2K_2 = \frac{3EI_1}{\ell^3} + \frac{4EI_2}{\ell^3}$$

$$= \frac{E}{\ell^3}\left[3I_1 + 4I_2\right]$$

BEAM DEFLECTION UNDER LOAD P.

$$\Delta_p = \frac{P\ell^3}{E}\cdot\frac{1}{(3I_1 + 4I_2)} = \frac{P\ell^3}{E(3I - 2I_2)}$$

$$= \frac{P\ell^3}{3EI}\left(\frac{1}{1 - \frac{2I_2}{3I}}\right)$$

By Binomial Expansion, $\simeq \frac{P\ell^3}{3EI}\left(1 + \frac{2I_2}{3I} \cdots\right)$ but $2I_2 \doteq I - I_1$

$$\Delta_p \simeq \frac{P\ell^3}{3EI}\left(\frac{4}{3} - \frac{I_1}{3I}\right) \text{ or } \frac{P\ell^3}{3EI}\left(\frac{4}{3} - \frac{b_1}{3b}\right).$$

If Pe^3/EI is the deflection of a beam of constant width (b) then;

The additional deflection due to taper is, therefore,

$$\delta_T = \frac{Pl^3}{3EI} * \left(\frac{2I_2'}{3I}\right) \quad \text{where } 2I_2' = I - I_1$$

$$= \frac{Pl^3}{3EI} * \frac{1}{3}\left(\frac{I - I_1}{I}\right)$$

$$\delta_T = \frac{Pl^3}{3EI} * \frac{1}{3} * \left(1 - \frac{I_1}{I}\right)$$

$$\delta_T = \frac{Pl^3}{3EI} * \frac{1}{3} * \left(1 - \frac{b_1}{b}\right)$$

NASA
National Aeronautics and Space Administration

Report Documentation Page

1. Report No.	2. Government Accession No.	3. Recipient's Catalog No.
NASA CR-177586		

4. Title and Subtitle	5. Report Date
Soft Hub for Bearingless Rotors	June 1991
	6. Performing Organization Code

7. Author(s)	8. Performing Organization Report No.
Peter G. C. Dixon	A-91158
	10. Work Unit No. 505-59

9. Performing Organization Name and Address	11. Contract or Grant No.
Advanced Technologies, Inc. 812 Middle Ground Blvd. Newport News, VA 23606	NAS2-13157
	13. Type of Report and Period Covered Contractor Report
12. Sponsoring Agency Name and Address Ames Research Center Moffett Field, CA 94035-1000	14. Sponsoring Agency Code

15. Supplementary Notes

Point of Contact: Benton Lau, Ames Research Center, MS T-042, Moffett Field, CA 94035-1000
(415) 604-6714 or FTS 464-6714

16. Abstract

Soft hub concepts which allow the direct replacement of articulated rotor systems by bearingless types without any change in controllability or need for reinforcement to the drive shaft and/or transmission/fuselage attachments of the helicopter have been studied. Two concepts have been analyzed and confirmed for functional and structural feasibility against a design criteria and specifications established for this effort. Both systems are gymballed about a thrust carrying universal elastomeric bearing. One concept includes a set of composite flexures for drive torque transmittal from the shaft to the rotor, and another set (which is changeable) to impart hub tilting stiffness to the rotor system as required to meet the helicopter application. The second concept uses a composite bellows flexure to drive the rotor and to augment the hub stiffness provided by the elastomeric bearing. Each concept has been assessed for weight, drag, ROM cost, and number of parts and compared with the production BO-105 hub.

17. Key Words (Suggested by Author(s))	18. Distribution Statement
Hub, Composite, Bearingless, Flexure, Elastomeric, Hub Moment, Bellows, Rotor	Unclassified-Unlimited Subject Category – 05

19. Security Classif. (of this report)	20. Security Classif. (of this page)	21. No. of Pages	22. Price
Unclassified	Unclassified	100	A05

NASA FORM 1626 OCT 86

For sale by the National Technical Information Service, Springfield, Virginia 22161